Applying the Herman-Beta probabilistic method to MV feeders

Statistical MV Distribution Network Planning

Author: Munyaradzi Justice Chihota

Supervisors: Prof. Charles Trevor Gaunt

Dr Ron Herman

A Dissertation
Submitted to the Faculty of
Engineering and the Built Environment
University of Cape Town
in Fulfilment of the Requirements for
the **Degree of Master of Science**
in Electrical Engineering

November 2015

DECLARATION

I know the meaning of plagiarism and declare that all the work in the document, save for that which is properly acknowledged, is my own.

Signed by candidate

Signature removed

Department of Electrical Engineering
University of Cape Town
South Africa

25 November 2015

ACKNOWLEDGEMENTS

I would like to express my sincere gratitude to my supervisors, Professor C.T. Gaunt and Dr Ron Herman for the guidance throughout this work. So much knowledge was imparted in the period of academic interaction through this work. This has raised my standards of research and knowledge in power systems engineering.

Great appreciation again to my supervisor for setting up the necessary funding required for this research. I extend this note to the Dutkiewicz Family Scholarship Fund for the supplementary financial support to this work.

I also stretch my appreciation to my family for their unswerving support in my academic life up to this very day. My friends and colleagues are also worth mentioning as they contributed notably to the success of this work through encouragements. I give all honour to God for the ability to undertake this work.

ABSTRACT

The assessment of voltage drop in radial feeders is an important element in the process of network design and planning. This task is however not straight forward as the operation of modern power systems is highly influenced by a variety of uncertain and random variables such as stochasticity in load demand and power generation from renewable energy resources. Classic deterministic methods which model load demand and generation with fixed mean values consequently turn out to be inadequate and inaccurate tools for the analysis of power flow in the uncertainty-filled system. Statistically based methods become more suitable for such a task as they account for input variable uncertainties in their calculation of load flow.

In the South African context, the Herman Beta algorithm, a probabilistic load flow tool developed by Herman *et al.* [1] was adopted as the method for voltage assessment in Low Voltage (LV) network [1], [2]. The method was shown to have significant advantages compared with many other probabilistic methods for LV feeders, as investigated by Sellick and Gaunt [3]. Its performance with regards to speed and accuracy is superior to deterministic, numeric probabilistic and other analytical probabilistic methods. The evolving connections of smaller generators, referred to as Distributed Generators (DGs), to the utility grid inspired the extension of the HB algorithm to active LV distribution networks.

The HB algorithm was however formulated specifically for LV feeders. The assumptions of purely resistive feeders and unity power factor loads make it unsuitable for the Medium Voltage (MV) distribution network. In South Africa, deterministic methods are still being used for network design in MV distribution networks. This means that the drawbacks of such methods, for example inaccuracy and computational burden with large systems, are characteristic of the quality of network design in MV feeders. The performance of the HB algorithm together with the advantages and superiority of load modelling using the Beta probability density function (Beta pdf)[4] suggested that modifying the input parameters could allow the HB algorithm to be used for voltage calculations on MV networks.

This work therefore involves the adaptation of the way the HB algorithm is used, to make it suitable for voltage calculations on MV feeders. The HB algorithm for LV feeders is firstly analysed, coded into MATLAB, tested and then validated. Following this, the input parameters for feeder impedance and load current are modified to include the effects of reactance and non-unity power factor loads, using approximate modelling techniques. For reactance, the modulus or absolute value of the complex impedance is used in place of the resistance, to compensate for the line reactance. The load current is adjusted by inflating it by the power factor. The results of calculations with the HB algorithm are tested against a Monte-Carlo Simulation (MCS) solution of the feeder with an accurate model (full representation of feeder impedance and load power factor). The approach is extended to include shunt capacitor connections and DG in voltage calculations using the HB algorithm and testing the results with MCS.

The outcomes of this research are that the approach of adjusting the input parameters of line resistance and load current significantly improves the accuracy of calculations using the HB algorithm for MV feeders. Comparison with the results of MC simulations indicates that the error of voltage calculations on MV feeders will be less than 2% of the 'accurate probabilistic value'. However, it is not possible to predict the error for a particular application.

TABLE OF CONTENTS

LIST OF FIGURES

LIST OF TABLES

ACRONYMS AND ABBREVIATIONS

ADMD	After Diversity Maximum Demand
C_{1i}-C_{6i}	Network constants
DFL	Deterministic Load Flow methodologies
DG	Distributed Generation or Dispersed Generation
dV_i	Complex voltage drop due to node
dV_{R-i}, dV_{I-i}	Real and imaginary components of voltage drop at node
dV_{R-t}, dV_{I-t}	Total real and imaginary voltage drop components over feeder respectively
E (X)	Expected Value of X
FDLF	Fast Decoupled Load Flow
FLF	Fuzzy Load Flow algorithms
FOSM	First Order Second Moment
GA	Genetic Algorithms
GMM	Gaussian Mixture Model
HB	Herman-Beta probabilistic design tool
IDMTL	Inverse definite minimum time lag
k	Ratio of phase impedance to neutral impedance
LV	Low Voltage distribution systems
MCS	Monte-Carlo Simulation
MV	Medium Voltage distribution systems
NERSA	The National Energy Regulator of South Africa
OLTC	On-Load-Tap-Changing
P	Real Power consumed or supplied by loads or generators respectively
PEM	Point Estimate Method
PLF	Probabilistic Load Flow methods
$Q_{L,C}$	Reactive power drawn or supplied by a load or shunt capacitor bank respectively
R_n	Neutral conductor with resistance
R_p	Phase conductor resistance given
S	Apparent power
SVC	Static Var Compensators

V_{con}	Consumer voltage
V_s	Supply voltage
X_p	Phase reactance

Chapter 1

1. INTRODUCTION

The purpose of this work is to provide a network design tool for Medium Voltage (MV) distribution systems. Its focus is centred on the development of a statistical tool for voltage drop calculation along distribution feeders. This is done through modification of the input parameters in the Herman-Beta (HB) probabilistic design tool for Low Voltage (LV) distribution systems to include line reactance and to cater for non-unity load power factor. To establish validity of the generated tool, a Monte-Carlo simulation is used to assess the performance of the tool in terms of both accuracy and computational speed.

This chapter introduces the research problem, voltage drop calculation for MV feeders in the South African power system network. The work presented here includes a look into the background of network planning and design tools used for MV networks. Shortfalls and inadequacies of existing tools are identified leading to the formulation of the research hypothesis.

1.1. Background

An electric power system can be described as a network of electric components used to produce, transmit, supply and use electric power. The power system definition can be simplified by looking at it as an entity comprising of power generation plants, power consuming loads and infrastructure connecting the two. Classical power systems were designed hierarchically with generation at the top end of the system, high voltage transmission networks bridging the generation to distribution networks of medium and low voltage classification [5]. This system was configured for radial operation such that power flows from centralized generators at the high voltage end of the system down to loads along radial feeders only in one permissible direction [6]. This setup has however ceased to be consistent with the modern structure of the power system.

The present day scenario in power systems is characterised by the interconnection of small to medium generation plants to the distribution system, both low and medium voltage. This infrastructural change makes the power system an active network with distributed generation. The term Distributed Generation or Dispersed Generation (DG) refers to the small/medium scale power generation units within the distribution network which are usually close to the loads (customers) [7]. These remotely located plants are mostly based on renewable energy technology since power generation from fossil-fuels is increasingly receiving resentment due to its impacts on the environment and also the decline of the Energy Return On Investment (EROI) associated with it. In Low Voltage (LV) networks, photovoltaic plants are the most common whereas in Medium Voltage (MV) networks, wind energy and combined heat and power (CHP) plants are common. The role of distributed generation in complementary power production is expected to increase in future power systems. This is driven by the increased imbalance between power generation and the ever increasing load demand in modern societies. The need for more flexible electric systems, changing regulatory and economic scenarios, energy savings and environmental impact are further providing impetus to the development of DG [8].

Although the integration of DGs to power systems proves to be beneficial with regards to power system reliability and power quality, DGs bring new elements of uncertainty in power systems. This results from the unpredictable nature of their power production as generation is intermittent and also stochastic [9], [10]. Besides the uncertainty introduced by the integration of DGs, some other sources of uncertainty such as the intrinsic variability of power consumption exist in the system. The electric network load shows dependency on weather patterns, network operating parameters and is also stochastic in nature [11]. The environment around power system planning is therefore full of uncertainty. This makes power system design a non-trivial task requiring the use of well-developed tools to ensure economic and effective network design.

1.2. Power System Design

System design in the context of power systems involves the determination of electrical component sizes and their respective placement on the network. This is necessary so as to ensure optimal system performance as guided by power network regulations.

1.2.1. Design Guidelines and Milestones

The main objectives in power system design are as follows:

- To achieve an economical supply of electricity in adequate quantities to the customers in the network. This objective spreads to the requirement of the power system to be optimised for minimal power losses, voltage drop and reinforcement investments[12].
- To ensure the power system infrastructure is safe for the public, consumers and any persons that interact with it.
- To provide power supply with high reliability. This regards the capability of the system to supply electric power and serve the load demand at all times with consideration of scheduled or unscheduled outages of system components.

- To ensure power quality, which means the delivered power is within specified statutory limits necessary for consumer electric equipment to operate normally without damage. These limits for MV networks in South Africa are such that the voltage is within ±5% of whatever the nominal voltage is (Typical Nominal Values being: 11 kV, 22 kV, 44 kV etc.). The NRS048 standard also stipulates frequency deviations of up to ±2% and ±2.5% for grid and island connection types respectively; where the nominal frequency is 50 Hz. Other quality assessment indicators such as phase deviation, harmonics content and voltage unbalance are also specified [13].

The tasks necessary in achieving the above listed set of objectives encompasses the sizing and positioning of networks feeders, transformers, shunt capacitors and DGs. Other important aspects in this regard include penetration assessment for DGs and capacitors, as well as load balancing. These tasks depend on an analysis of bus voltages, their angles, and current flow in the system. This forms the basis for a requirement of assessment methods in power systems that give details about the state of the system at any required instant. This is what is termed the Load Flow Problem.

1.2.2. The Load Flow Problem

Load flow or power flow analysis is the most fundamental tool used by power system engineers to analyse the steady state of power systems with regard to bus voltages, real and reactive power flows, line losses and faults. Through load flow analysis, consumer (bus) voltages and angles at steady state can be obtained. This is essential as these parameters are meant to be within specified limits as discussed earlier on. Load flow studies are therefore crucial tools in network planning and design in the field of power system engineering.

Power flow methodologies began around the mid-1950s with a method by Hale and Ward[14]. Since this development, a lot other methods have evolved from it. Well known methods include the Gauss-Seidel and Newton-Raphson which are based on matrices and iterated calculations. A review of power flow computational methods can best be done by categorising the methods based on the manner in which the solutions are obtained.

Deterministic Load Flow – Classical Approach

Deterministic Load Flow (DFL) methodologies use specified (fixed) values of power generation, loads and network parameters to compute system steady-state operating conditions without taking into account any sources of uncertainty affecting the power system. The use of these traditional methods consequently becomes inaccurate and therefore less reliable amidst uncertainty. This is simply because the DFL methodology disregards uncertainty elements of the power system such as failure rates, intermittent power generation and the general stochastic customer load variations [15].

In the MV network, the deterministic approach to power flow studies remains prevalent in many countries. This approach is based on a non-statistical load modelling methodology that represents loads with mean values referred to as After Diversity Maximum Demand (ADMD) together with correction factors that attempt to address diversity and imbalances in loads. South Africa also utilises DLF methods for voltage drop analysis on MV feeders. Though the load represented by MV/LV transformers is modelled statistically, it is converted into a fixed value at the transformer terminals in order to apply DFL tools. The loads from direct MV customers are represented through ADMD values. A deterministic load flow calculation with the consideration of power factor and reactance is then done in the assessment of consumer voltage in the network. Though this was found to be adequate within customer load variability, the uncertainties of DGs are likely to cause inaccuracies in this method [16].

Inaccuracy and inefficiency cannot be freely tolerated in power systems as design parameters are directly linked to the overall system cost, magnitude of losses in the network and power system reliability. Design uncertainties therefore pose a great impact to network planning and design [17]. Hence, the explicit consideration of uncertainties requires the deployment of probabilistic approaches so as to provide the ability to manage the wide spectrum of all possible values of the input and state variables [18].

Probabilistic Load Flow – Modern Approach

In order to account for the uncertainty elements in the power system, probabilistic methods are required to cater for the stochastic variance in the generation as well as the load profiles. Probabilistic Load Flow (PLF) methods were first proposed in 1974 by Borkowska [19] and have since been developed over the decades. PLF methods regard both loads and DG sources as random variables due to their stochastic unpredictable natures. These methods have resulted in more reliable and accurate results than the classic deterministic (DLF) methods [15]. PLFs make use of probability or cumulative density functions allowing the analysis of the load flow or feeder voltage drop within risk or confidence intervals.

The choice as to which probability density function to use in the modelling of loads is an area of evolving research till present day. According to Neimane [20] the normal, log-normal and beta pdfs adequately fit MV load data as demonstrated through Chi-square fitness tests. It was however found that in cases where the data was not symmetrical, the beta and log-normal pdfs were more appropriate. Most PLF methods for voltage computation in MV systems are based on a Gaussian model.

With the use of pdfs, PLFs are able to account for the uncertain power production and load variations through an iterative selection of random input values from the distributions to represent the possible input variables. The Monte-Carlo method is quite a renowned tool in this class of numeric PLF methods. High computational time as a result of the iterations has however downplayed these methods. An attempt to address this inadequacy led to the development of other tools.

Fuzzy methods have been implemented in load flows for both LV and MV systems. These methods, sometimes called Fuzzy Load Flow (FLF) algorithms, model input uncertainties as imprecise or vague fuzzy numbers. Both loads and DG inputs are modelled through fuzzy methods, demand as positive and generation as negative loads [21]. The calculations for FLF are somewhat simple and they are represented as linearized functions. However, most of the FLF methods result in distorted uncertainties and the results are mostly impractical [22]. Souza *et al.* [12] employed a power flow method based on the sum of currents together with Genetic Algorithms (GAs) as optimisation tools to investigate the impact of DGs on MV networks. This method is an iterative optimisation tool that uses binary encoding and standard genetic operators. This Sum of Currents method obtained a reasonable performance in small power systems but it gains computational expense with larger distribution systems [21]. Celli *et al.* [23] used normally distributed loads and generation from DGs as the modelling approach in their work on MV networks. The PLF method was based on the mean and variance of the input random variables and was used to compute similar parameters for the consumer voltage. This PLF method was embedded in an iterated heuristic program for network optimisation along power loss and total system cost parameters. The method proved successful but it however restricts the modelling of input data to a Gaussian fit without skewness. This shortfall can be addressed by PLF methods based on pdfs that allow modelling of input variables with flexibility of skewness such as the beta function.

The implementation of such pdfs was proposed and developed for LV feeders by Herman and Gaunt [1], [4], [24] in 1994. Their approach referred to as the Herman-Beta (HB) method is an analytical statistical method used for LV voltage drop computation in South Africa [2]. This method is based on statistical moments, using the first two central moments to represent beta distributed currents drawn by loads and those injected by DGs. It is therefore a non-iterative approach which has proven to be superior to other methods as investigated by Sellick and Gaunt [25].

Though the HB method was designed specifically for LV networks, Siebert *et al.* [15] applied it without modification to MV feeders. A comparison of its performance against a DLF method and the Monte-Carlo simulation indicated that the HB method was faster but is however less accurate than the other methods.

1.3. Research Motivation

The stochastic behaviour of loads on MV feeders calls for a probability-based approach to voltage drop calculations [26]. More effective and accurate network decision can be made if network approximations and uncertainties are carried through to the load flow solution, thus allowing power system engineers to have a full understanding of the network and the implications of their design and operational decisions [22]. Accuracy in load flow computation is not the only essential characteristic of an appropriate PLF technique. Another dimension to the requirements in network planning and design is computational speed. In some cases, operational decisions need to be made within very short periods of time. For instance, in a modern power system setting (smart grid), network decisions may need to be made promptly to avoid power system reliability and quality issues, as investigated by Siebert *et al.* [15]. This requires a fast network voltage analysis using appropriate load flow techniques that allow an accurate representation of stochastic loads.

Deterministic methods result in unreliable and often misleading results as they fail to account for the uncertainty in power systems. These methods, as described by Seibert *et al.* [15] should be used with caution. Probabilistic approaches are the most appropriate tools for voltage calculations for a power system with uncertain random variable inputs such as load data and power generation. These have substantially proved to be better than deterministic approaches as they employ better input data representation through probability density functions. However, numeric orientated approaches in this class of load flow methodologies lack computational speed. This is the case with the renowned PLF tool, the Monte-Carlo Simulation (MCS). Most analytical methods are currently based on the normal distribution approach to load data and power generation [23].

The Herman-Beta algorithm is based on the Beta pdf which allows for load or power production data skewness. The advantage lies in that the beta pdf can also model symmetrically distributed load profiles which makes it a better tool than the Gaussian model. The HB method has shown immense capability in voltage computation on LV feeders, both passive and active [27]. Its superiority in performance as compared to other methods has seen it accepted and endorsed by the power utility company Eskom as the only valid design algorithm for use in South Africa[2]. The HB method was applied to MV systems, without any algorithm modifications, in Rio de Janeiro, Brazil [15]. However, the manner in which it was applied is questionable since the assumptions of negligible reactance and unity power factor loads cannot be extended to MV systems. The reactance and resistance quantities are nearly of the same value in MV networks as opposed to the dominant resistive component in most LV networks [23]. A modification to accommodate these missing elements in the HB algorithm may result in a functional PLF method for voltage computation on MV feeders. This development will allow optimisation of conductor sizing in both passive and active radial distribution networks. A probabilistic approach to power flow analysis on MV networks in South Africa will also mean the ability to perform network planning and analysis for DG penetration. Surely, the possibility of that development is an avenue worth exploring.

1.4. Research Contributions

The voltage drop methodology used in this research is an already existing algorithm tested and in implementation in the South African power system on the LV network. The methods of load modelling for both loads and generators are well known and have been discussed before.

The main contribution of this dissertation is to test an extension of the HB algorithm to MV feeders through the modification of input parameters to accommodate reactance and non-unity power factor loads in the calculation of voltages. A further extension to accommodate active DG connection on the network and also perform load flow analysis for feeders with capacitor compensation is also made.

The overall contributions can be summarised as follows:

- An analysis and verification of the HB algorithm for voltage drop calculation, as provided in literature mainly the NRS034-1 [2] and the main paper describing the method [27]. This analysis leads into the development of errata documents on the presentation of the HB algorithm in literature.
- Validation of the HB algorithm through a Monte-Carlo simulation for voltage drop calculation in LV feeders.
- A PLF method based on the original HB algorithm for LV systems to incorporate line reactance and non-unity power factor load flow through the adjustment of input parameters linked to these factors.
- An analysis of the effects of shunt connected capacitors used for voltage regulation on MV feeder voltage.
- An approach for voltage calculations on active MV feeders, allowing power systems engineers to compute voltage drop along radial feeders with DG modelled as negative loads.

1.5. Research Hypothesis

The HB algorithm is the current voltage drop computation tool adopted by Eskom utility company for distribution network planning and design in LV networks in South Africa. The HB method has been proven to be an effectual tool for voltage drop calculation superior to other methods. However, for MV networks, deterministic tools are still being used for feeder sizing and network planning in MV in South Africa.

Based on the analysis thus far, the following suppositions can be made:

- The differences in network models between the LV and MV systems necessitate modifying the application of the HB algorithm for calculating voltage drop on MV systems. This is potentially the reason why limited accuracy was obtained on the application of the original HB algorithm on MV networks by Siebert *et al.* [15].
- The work by Siebert *et al.* however promises applicability of the HB algorithm to MV systems.

The findings as noted above are adequate to inspire investigation of the possibility of extension of the HB algorithm to MV systems.

The hypothesis of this research can therefore be worded as follows:

The Herman-Beta algorithm can be adopted for voltage calculation on Medium Voltage (MV) feeders through inclusion of line reactance and power factor variations in the formulation of the input parameters. Following validation of this new approach with a Monte-Carlo simulation, it is possible to further extend the application for voltage calculation on feeders with shunt capacitor compensation.

1.6. Research Questions

In order to guide the course of this research and to fully establish its aims and purposes, the following research questions are necessary to be posed:

I. What are the key components of an MV network, its configuration, topologies and parameters? How is it different from the LV network?

II. Can MV loads be modelled by a Beta distribution function as done in LV systems?

III. What other approaches have been used to model MV loads?

IV. What methods have used to calculate voltage drop in MV systems?

V. What assumptions were made in the formulation of the Herman-Beta algorithm? Are these assumptions still valid in an MV network context?

VI. How can the input parameters in the HB algorithm be modified to make the HB algorithm suitable for voltage calculations in MV networks? Does the new application agree with proven methods such as the Monte-Carlo Simulation for voltage calculation?

VII. How can the new approach to voltage calculations on MV feeders be extended to accommodate an active network with DG interconnections?

VIII. How can the HB algorithm for MV be extended to allow for voltage calculations on shunt capacitor compensated feeders?

1.7. Research Scope and Limitations

This research is based on the adoption of the Herman-Beta algorithm as a statistical tool for voltage calculation in MV feeders. Since the HB method is based on beta-distributed load current inputs, the beta pdf is assumed to be the best fit for load data since load data is not readily available. The same assumption is considered for generation data that is also not readily available. Also, the load data used in the research is based on assumed models rather than actual measurements. These load pdfs may or may not be at the time of maximum demand.

The work covered in this research covers 3-phase 4-wire MV systems only. The other MV technologies such as 3-phase 3-wire, single phase and SWER will not be covered in this work.

Precisely, the work in this research covers the adoption of the HB algorithm for application to MV networks and its extension to capacitor compensated feeders. In this coverage, validation of the developed algorithms will be done through tests with the Monte-Carlo simulation.

1.8. Dissertation Structure

Chapter 1 introduces the research problem, voltage drop calculation for MV feeders in the South African power system network. The work presented here includes a look into the background of network planning and design tools used for MV networks. Shortfalls and inadequacies of existing tools are identified leading to the formulation of the research hypothesis.

Chapter 2 extensively covers the relevant literature around the research objectives in this work. It provides answers to some of the proposed research questions. The discussion of network design in MV networks forms the heart of this chapter with the main focus being on MV network topologies, load modelling, voltage drop computation and distributed generation integration.

Chapter 3 gives the description of the Herman Beta algorithm as a method for voltage drop computation in power systems. Its application to LV systems forms the foundation of this chapter. An analysis of the MV network topology is performed and the differences in network parameters from those of the LV network noted. A sensitivity analysis on the different parameters is conducted to establish the need for modification.

Chapter 4 covers the development of the programming tools necessary for voltage computation and analysis in the scope of the project. The Herman-Beta algorithms for voltage calculation in passive and active LV feeders are translated into MATLAB code. Tests are subsequently done to check for errors in the code. The error-free software is then validated against the Monte-Carlo counterparts programs.

Chapter 5 deals with the modification of the resistance input parameter to the HB algorithm to include the effects of feeder reactance on voltage drop. Tests on this new approach are done and results compared to voltage calculations with the MCS.

Chapter 6 involves the modification of the load current parameter to include the effects of non-unity power factor loads on voltage drop. Following the adjustment, the method is tested for errors and validation done through comparison with voltage calculations using the Monte-Carlo simulation.

Chapter 7 covers the application of the HB algorithm for LV active feeders to MV feeders. Modifications to the input parameters for feeder impedance and load current are done in a similar way to those done in Chapter 5 and 6. The resulting voltage calculation approach is tested and its performance assessed through comparative studies with the Monte-Carlo Simulation. Validity is concluded based on the findings.

Chapter 8 concerns the extension to compensated feeders, of the approach to voltage calculations on MV feeders using the HB algorithm. The testing of the extended approach is done and validation performed through comparison of voltage calculation outcomes with the MCS.

Chapter 9 assess the level of improvement that the modifications to the application of the HB algorithm presented in chapters 5-8 make compared to the original unmodified algorithm. Different test scenarios are used to assess the performance of the algorithms on the basis of expected results from the MCS.

Chapter 10 concludes the dissertation with a presentation of concluding remarks, future work projections and final thoughts. It also gives a report on the extent to which the research outcomes answer the research questions and validate the research hypothesis.

Appendices contain other relevant information concerning the dissertation that is useful in the understanding of the work.

Chapter 2

2. POWER SYSTEM NETWORK DESIGN PRINCIPLES

This chapter extensively covers the relevant literature around the research objectives in this work. It therefore seeks to answer the proposed research questions. Network design in medium voltage networks forms the heart of this chapter with the main focus being on MV network topologies, load modelling, voltage drop computation and distributed generation integration. Some voltage drop calculation methods used for LV systems are also included so as to get a wider scope on voltage computational methodologies.

2.1. Distribution Networks Overview

A power system is mainly characterised by three sub-systems namely generation, transmission and distribution. Though it can be broken down into just these three parts, power systems are very complex structures with a lot of components such as generators, transformers, feeders, circuit breakers and loads. The sole role of the power system is to transport power over considerable distances from the generation end to customers connected via the distribution network[28]. There are however constraints in the design of a power system. A power system is meant to effectively perform the task of power distribution with minimal power losses, inexpensive infrastructure, good quality of supply, reliability and minimal reinforcements (or maintanance). These constraints point to the need for excellent power system design and operational planning. This task is usually characterised by objectives such as cable and transformer sizing, shunt capacitor positioning, reinforcement power generation placements and phase load balancing [12].

Power generation was classically done from centralized large power plants based on fossil-fuel. These would generate high voltage power that feeds into the transmission systems of the network. Such centralized generation is classified under passive power systems since power flow was maintained only in one direction from upper voltage levels down to customers along radial feeders [29]. In most modern power systems, generation is no longer a centralised process as smaller generators are now connected to the distribution system usually closer to the customers [6], [7], [12], [28], [30]. These modern power systems have been referred to as active power systems owing to the generation of power at distribution level.

The power generated from power plants is injected into the transmission system whose sole role lies in transporting the power to the distribution system. The necessity of the transmission system arises from power plants (usually centralized ones) being distances away from the place of demand. Power transmission is usually characterised by high voltage underground and overhead cables over long distances. The transmission at high voltage is such as to minimise power losses in the process. Transmission networks terminate at transformers bridging into the distribution network.

Transformers play an important role in power systems as they step up or down voltages to required voltages at different points in the network. In the generation component of the system, transformers are responsible for voltage step-up for transmission purposes. At the distribution level, they step down voltages to the customer's required range. In the distribution system, two subsystems are found based on the range of consumer voltage. The Medium Voltage network starts from the secondary HV/MV transformer side up until it runs into Low Voltage networks on the primary side of MV/LV transformers. Table 2.1 below shows the network voltage ranges and classification as stipulated by the Eskom Distribution Code Definitions (2007).

Table 2-1: Power System Voltage Classification

DISTRIBUTION SYSTEM CLASS	VOLTAGE RANGE
High Voltage (HV)	44 kV ≤ V_{HV} ≤ 132 kV
Medium Voltage (MV)	1 kV < V_{MV} < 44 kV
Low Voltage (LV)	V_{LV} ≤ 1 kV

This work will focus on the MV distribution network and its interconnections with both the HV and LV networks through transformer units. A broader insight into the MV network is therefore necessary and is given in the section that follows.

2.1. The Medium Voltage (MV) distribution system

2.1.1. MV Distribution Network Topology

The MV network in South Africa is categorised into rural overhead MV networks (1-22 kV), Urban MV networks (1-22 kV) and another class of MV networks with customers drawing power at voltages exceeding 22 kV (22 kV-44 kV) [13]. MV feeders are typically short since long feeders result in more voltage drop due to their impedances. The main MV technologies implemented are three phase 3-wire, three phase 4-wire, single phase and the Single Wire Earth Return (SWER) system. The characteristics of these technologies are outlined in Table 2.2.

Table 2-2: MV Network Technologies and properties

MV Technology	Connection Type	Typical Nominal Voltage
3 phase 3-wire	Phase to Phase	11 kV, 22 kV, 33 kV
3 phase 4-wire	Phase to Phase	11 kV, 22 kV, 33 kV
Single Phase	Phase to Phase	11 kV, 22 kV, 33 kV
SWER	Phase to Neutral	19 kV

Most MV feeders are configured radially and characterised by low X/R ratios close to unity. Masters [31] and Celli et al [32] emphasized the importance of including line reactance in the feeder modelling as is it not a negligible quantity in MV systems. This is one of the major differences between MV and LV feeders that may affect voltage computation.

In this research, the method developed will be tested and implemented on 3-phase 4-wire MV feeders. The application of the developed method to the other MV technologies is considered for future work.

2.2. Voltage Compatibility Levels and Limits

Quality of supply is a crucial element in power systems. It can be thought of as a measure of the fitness of delivered power for consumer appliances. There are three main attributes that are considered in this regard; these are voltage levels, phase magnitude and frequency. These attributes of power supply are necessary for the optimal appliance performance and efficiency. Most researchers have found out that the most critical power supply attribute is voltage level (conversely voltage drop). Compatibility levels stipulate non-deviations from the nominal voltage expected at the consumer terminals. According to the NRS048 standards, it is recommended that the declared voltage be within 5% of the nominal voltage. Deviation from this stipulated margin is not allowed to occur for a period longer than 10 consecutive minutes [13]. In addition to voltage compatibility levels, voltage limits are enforced so as to restrict allowable out of range voltages for system and appliance protection. The same guideline to quality of supply stipulates a maximum deviation from the standard voltage levels by up to 10% for voltages less than 500V. This information is instrumental in the design context as it directly affects cable sizing in feeders.

2.2.1. Consumer Phase Assignment

Voltage drop in a feeder is affected by the way customers are connected to the supply [2]. De Souza et al [12] investigated the effect of phase load balancing on voltage levels in networks. Their findings reflected that phase load imbalance on a feeder may result in increased voltage drops in the network. Gaunt and Sellick [24] also undertook investigations on the effect of phase allocation on voltage drop in LV networks using the HB algorithm. They came to a conclusive finding that the best case of voltage drop is obtained when the loads are evenly distributed across the phases. The investigations involved the implementation of different phase allocation patterns and observing the effects on voltage drop. The main patterns that were found to achieve phase load balancing and thus minimal voltage drop in the feeder were the cosine, cyclic and balanced allocation methods. These are illustrated with examples in Table 2.3 below.

Table 2-3: Phase Allocation Methods for optimum network design

Allocation Classification	Phase Assignment Pattern	Phase	Node 1	Node 2	Node 3	Node 4	Node 5	Node 6	Total Load
Cyclic 211	R,W,B,R,W,B,R,W,B	A	2	1	1	2	1	1	8
		B	1	2	1	1	2	1	8
		C	1	1	2	1	1	2	8
Cosine 400	R,W,B,B,W,R,R,W,B	A	4	0	0	0	0	4	8
		B	0	4	0	0	4	0	8
		C	0	0	4	4	0	0	8
Bal 222	Equal customers in every phase at every node	A	2	2	2	2	2	2	12
		B	2	2	2	2	2	2	12
		C	2	2	2	2	2	2	12

As shown in the table above, the phases in all cases are equally loaded at the end of every 3 nodes. This allows even voltage drops on the network thus avoiding heavy loading and poor voltage levels in any individual phase. An understanding of phase allocation is therefore a tool for voltage regulation in power systems.

2.2.2. MV Distribution System Protection

In MV networks, especially in underground and bare overhead conductor systems, feeder protection against over-currents is designed through implementation of non-directional inverse definite minimum time lag (IDMTL) over-current and earth fault protection relays [2]. For MV ABC systems, extreme inverse over-current and earth fault protection relays are used to counter over-current faults. MV transformers are protected through rupturing or expulsion over-current fuses. Circuit breakers, trip coils, time-lag fuses or relays with unshunted earth fault trip coils may also be used.

2.2.3. MV feeder voltage regulation

One of the most important characteristic of quality of supply in power systems is voltage quality. Power supplied to consumers is required to be delivered in specified limits of voltage, current and frequency. This proves to be a challenge in power systems since the transmission and distribution of current flow over distances results in power losses and voltage drops. Moreover, the flow of reactive power increases the thermal loading of feeders resulting in further drops. Customers connected far from the generators are then likely to receive voltages below the stipulated supply margin.

The condition of under-voltage is not the only violation of voltage limits possible. Over-voltages also occur in power system as a result of load imbalances, current injection from DGs and shunt capacitors. Both cases of voltage violation are undesirable as they affect the normal functionality of consumer appliances. To avoid this, voltage regulation is required.

Voltage support is used to maintain the bus or nodal voltages within stipulated margins. Maintenance of bus voltage involves the increase or decrease of line voltages in cases of under-voltages or over-voltages respectively. In this regard, methods like transformer On-Load-Tap-Changing (OLTC) have been used vastly in power systems. Another way to obtain voltage correction is through reactive power compensation and power factor correction.

Reactive power compensation is used to reduce the thermal loading in the system. This is achieved through reactive power supply to the loads thereby reducing reactive power flow in the system. A reduced flow of current then results in reduced voltage drops and conversely increases in bus voltages. A lot of compensation techniques have been implemented in power systems to mitigate the effects of reactive power flow in power systems. Series and shunt capacitors, Static Var Compensators (SVCs), Pulse Width Modulation (PWM) inverters and in some cases switched reactors are amongst other reputable methods. Recently, voltage regulation through Distributed Generators (DGs) has been used for complimentary real power generation as well as for reactive power compensation.

2.3. Distributed Generation in MV Systems

2.3.1. Introduction

Electrical power systems were traditionally designed mainly to distribute power from large, centrally situated power plants to loads over considerable distances. From the past few years, there have been extensive interests in the connection of other power plants to the power system at the distribution system level [5]–[7], [9], [23], [33], [34]. This interconnection of non-centralized power plants is called Distributed Generation or in some cases, Dispersed Generation (DG) or Embedded Generation. Typically, DGs vary from small to medium scale plants generating power in the order of kilowatts (kW) up to tens of megawatts (MW). These plants are not part of the large central power source and are usually installed close to the loads they supply. DG sources which include photovoltaic plants, wind turbines, small hydro plants, storage technologies and CHP (combined heat and power) [1] are mostly connected to LV and MV distribution networks rather than the high voltage transmission network [13]. The resulting network no longer exists to be passive but active with non-unidirectional power flow as a result of power injections from generators at customer level [15].

The move to DG integration has thus far increased as motivated by the need to deregulate the energy markets, improve power system reliability, adequately supply an ever-increasing load and increase energy system efficiency amongst other reasons [5]. Countries like Germany, UK, Denmark and Portugal have experienced an accelerated implementation of distributed generation in their power systems. This has been motivated by incentive and benefit schemes such as simplified access to the grid and priority in dispatching such as to promote DG integration [4]. South Africa is also another country in which DG integration has recently received attention. The National Energy Regulator of South Africa's (NERSA's) has recently looked into developing a regulatory framework for "distributed power generation" in South Africa, including how "prosumers" could be empowered to feed surplus electricity into the grid. This is potentially a gateway to a DG prominent network.

The connection of DGs to power systems has been found in literature to have benefits to the electric network; however literature also reveals a lot of issues with this interconnection. Some of the benefits and issues as discovered in current literature are discussed in the proceeding section.

2.3.2. Benefits of DG

A variety of benefits to consumers, DSOs and energy service companies are seen with the integration of DG.

- *Green power* - the implementation of DGs has been hailed for its use of renewable energy sources and combined heat and power technologies. The high efficiency in CHP and the low carbon footprint associated with renewables results in DG posing less impact on the environment than fossil-fuel based technologies which have higher greenhouse gas emissions [1], [4] .
- *System flexibility and reliability* - the deregulation of the energy market through access to the grid has allowed new energy suppliers to connect to the distribution system in many cases improving system reliability in the network [5], [28].
- *Peak shaving* - the grid connection of DG can also be utilised as a source of peak demand power thereby used for peak load shaving [1].
- *Grid support* - the installation of DGs to the distribution system and in many cases closer to the load typically reduces power lost through transmission over long distances. Increased efficiencies in the power system are therefore obtained and utility investments for

reinforcements deferred [5], [7], [16], [23]. Dondi *et al.* [5] and other researchers affirm that the injection of real and reactive power from DGs can be used to perform power factor correction in the network. Safigianni [28] also concurs but quantifies this effect of improved power factor as minimal.

2.3.3. Issues with the connection of DGs

The connection of DGs has been proven to have some negative impacts on the power system. Firstly, the presence of generation nodes in the distribution system can cause over voltages in some points of the network. This effect is prevalent to nodes closer to the generators. However, the extent to which voltage rise occurs depends particularly on the transformer control system used. In some systems, voltages at the busbar are lowered through adjustment of the OLTC thereby decreasing effects of voltage rise. However, it can generally be said that the interconnection of DGs to the utility grid causes conditions of voltage rise [5]–[7], [23], [34], [35].

Researchers have discovered increased complexities in power system planning as a result of the penetration of DGs. This is mainly because of the stochastic power production by DG units which results in increased levels of uncertainties in Power systems [9], [23]. Delfanti and many other authors also claim negative impact on system operation, control, protection and reliability if DGs are incorrectly placed and/or connected to the grid[5], [6].

A study on the effects of penetration of mixed generation by Safigianni *et al.* [28] led to a conclusion that the main impact of DGs is expressed on the voltage profiles in the network. This was found to occur during the condition of maximum generation with minimum load leading to voltage rise. The majority of the voltage nodes therefore exceeded the regulatory limits of voltage. To address this problem, researchers have resorted to worst case design approach especially the "maximum DG production minimum demand" case [9]. The other critical case in the design task is the extreme combination of maximum load and minimum DG production.

A high degree of penetration of DG into the distribution system has considerable impacts on the operation, control, protection and reliability of the power systems. Principally, as been stated earlier, the traditional power systems were designed for a radial power flow from high voltages associated with generation down to lower voltages where consumption occurs. The integration of DG may pose reverse power flow effects in the network [4]. For this reason, it is advised that an appropriate analysis on the possible effects of increased penetration on the system should be undertaken before installation of DGs is done. This is a current ongoing research endeavour in power system distribution studies [5], [34] The effect of DGs can be disregarded if the diffusion is low in comparison with the load. However, when the diffusion of DG becomes comparable with the demand of the distribution network to which it is connected, the uncertainties introduced cannot be disregarded

2.4. Load modelling in power systems

2.4.1. Deterministic Approach – ADMD

The design of MV and LV distribution systems in some countries remains a deterministic approach based on estimated After Diversity Maximum Demand (ADMD). ADMD is the average maximum demand of power per customer after diversity has been considered[36]. ADMD is seen to vary with the number of customers considered. This value decreases with the number of customers as a result of the stochastic nature of the individual demand. The variation of the ADMD with the total number of customers and demand intervals is usually expressed graphically and used for network design. The meaning of ADMD is therefore only valid in the interval of interest, the averaging window. To use the ADMD curves correctly, information on the number of customers and interval of demand is required. ADMD is usually expressed wither in KW, KVA or in Amps.

In order to incorporate the diversity of demand along the feeder and for different types of customers, a diversity factor is used to inflate the ADMD value to more appropriate values. A diversity factor can be defined as the ratio of the sum of the individual maximum demands of the various subdivisions of a distribution system to the maximum demand of the whole system [37]. This factor is essential in expressing diversity of customer loads in a distribution system. Another factor called a coincidence factor is merely a reciprocal of the diversity factor.

Barry [38] investigated the variation of maximum demand with the total customers connected in a distribution feeder. His findings led to a proposal of an empirical formula that dictates this relationship. This method has been vastly used in many countries, including South Africa, in performing deterministic load calculations. The relationship is as shown below:

$$E_n = E_\infty + \frac{1-E_\infty}{n} \quad where\ E\ denotes\ the\ coincidence\ factor\ ; \qquad (2.1)$$

$$n - number\ of\ customer$$

Barry hypothesised that the term E_∞ was dependent on the class of customers, appliances used, weather and other climatic conditions. Other researchers such as Hamilton [39] and Rusck [40] extended the concept of coincidence factors to statistical grounds. The coincidence factor according to them was a measure of the spread of consumer demands during the interval of maximum demand. Rusck stated that the general distribution of a customers demand was not normally distributed.

However, during the instant of maximum demand this distribution could be assumed to be normally fitted. The summation of these individual distributions using their means and variance would result in a normally distributed total demand. To sum up his work, his mathematical description of coincidence factor is as given below:

$$C_n = C_\infty + \frac{1-C_\infty}{\sqrt{n}} \qquad where\ C\ denotes\ the\ coincidence\ factor\ ; \qquad (2.2)$$

$$n - number\ of\ customer$$

An introduction to statistical confidence intervals on the load estimate was brought by Davies and Paterson with the concept of 'loss of diversity factor'. This work was based on the same assumption of Normal distributivity as claimed by Rusck. The study investigated the loss of diversity with diminishing number of customers in a load sample. In line with this, findings made by Gaunt and Ferguson on a load modelling study reflected that typical small number of rural network customers brought uncertainty in the ADMD correction factors [41]. The correlation between the number of customers and correction factors introduces errors in the estimation of ADMD.

The use of the ADMD values in design as described in the literature review above is dependent on the availability of load information usually obtained from recording customer load usage in defined intervals. Usually, in MV systems not much of this information is available. In most cases only yearly energy consumption indices are given. Velander described a formula that transforms annual energy consumption into maximum consumer demand.

$$P_{peak} = k_1.E + k_2.\sqrt{E} \qquad where\ E\ is\ the\ annual\ consumption \qquad (2.3)$$

$$k_1 and\ k_2 being\ empirical\ coefficients$$

The developments of load modelling, especially those looking into the spread of loads, instigated a better analysis on loads and their representations for power system design. The literature reviewed showed a surge in development of load modelling using statistical approaches with intention to fully represent the spread of customer demand in the load models.

2.4.2. Statistical Modelling

Electrical network load data measurements reflect dependency of load size and patterns on weather, network parameters such as circuit breaker limitation and customer profiling [17]. Customer profile characteristics such as income, occupants per household and community habits were some of the parameters found to have great impacts on loads in LV systems in a research by Gaunt and Herman [24]. This stochasticity of customer load necessitates the need of a statistical approach to load modelling.

Literature reveals the Gaussian model as the most commonly used means of load modelling in power systems [42]. In a study on MV network planning, Celli *et al.* used the normal distribution to represent the loads as powers [23]. In their work, they found shortfalls of the Gaussian method in fully fitting the variation of customer load. However, their research also pointed to the fact that more precise representation of loads and generation with other distribution types is unfeasible as the increase in computation time gets dramatic. Other authors also share the same sentiments on the inadequacy of the Gaussian method. Studies reveal that the Gaussian method applies precisely to a large number of consumers and is least accurate when there are less than 30 connected customers [17] . Stemming from this find, considerable research effort has been spent attempting to represent varying customer load more accurately.

Herman and Kritzinger investigated the modelling of load data using various distribution functions in efforts to find the most fitting distribution. In their research, the Weibull, normal, Erlang and beta pdf were assessed through Chi-square goodness of fit tests. The conclusion was that the Beta distribution function was the most appropriate tool for representation of load data in LV systems [4]. Ghosh *et al.* also investigated the same and came to a similar conclusion with the exception that the log-normal was in some cases a better fit that the beta pdf [37]. Consequently, Carmona-Delgado amongst other authors then argue that there is no standard distribution function that would precisely represent customer load data for the nature of load seen in MV and LV networks [43].

The Gaussian Mixture Model (GMM) has evolved in literature in effort to model loads more accurately[42], [43]. The GMM approach can represent any type of load distribution as a combination of several Gaussian components and represents a parameter estimation problem. The estimation of the distribution improves with increasing Gaussian components. However, this increases the parameters to be estimated and therefore increases the computational burden [43]. The GMM method has been compared with other pdfs like the Beta, Gauss and was found to give a better fit using the Chi-square goodness of fit test. However, this procedure is iterative and has high computational times [42].

In literature, there hasn't been a clear distinction between methods used for load modelling in LV and MV systems. Most methods that apply to LV networks have been also applied impeccably to MV systems. There is however a problem in that there is a substantial lack of collection of load data in MV networks in comparison to LV networks [9], [36], [43]. In cases where data is unavailable, standard distributions such as the Normal, Weibull and Beta have been used to estimate the load profiles using available annual usage data or other periodic seasonal load curves.

The presentation of loads for a statistical analysis of voltage drop in power systems either as currents or voltages forms another important aspect of load modelling. Literature reveals three main techniques of load characterisation sometimes referred to as the ZIP models [44] in which the loads are represented in the following parameters or as hybrids:

i) Constant impedance (Z)
ii) Constant current (I)
iii) Constant power (P)

Herman and Gaunt [1] in a research on voltage drop computation using the Herman-Beta algorithm made use of a current model to represent residential loads. They based their choice of methodology on the basis of the following facts:

- The magnitude of the load current is independent of the voltage drop along the feeder or distance of load from the source.
- The measurements of loads as currents can be carried out more accurately and economically.
- The alternative modelling, that of power could only be applied to an iterative voltage drop computational method.
- The representation of load as currents is consistent with the nature of real (close to unity power factor) residential loads.

Although some of the reasons given by Gaunt and Herman suggest restriction of current modelling to LV systems, the same method has been applied plausibly in MV systems

The vast majority of authors [9], [23], [34], [36], [42], [43] represent consumer loads as power pdfs for network analysis in MV distribution systems. In most of these presentations, the known nodal power is however used to compute nodal currents which are then treated as the random variables for the statistical voltage computations. This is the way in which Celli *et al.* [23] represent consumer loads. Ghosh et al used real power load data and substation power factor information to obtain reactive power load demand profiles [37]. This is very useful in cases where only real power demand data is available.

2.5. DG modelling techniques

As discussed earlier, the interconnection of DG to the power system changes the network configuration resulting in the need of adjustments in the modelling. In power flow analysis using probabilistic methods, DG connections have been commonly regarded as negative loads. This is because DG cannot be modelled as a power source connected in parallel with the utility source. This according to Brown and Freeman [45], would result in a non-radial system on which radial power flow algorithms cannot be applied. The modelling of DG as a negative load therefore preserves the radial network structure and also makes power flow analysis easier. In addition, Kim and Hwang [46] reported the convenience of this representation of DG in islanding detection studies. In their work they made findings that the 'negative load' approach for DG is reasonable since in cases of faults and in the absence of a utility source, the DG is required to be disconnected allowing faults to clear and ensure safety. The representation of generators as negative loads has since been adopted by a lot of researchers, including Gaunt *et al.* [10] for implementation on both MV and LV feeders.

2.6. Voltage drop calculation methodologies

2.6.1. Deterministic Load Flow

In the past decades various algorithms have been developed for solving the power flow problem. These algorithms differ very much in their characteristics, performances, as well as in their mathematical foundations. Generally, traditional power flow methods are very accurate and allow detailed modelling of the system. These methods work with fixed, deterministic type inputs. Therefore DLF methodologies disregard power system uncertainties such as load stochasticity [8], [15], [19], [47]–[50]. Most deterministic methods of voltage computation are based on mean maximum demand values [7]. Newton-Raphson and some fast decoupled methods with deterministic inputs have also been used to calculate voltage drop in MV networks. However, the computational effort that arises because of the increase in matrix dimensions with network size is undesirable [12], [15].

Many authors have used the backward/forward sweep sum of currents for the calculation of the power flow in both LV and MV network design [12], [15]. This is an iterative method in which calculation of feeder nodal currents is done using initial estimates of nodal voltages from the bottom of the network tree up to the top (node closest to supply transformer). This is then followed by a computation of nodal voltages using the initial values of currents from the transformer to the most distant nodes. This is iterated until the difference between successive iteration is within a certain stipulated tolerance. Genetic algorithms were then employed to optimise an objective function to minimise power losses, voltage drops and installation costs [12]. The back/forward sweep method is advantageous in that it doesn't require matrix representation in its calculation but the requirement for iteration leads to a time consuming calculation.

2.6.2. Probabilistic Load Flow

DLF methods have been proven ineffective in modern power system planning and design due to their failure to cater for power system uncertainties. The levels of uncertainties and stochasticity in the power systems inspired statistically based methods of voltage computation to evolve [47], [48].

Methods used for voltage computation which are statistically based have been referred to as Probabilistic Load Flow (PLF) methods. These methods are becoming renowned tools in distribution system design as they take into account the uncertainties in power systems which include the stochastic nature of power demand and the intermittent power generation by Distributed generation sources [34], [43].

By means of modelling the input variables through statistical tools like the Normal, Gaussian and Beta pdfs, the PLF methods function like transforms which translate the statistical inputs into statistical outputs of the same distribution. These outputs give the likelihood and confidence levels in the power system network variables such as bus voltage [15]. This is the main supremacy of PLF methods over DLF methods which do not incorporate uncertainties and the concept of chance [43].

PLF methods evolved through a researcher Borkowska, in 1974 [19] and have been progressively taking over from DLF methods with a focus on effectiveness and accuracy either on the uncertainty modelling of the loads or bus voltage calculations. PLF methods can be categorised into analytical and numerical based on the way the PLF is solved.

The Monte-Carlo Simulation (MCS) method is one of the most commonly used numerical methods in power system planning and design. The MCS method is typically an iterated deterministic load flow calculation based on AC load flow. In each iteration, a different set of random input variables such as customer load demand and DG power production are used in the DLF calculation [34]. Literature hails its degree of accuracy amounting from its precise modelling with inclusion of all network elements like reactance and power factor in its computations without assumptions. The MCS method has been applied as a tool for voltage computation in MV networks. Zio *et al.* [7] undertook an assessment of DG penetration in MV distribution systems using the MCS method. The MCS method was based on a Newton-Raphson power flow analysis. It was concluded that the PLF method is more appropriate in power flow analysis than the DLF one, due to a more realistic presentation of load demand and power injections.

The MCS method is however pulled down by the huge computational effort required to arrive at a single solution. The iterations required in a MCS calculation for acceptable degrees of accuracy are in the order of tens of thousands. This makes the method very slow and ineffective in cases where quick network decisions need to be made e.g. in smart power systems. However, because of its high accuracy, the MCS method continues to be used as tool for validation on other PLF methods.

The MCS method is also vastly used in the assessment of DG penetration in power systems [34]. El-Kattham *et al.* [49] investigated the performance of distribution systems with DG using the MCS method. The work extended into investigations of the effects of DG positioning on bus voltages. It was found that the random operation of DG units can dynamically affect the overall performance of the power system.

Literature reveals several attempts to improve the speed and computational burden associated with the MCS method. A multi-linear Monte Carlo method suggested by Carpinelli *et al.* [50] utilizes the total active power as a criterion for determining different linearization points. This allows for a wider coverage of the uncertainties in the input data. Results obtained revealed that the multi-linear MCS requires less computational time than other versions of the MCS method such as the linear-MCS and the non-linear-MC. Another method, the Quasi Monte-Carlo is tailored to generate input samples which are more uniformly distributed. This method uses less input samples yet obtaining more accurate results than the normal MCS method [51]. Though these modifications do reduce the computational effort in the MCS method, the time is still considerably long.

The problem of computational rigour is better addressed by probabilistic analytical methods, which are computationally more efficient compared to MCS. Among these, two of the most popular techniques developed for the reduction of the computational burden are:

1. *Conventional convolution*

Convolution techniques have the advantage of considering all possible network load usage profiles. This methodology allows all possible load patterns to be used in the computation of mean, standard deviation and variance of the output variable without restriction to normal distributivity [52]. However, this property results in increased computational time which may be undesirable.

Most convolution methods use network models that are linearized at an expansion point in order to avoid complexity posed by the non- linearity of the network. One of the major drawbacks is the increasing inaccuracy for wide spread probability density functions such as those for wind power injections [47].

Schwippe proposed an improved convolution method that was based on a Fast decoupled load flow (FDLF). In this method, the linearization of network equations was only dependent on the feeder topology and network parameters. The extension of the convolution method by Schwippe reduces the inaccuracies brought about by the process of linearization. This was found to minimize feeder voltage deviation from the actual value and also decrease computational time [47].

2. *Mathematical series based approaches*

Existing literature also reveals reduction of computational burden through analytical methods based on Fast Fourier Transformation (FFT) convolution and those that make use of Cumulants and Gram-

Charlier series expansion (usually Type A). The FFT method is however drawn back by the need of a great deal of data storage for intensive computational loops. The methods based on the Cumulants and Gram-Charlier series is reported to significantly reduce computational time and accuracy but has complex formulations [53].

3. *Point Estimate Method (PEM)*

The PEM method is a deterministic power flow based approach that chooses representative points from the input variables and models them as weights which are then used in a deterministic load flow calculation to obtain statistical moments of the outputs [48], [51]. The PEM approach can handle non-Gaussian load models. However, the PEM method is characterised by a complex linearization process [43]. Some authors have worked on improving the PEM method especially on the reduction of complexity through sampling methodologies. Xiao's PEM method utilizes a better approach to the selection of representation points and the weighting as well. The determination of correlation between random variables is also done directly in this approach. The result is a more efficient and accurate PEM method [51].

4. *Methods based on statistical moments*

The Herman Beta algorithm developed by Herman and Gaunt in 1994 [1] solves the PLF problem only in one iteration using the input variable statistical moments. The two values obtained from the input variable pdf are sufficient to estimate the end voltage pdfs through statistical calculations. The method obtained adequate accuracy and high computational speeds as investigated by Gaunt and Sellick [25] on residential LV networks. The same method without alteration was implemented on MV systems by a group of Brazilian researchers[15]. It was concluded that the HB algorithm was less accurate than the MCS and deterministic methods, however it was faster. In the results achieved, the HB algorithm was seen to over-estimate voltage drops thus obtained lower nodal voltages than the MCS and a DFL method. However, the finding showed a promise in the calculation of voltage drop in MV systems using the HB algorithm.

Another analytical probabilistic method is the First Order Second Moment (FOSM) suggested by Wan [48]. This method is very similar to the HB method in that they both use first and second moments in the calculation of voltage drop. However, in the FOSM they use a second moment centred around the mean (variance) whereas in the HB method a central (zeroed) second moment is used

In a similar fashion, Celli *et al.* [23] utilised the mean and variance of the customer loads and power generation from DGs to compute the same statistical parameters for the consumer voltage in MV networks. In their work, they employed linearization around the operation point (instant of maximum demand) in order to omit the problem of non-linearity. The major difference between this method and the HB algorithm is the method of load modelling used. Celli *et al.* based their work on normally distributed inputs whereas the Beta pdf is used with the HB algorithm [23]. However, both methods closely mirror the FOSM method discussed earlier. Celli *et al.* also utilised a heuristic algorithm to optimise the design solution for minimal losses and overall cost. This algorithm is an iterated routine that eventually stops if the solution ceases to improve. Overall, the findings proved the supremacy of PLF methods over DLF for MV distribution network design. Celli *et al.* also reiterated the necessity of new tools better suited for the modern power system faced with increased DG penetration. This was motivated by the evident ineffectiveness and unreliability of deterministic approaches on uncertainty-filled systems. The method presented has great computational speed and accuracy but it is restricted to normal distributed loads. According to the authors, non-normal distributions would increase computational time dramatically and make the method unfeasible.

The main concerns about analytical methods, apart from the complicated mathematical computation, include the requirement of mathematical assumptions such as linearization of equations and independence between input variables, which leads to inaccurate results [43].

2.7. Design risk in network planning and design

The concept of design risk is a measure of how uncertain the outcomes of a designed system are. PLF methods such as the HB algorithm apply the concept of risk in the form of statistical confidence intervals on the output pdf of a desired parameter (consumer voltage). Confidence intervals are a reciprocal to design risk. They denote the extent or interval to which the value of a random variable described by a probability density functions is certain. To explain this simply, a 90% confidence interval is interpreted as a 10% design risk. In power systems, risk has impacts on network planning and design. High risk (low confidence interval) indices imply an unreliable design with a higher probability of violation of permissible voltage values at the consumer end. Conversely, a low risk index (high confidence interval) yields a safer design but might result in a costly over-designed system. A careful choice of the design risk is therefore an important task in distribution network design.

Most probabilistic designs apply an uncertainty factor or design risk of 10% (Confidence interval of 90%). Stated simply, this means that when the actual load reaches its design level, the designer is 90 % confident that all of the consumers will receive a voltage within the statutory limits [2]. The representation of this on consumer voltage profiles for passive and active networks is however different. In passive networks, there is a major concern on voltage drop. This means that the design's objective is to make sure that the majority (90%) of the customers have voltages greater than the minimum permissible voltage, $P(V_i > V_{min}) = 0.9$. For active networks, a 10% risk is reflected by the majority having voltages less than the maximum permissible voltage, $P(V_i > V_{max}) = 0.9$. In statistics the confidence interval is however described by the statistic,

$$P(V_i < V_x) = CI\% \quad (2.4)$$

where: V_i *is a variable on the distribution,*

V_x *is the percentile voltage at the confidence level CI*

This means that for passive networks, the percentile voltage that correlates to a 90% design confidence (10% risk) is obtained by the computation of the percentile voltage at 10% confidence level (in MATLAB) as shown below.

$$P(V_i < V_x) = 1 - P(V_i > V_x) \quad (2.5)$$

$$P(V_i < V_x) = 1 - 0.9 = 0.1 \quad (2.6)$$

This does not mean that the risk is now 90%, it is only used for the extraction of percentile voltages from statistical packages such as MATLAB or EXCEL. For active feeders, no change is effected since the objective statistic $P(V_i < V_x)$ is the same as the MATLAB description of confidence interval. Fig. 2.1 and Table 2.4 below illustrate this.

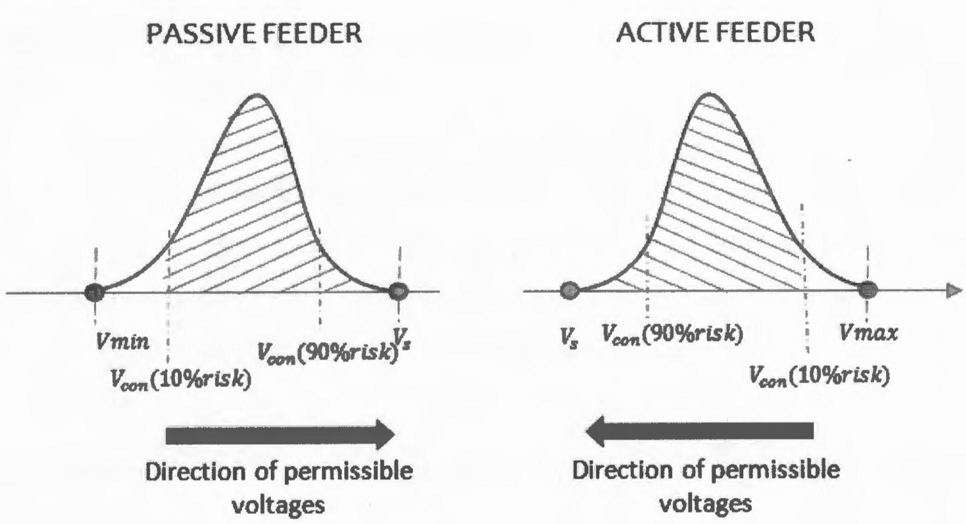

Figure 2.1: Design risk and confidence in statistical voltage calculations

Table 2-4: Risk and Confidence levels in Statistical Voltage Calculations

Feeder Type	Risk	$P(V < V_{con}\%)$ MATLAB Confidence Level	$P(V > V_{con}\%)$ Design Confidence
Passive	10%	10%	90%
	90%	90%	10%
Active	10%	90%	90%
	90%	10%	10%

2.8. Concluding Remarks

The literature review undertaken in this chapter has resulted in the following conclusions and study projections:

- Medium voltage distribution networks have substantially higher reactance than low voltage networks. The network model for an LV network which assumes negligible reactance is therefore inapplicable. It is therefore necessary to investigate the effects of reactance on the computation of voltage drop so as to conclude whether it can be ignored or not.
- Modelling of MV loads has been done mostly with normal distributions. However, since part of the load in MV networks are MV/LV transformers supplying residential networks, the assumption of Beta distributed loads can be carried over to MV networks.
- The modelling of generators as negative loads is an acceptable design strategy for DGs connected to MV networks.
- MV load composition is made up of directly connected loads and MV/LV transformers supplying residential areas. The total load is therefore in most cases of non-unity power factor. However, the MV/LV transformers are still assumed to be loads at unity power factor. The differences in load composition are expected to affect voltage drop calculations. Hence, the effect of power factor in MV feeder sizing should thus be investigated.
- Voltage regulation through shunt capacitors is a common practice in medium voltage networks. The effects of these network elements on the computation of voltage drop are worth investigating.

The HB algorithm can be extended to MV networks for computation of voltage drop if modifications are done to reflect the differences between the network topologies and characteristics. Therefore, a necessity to look further into the formulation of the HB algorithm arises. This is essential in establishing a firm understanding of the formulation then creating capacity to modify the application of the algorithm to suit MV networks. This forms the basis of the next chapter.

Chapter 3

3. THE HERMAN BETA ALGORITHM, A VOLTAGE DROP COMPUTATION TOOL IN POWER SYSTEMS

This chapter involves the description of the Herman Beta algorithm as a method for voltage drop computation in power systems. Its application to LV systems forms the foundation of this chapter. Following this, an analysis of the MV network topology is performed and the differences in network parameters from those of the LV network noted. A sensitivity analysis on the different parameters is conducted to establish the need for modification.

3.1. Overview of the Herman Beta Analytical Method

Power flow computation remains an important aspect of power systems analysis and design. Inaccuracy and inefficiency cannot be freely tolerated in power system network as design parameters are directly linked to the overall system cost, the magnitude of losses in the network, power system reliability and quality of supply. To ensure a good index of power quality of supply, the consumer voltage at any part of the power system has to be within a stipulated margin as directed by the national regulations and standards for electricity distribution. This implies that an accurate voltage calculation on the network is of essence. Accuracy is usually enough if the power system is small and if the outcome of results is not time constrained. However, in larger power systems, voltage analysis becomes a huge computational burden that can take too long especially in cases where results are required for immediate network decisions e.g. in smart power systems. As a result, there is a need for fast and accurate means of voltage computation in power systems.

The Herman Beta algorithm is a proven fast and accurate analytical probabilistic approach to voltage drop calculation in power systems specifically for low voltage networks. It can be thought of as a transform that takes beta distributed load currents as inputs mapping them into beta distributed output voltages. The nature of the inputs is such as to accommodate stochasticity in customer load currents during the instant of maximum demand. The algorithm has been proven to be an effective tool and was adopted nationally in South Africa as the only recommended and accepted means of voltage drop computation in LV networks. It has been successfully applied to single phase, bi-phase and 3-phase networks [17], [27].

3.2. Key assumptions in the HB algorithm

The Herman-Beta algorithm like most mathematical theories and formulae has a set of assumptions and/or simplifications. This is a very important part of the algorithm as it describes the domain of applicability of the algorithm beyond which the performance of the algorithm is not guaranteed. The assumptions made in the HB algorithm for LV networks are as follows:

1. Maximum voltage drop occurs during the interval of maximum demand.
2. The loads are represented as currents at unity power factor – valid for residential loads near interval of maximum demand.
3. The load currents can be represented as a statistic which is distributed by a Beta probability density function.
4. The customer load currents are considered as independent statistical variables – valid if the statistic is considered at a single time interval.
5. In the network model of the LV system, the feeder impedance is regarded as resistive with negligible reactance.

The above listed assumptions are adequate for application to passive networks. For active networks, the extended algorithm incorporates the following addendum of assumptions:

1. Generators can be modelled as negative loads.
2. The generation by the DGs can be modelled as beta distributed currents injecting into the power system through nodes along the feeder.
3. The generation units are connected to the feeder at nodes separate from the normal loads (current drawing loads) so as to keep the direction of current unambiguous.

3.3. Outline of the derivation of the HB algorithm

The HB algorithm uses a concept of statistical moments to calculate voltage drop non-iteratively for a system with probabilistic inputs. This computational approach utilises the first and second raw moments (about zero) of the current statistic in its calculations [1].

NB. The derivation given here is only an outline which reveals some of the important parts of the algorithm that are essential in the successful extension of the approach to MV networks. The full algorithm is given in Appendix A, which is a corrected list of equations different from the ones presented in the NRS034-2 document.

In the analysis that follows, a single node feeder is used for simplification purposes. The superposition theorem is applied to extend the voltage equations to successive nodes on the feeder. A 3-phase 4 wire network configuration is used to discuss the application of the HB method in feeder voltage calculations. The application to bi-phase systems will not be covered in this text since this research is focused on 3-phase systems.

3.3.1. Network Configurations

A network configuration dictates the equations used for voltage drop calculation in a power system. It is therefore crucial to get the network model right in any voltage analysis exercise otherwise the whole calculation will be meaningless. As mentioned before, the feeder impedance for most LV networks can be assumed to be resistive owing to the small reactance associated with them. The network model for a 3-phase system as given in Figure 3.1 below is therefore acceptable.

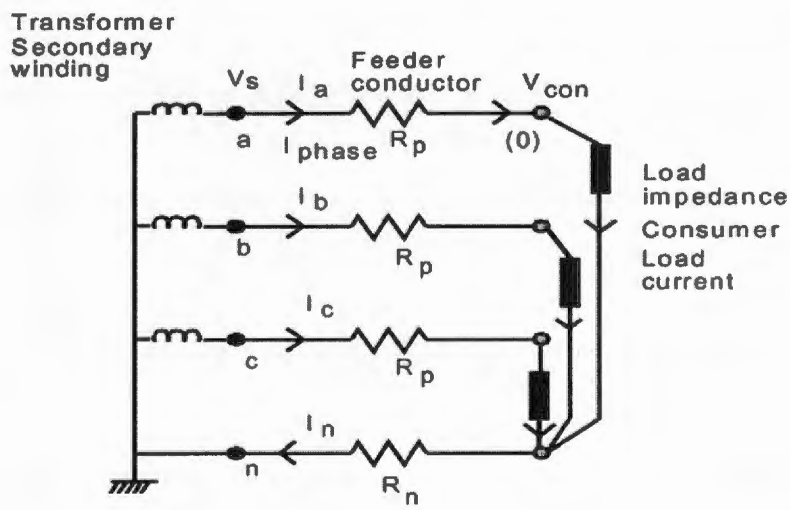

Figure 3.1: Network model for 3 a phase LV feeder [1]

In the diagram above, the secondary side of an MV/LV transformer is connected to an LV feeder with phase conductors of resistance R_p in each phase and a common neutral conductor with resistance R_n. The resistance of the neutral conductor is directly proportional to that of the phase through a network constant k. The load impedance shown on the diagram is a summated value for all consumers connected at that particular node in that phase. The load current, which is the same as the phase current, represents the total drawn current at that node as a result of the connected consumers.

Customer Load Currents

Since the load demand is of statistical nature, individual load currents are considered as randomly drawn variates drawn from a population modelled by a beta distribution function with parameters α and β. For each individual load connected at node i, current at any instant is represented as a product of the random variable, Y_i in the inclusive range (0, 1) and a scalar quantity, C, which is usually in the form of the circuit breaker size or higher. The phase current at that node is then a summation of the individual load currents as demonstrated mathematically below.

$$\textit{individual customer current:} \quad Y_i \in [0,1] \tag{3.1}$$

$$\textit{phase current:} \quad I_{a(b,c)} = C.\sum_{i=1}^{m_{a(b,c)}} Y_i \tag{3.2}$$

where: $m_{a(b,c)}$ *denotes the total connected consumers to phase A, B and C respectively*

3.3.2. Circuit analysis and voltage equations

The formulations presented in this section refer to the red phase. Where phase identifiers *a, b* and *c* are not explicitly given, the variable or quantity in question refers to the red phase.

A circuit analysis on the network model as given in Figure 3.1 above results in the following voltage drop equations:

$$dV_i = \boldsymbol{I_a} R_p + \boldsymbol{I_n} R_n \tag{3.3}$$

Since the neutral current is a sum of the phase currents, equation 3.3 can be written as follows:

$$dV_i = \boldsymbol{I_a} R_p + (\boldsymbol{I_a} + \boldsymbol{I_b} + \boldsymbol{I_c}).R_n \tag{3.4}$$

In the equations 3.3 and 3.4, the boldface characters represent phasor quantities whilst ordinary text represents scalar quantities. Considering the red phase (A) as the reference phase, the blue (B) and white phases (C) are angularly displaced 120 ^{0} to each side of the reference. The phasor currents $\boldsymbol{I_b}$ and $\boldsymbol{I_c}$ can then be resolved into their respective quadrature components as illustrated below.

$$\boldsymbol{I_a} = I_a \angle 0° = I_a + j0 \tag{3.5}$$

$$\boldsymbol{I_b} = I_b \angle 120° = I_b\left(-\frac{1}{2} + j\frac{\sqrt{3}}{2}\right) \tag{3.6}$$

$$\boldsymbol{I_c} = I_c \angle -120° = I_c\left(-\frac{1}{2} - j\frac{\sqrt{3}}{2}\right) \tag{3.7}$$

The voltage drop equation then becomes a complex quantity given by:

$$dV_i = dV_{i-R} + jdVI_{i-I} \tag{3.8}$$

$$\textit{where:} \quad dV_{i-R} = I_a R_p(1+k) - \frac{1}{2}(I_b + I_c).k.R_p \tag{3.9}$$

$$dV_{i-I} = \frac{\sqrt{3}}{2}(I_b - I_c).k.R_p \tag{3.10}$$

It is from equations 3.9 and 3.10 that the HB algorithm is formulated. Since phase currents are a sum of random variables drawn from a beta probability density function, it can then be shown that the voltage drop in each phase is also beta distributed and so is the consumer voltage V_{con}. The derivation of the consumer voltage pdf parameters forms the principal objective in the calculations in the HB algorithm. The consumer voltage, which is beta distributed with parameters α^* *and* β^*, can be expressed in terms of the voltage drop dV_i and the supply voltage V_S through the following equations.

$$V_{con} = V_s - dV_i \tag{3.11}$$

$$V_{con} = \sqrt{(V_s - dV_{i-R})^2 + {dV_{i-I}}^2} \tag{3.12}$$

The exponential degrees on the voltage drop variables give an indication on the order of statistical moments required in the computation of consumer voltage. In this case its 2nd order, therefore 1st order and 2nd order moments are used in the HB algorithm. Before the discussion delves into the calculation of moments, the voltage calculations presented up to this point are extended to cover a multiple nodes on the feeder.

3.3.3. The principle of Superposition

In order to extend the voltage calculations, initially derived for a single node, to an N-node feeder, the principle of superposition is applied. In the calculation of voltage drop due to a node i, a summated value of the resistances of the preceding feeder sections and the phase current due to the consumers connected at that node are used. The consumer voltage at the end of the feeder is given by the difference between the supply voltage and the summated voltage drops due to the individual nodes on the feeder. For voltage drops, subscript $'t'$ is adopted to represent summated quantities whilst $'i'$continues to denote singular, nodal quantities. For conductor resistance, the variables R_n and R_t now imply the total resistances on the whole feeder; which is a summation of inter-nodal resistances denoted by R_s and R_t respectively.

$$R_p = \sum_{i=1}^{N} R_s \qquad , R_n = \sum_{i=1}^{N} R_t \tag{3.13}$$

$$dV_{t-R} = \sum_{i=1}^{N} dV_{i-R} \qquad , dV_{t-I} = \sum_{i=1}^{N} dV_{i-I} \tag{3.14}$$

Using the new variables for voltage drop as given above, the consumer voltage at the Nth node is given by the expression,

$$V_{con} = \sqrt{(V_s - dV_{t-R})^2 + {dV_{t-I}}^2}\,. \tag{3.15}$$

3.3.4. Calculation of Statistical Moments

In order to solve for the unknown consumer voltage beta parameters α* and β*, two or more distinct equations involving the unknown terms are required. The HB algorithm uses equations 3.16 and 3.17 describing the first two statistical moments of the consumer voltage to solve for these parameters.

$$E(V_{con}) = \frac{\alpha^*}{\alpha^*+\beta^*} \tag{3.16}$$

$$E(V_{con}^2) = \frac{\alpha^*(\alpha^*+1)}{(\alpha^*+\beta^*)(\alpha^*+\beta^*+1)} \tag{3.17}$$

$$where, \quad V_{con}^2 = (V_s - dV_{t-R})^2 + {dV_{t-I}}^2$$

The Taylor's approximation is used to simplify the equation for V_{con} so as to be able to obtain the expected value of the expression. The equation is firstly written in Taylor's argument form as below.

$$V_{con} = (V_s^2 - 2.V_s.dV_{t-R} + dV_{t-R}^2 + dV_{t-I}^2)^{1/2} \tag{3.18}$$

$$\frac{V_{con}}{V_s} = \left[1 + \left(\frac{dV_{t-R}^2+dV_{t-I}^2}{V_s^2} - 2\frac{dV_{t-R}}{V_s}\right)\right]^{1/2} \tag{3.19}$$

Using the Taylor expansion up to the 2[nd] order term, the following estimation to consumer voltage is obtained.

$$V_{con} = V_s - dV_{t-R} + \frac{1}{2}\left(\frac{dV_{t-I}^2}{V_S}\right) \tag{3.20}$$

The first and second statistical moments of the consumer voltage are therefore given by:

$$E(V_{con}) = V_s - E(dV_{t-R}) + \frac{1}{2}\frac{E(dV_{t-I}^2)}{V_S} \tag{3.21}$$

$$E(V_{con}^2) = V_s^2 - 2.V_s.E(dV_{t-R}) + E(dV_{t-R}^2) + E(dV_{t-I}^2) \tag{3.22}$$

$$where: \quad E(dV_{t-R}) = \sum_{i=1}^{N} E(dV_{i-R}) \quad , E(dV_{t-I}) = \sum_{i=1}^{N} E(dV_{i-I})$$

$$E(dV_{t-R}^2) = \sum_{i=1}^{N} E(dV_{i-R})^2 + \sum_{m=1}^{N}\sum_{\substack{n=1\\n\neq m}}^{N} E(dV_{m-R})E(dV_{n-R})$$

$$E(dV_{t-I}^2) = \sum_{i=1}^{N} E(dV_{i-I})^2 + \sum_{m=1}^{N}\sum_{\substack{n=1\\n\neq m}}^{N} E(dV_{m-I})E(dV_{n-I})$$

The equations listed above are also dependent on expected values of nodal voltages, both imaginary and real components. These are obtained by taking statistical moments of the voltage drop equations given in section 3.3.2. The derivation will not be covered here as it is quite a tedious task. The expressions for the expected values are rather given.

$$E(dV_{i-R}) = C_{1i}.R_p.C.G \tag{3.23}$$

$$E(dV_{i-R}^2) = R_p^2C^2(C_{2i}H + C_{3i}G^2) \tag{3.24}$$

$$E(dV_{i-I}^2) = R_p^2C^2(C_{4i}H + C_{5i}G^2) \tag{3.25}$$

$$E(dV_{i-R}) = C_{6i}.R_p.C.G \tag{3.26}$$

where:

$$G = E(Y) = C\frac{\alpha}{\alpha+\beta}$$

$$H = E(Y^2) = C^2\frac{\alpha(\alpha+1)}{(\alpha+\beta)(\alpha+\beta+1)}$$

$C_{1i} - C_{6i}$ *are network constants*

Y – *consumer current random variable*

The constants C_{1i}-C_{6i} are network constants that depend on the total number of customers connected to the phases and the feeder resistances. The expressions for each of these constants are detailed in Appendix A.

3.3.5. Scaling of consumer voltage for beta fit

In order to restrict voltage outcomes in the required range for beta distribution fitting, the worst case voltages (minimum and maximum) are used to scale voltages into the range (0, 1). The calculation of these voltages is therefore important and is shown here.

Maximum and minimum consumer voltages

In the discussion that follows, identifiers, *'max'* and *'min'* are used to denote variables associated with the calculation of maximum and minimum nodal voltages respectively.

1. **Maximum Voltage**

The maximum voltage in a given phase occurs under the condition of minimal loading in that phase and maximum loading in the other two phases. The HB method uses a worst case design approach to the calculation of these values. A zero load current is regarded as minimum loading whilst a load current equal to the circuit breaker rating is taken as the maximum. Using the nodal voltage drop equations, the voltage drops used in the calculation of the maximum voltage $Vmax_i$ are:

$$dVmax_{i-R} = -\frac{1}{2}k.R_p.C.(m_{bi} + m_{ci}) \tag{3.27}$$

$$dVmax_{i-I} = \frac{\sqrt{3}}{2}k.R_p.C.(m_{bi} - m_{ci}) \tag{3.28}$$

$$where: \qquad m_{a(b,c)}.C.E(Y) = I_{a(b,c)}$$

$$m_{a(b,c)} - \textit{customers connected in that phase}$$

***Note: the quantities $dVmax_{i-R}$ and $dVmax_{i-I}$ are actually minimum voltage drops. The notation 'max' is used so as to identify the variables with the calculation of maximum nodal voltage.**

The resultant consumer voltage is then a vector difference between the sending end voltage, V_s and the voltage drops calculated above.

$$Vmax_i = \sqrt{(V_s - dVmax_{i-R})^2 + dVmax_{i-I}{}^2} \qquad (3.29)$$

2. **Minimum Voltage**

When a phase is maximally loaded whilst the other phases are minimally loaded, the voltage drop in that phase is high and therefore its end consumer voltage is minimum. Under the worst case design approach, the following expressions for minimum consumer voltage are arrived at:

$$Vmin_i = \sqrt{(V_s - dVmin_{i-R})^2 + dVmin_{i-I}{}^2} \qquad (3.30)$$

$$where: \qquad dVmin_{i-R} = C_b R_p m_{ai}(1 + k)$$

$$dVmin_{i-I} = 0$$

Calculation of scaled consumer voltages

In order to obtain consumer voltages within the permissible range (0, 1), the minimum and maximum voltage values given in the preceding section are used to scale the expected values of V_{con} . The resulting equations are denoted with an asterisk in order to differentiate them from the unscaled values.

$$E(V^*_{con}) = \frac{E(V_{con}) - V_{min}}{V_{max} - V_{min}} = \frac{\alpha^*}{\alpha^* + \beta^*} \qquad (3.31)$$

$$E(V^{*2}_{con}) = \frac{E(V^2_{con}) - 2.V_{min}.E(V_{con}) + V^2_{min}}{(V_{max} - V_{min})^2} = \frac{\alpha^*(\alpha^* + 1)}{(\alpha^* + \beta^*)(\alpha^* + \beta^* + 1)} \qquad (3.32)$$

Calculation of consumer voltage beta parameters

Equations 3.31 and 3.32 describing the statistical moments of the scaled consumer voltage can be solved simultaneously for the beta parameters. The solution to these equations is given below.

$$\alpha^* = \frac{E(V^{*2}_{con}) - E(V^*_{con})}{E(V^*_{con}) - \frac{E(V^{*2}_{con})}{E(V^*_{con})}} \qquad \beta^* = \frac{\alpha^*}{E(V^*_{con})} - \alpha^* \qquad (3.33)$$

Design risk

The risk incorporated in the network design for LV systems using the HB algorithm is usually 10%. This correlated to a 90% confidence interval on the voltage pdf. Generally, the consumer voltage at a design risk p%, or conversely within a q% confidence interval (where q=100-p) is given by an inverse beta function.

$$V^*_{con_{q\%}} = betainv\left(\left(\frac{p}{100}\right), \alpha^*, \beta^*\right) \tag{3.34}$$

Rescaling of consumer voltage to actual network values

The scaling of voltage is done so as to obtain values within the acceptable range for fitting the data into the beta distribution function. The actual voltages values are obtained through a reverse scaling process that involves a rearrangement of the scaling equation.

$$V_{con} = V^*_{con}(V_{max} - V_{min}) + V_{min} \tag{3.35}$$

In order to calculate the consumer voltage at the given risk factor, the above equation is used with $V^*_{con_{q\%}}$ in place of V^*_{con}. Other percentile voltage values can be calculated in the same fashion.

3.3.6. Extension of the HB algorithm to incorporate DG connections

The extension of the HB algorithm to LV feeders with DG is based on the modelling of DG as a 'negative load'. The feeder configuration of an active feeder is the same as the one in Fig. 3.1 only with added generator nodes separated from load nodes by little distances. This is done so as to maintain algebraic identity which makes analysis easier. With this consideration, the same algorithm for loads is used to calculate voltage drops at generator nodes only with slight modifications. In order to accommodate the effects on voltage calculations the current injection by DG causes, the following modifications are done.

1. Generators connected to a node are represented as 'negative customers'.
2. The quantity of generators connected to a node is specified as a negative quantity.
3. The variables m_{ai}, m_{bi} *and* m_{ci} ,which denote the number of customers connected to phase a, b and c at node i respectively, are replaced with their absolute values for the calculation of constants C_{2i} to C_{5i}.
4. The calculation of the percentile voltages using the beta inverse equation is adjusted to the following:

$$V^*_{con_{q\%}} = betainv\left(\left(\frac{p}{100}\right), |\alpha^*|, |\beta^*|\right) \tag{3.37}$$

5. Since generators have a reverse effect on voltages to that caused by loads, high generator currents are likely to cause over voltages unlike under-voltages in the case of loads. This

means that DG has reverse effects on the maximum and minimum feeder voltages. This effect is accommodated in the adjusted equations given below.

$$dVmin_{i-R} = -\frac{1}{2}k.R_pC_b(m_{bi} + m_{ci}) \quad (3.38)$$

$$dVmin_{i-I} = \frac{\sqrt{3}}{2}k.R_pC_b(m_{bi} - m_{ci}) \quad (3.39)$$

$$dVmin_{i-R} = C_bR_pm_{ai}(1 + k) \quad (3.40)$$

NB. A guideline to the use of the HB algorithm in voltage calculations on passive and active feeders is given in Appendix A. The documentation properly lays out the step by step sequence taken in the calculation of feeder voltages, along with the equations used in each step.

3.4. Analysis of 3-phase MV network models

The description of the HB algorithm given in the preceding sections applies to LV systems. Since LV and MV systems have different network models, the network parameters should also be different. The section that follows involves a circuit analysis of an MV network model resulting in the determination of the related voltage drop equations.

Network Configuration

Medium voltage network unlike the low voltage have higher feeder X/R ratios. The result is that reactance elements cannot be ignored in the network model. Consequently, phase and neutral impedance quantities become complex variables with real, resistive and an imaginary, reactive component. Figure 3.2 below shows a single node, 3-phase 4-wire MV network model used in the analysis in this section.

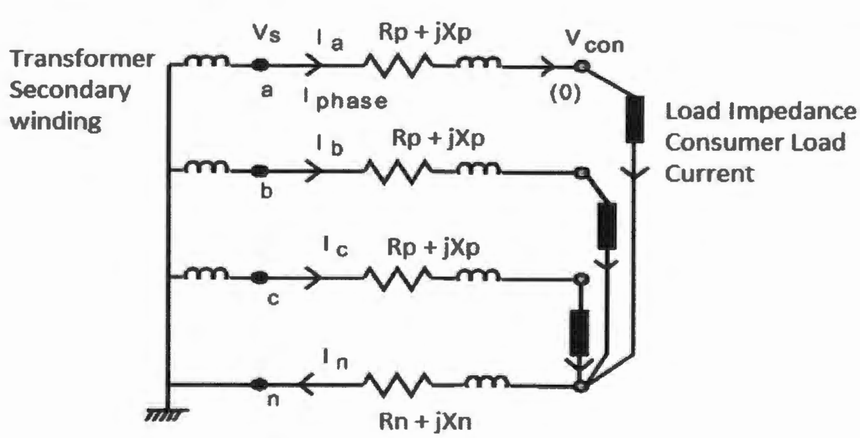

Figure 3.2: Network model for a 3 phase MV feeder

3.4.1. Effect of feeder reactance on voltage equations

The inclusion of reactance elements in the feeder network model results in changes in the voltage equations for the circuit as a new term Xp is introduced. The new equations with the inclusion of this term are given below.

$$dV_i = I_a Z_p + I_n Z_n \qquad where\ Z_{p(n)} = R_{p(n)} + jX_{p(n)} \tag{3.41}$$

$$dV_{i-R} = I_a R_p(1+k) - \frac{1}{2}(I_b + I_c).k.R_p - \frac{\sqrt{3}}{2}(I_b - I_c).k.X_p \tag{3.42}$$

$$dV_{i-R} = I_a X_p(1+k) - \frac{1}{2}(I_b + I_c).k.X_p + \frac{\sqrt{3}}{2}(I_b - I_c).k.R_p \tag{3.43}$$

In the network model in Figure 3.2, it is assumed that the ratio k between the phase and neutral conductor resistance is the same as that between the reactive elements. The new definition of k is extended to reactive elements in this way:

$$k = \frac{|Z_p|}{|Z_n|} = \frac{R_p}{R_n} = \frac{X_p}{X_n} \tag{3.44}$$

The consumer voltage at the end of the feeder, which is a function of the modified voltage drop equations, is found using equation 3.45.

$$V_{con} = \sqrt{(V_s - dVR_i)^2 + dVI_i^2}. \tag{3.45}$$

3.4.2. Effect of non-unity load power factor on voltage equations

One of the underlying assumptions in the application of the Herman-Beta algorithm on LV feeders is that of unity power factor loads during the instant of maximum demand. This is consistent with most LV networks but cannot be extended to MV networks as loads are usually characterised by lagging power factors which are non-unity. In the literature engaged with, both real and reactive power elements are considered in the computation of voltage drop in MV systems[7], [28], [32], [54]. Stojanovic [54] and Zio [7] , in their work on Medium Voltage networks, both agree on a close to unity power factor on loads represented by MV/LV transformers supplying LV systems. However, the other load component in MV systems, directly connected customers, is often of non-unity power factor. The results of this are complex load currents unlike the real variables encountered in LV networks.

$$\boldsymbol{I}_{a(b,c)} = I_{a(b,c)-R} + jI_{a(b,c)-I} \tag{3.46}$$

where: $\quad -R$ *and* $-I$ *denote the real and imaginary components*

If the new complex current variables are used in place of the real phase currents in the voltage drop equations derived in the preceding section, the following equations result.

$$dV_{i-R} = R_p\left[I_{a-R}(1+k) - 0.5k(I_{b-R}+I_{c-R}) + \frac{\sqrt{3}}{2}k(I_{b-I}-I_{c-I})\right]$$

$$+X_p\left[I_{a-I}(1+k) - 0.5k(I_{b-I}+I_{c-I}) - \frac{\sqrt{3}}{2}k(I_{b-R}-I_{c-R})\right] \quad (3.47)$$

$$dV_{i-I} = X_p\left[I_{a-R}(1+k) - 0.5k(I_{b-R}+I_{c-R}) + \frac{\sqrt{3}}{2}k(I_{b-I}-I_{c-I})\right]$$

$$-R_p\left[I_{a-I}(1+k) - 0.5k(I_{b-I}+I_{c-I}) - \frac{\sqrt{3}}{2}k(I_{b-R}-I_{c-R})\right] \quad (3.48)$$

The characteristic power factor of the connected loads in the calculation above is given by cos $\emptyset$ where the power angle is calculated as follows:

$$\emptyset = \arctan\left(\frac{I_{a-I}}{I_{a-R}}\right) \quad (3.49)$$

3.5. Sensitivity of consumer voltage to network parameters

The preceding two sections highlighted the differences in network parameters between LV and MV networks. The higher X/R ratios and non-unity power factors loads in MV networks introduce imaginary variables for feeder impedance and load current. The equations for voltage drop have shown changes as a result of these new terms. Hence, it is essential to quantify the resulting effects on voltage calculations and conclude whether the compensation of the new terms is necessary.

3.5.1. Variation of consumer voltage with feeder XR ratio

A Monte-Carlo simulation with an accurate MV network model (inclusion of line reactance and power factor effects) is used to investigate the variation of consumer voltage, Vcon, with increasing X/R ratios. This investigation lays a good foundation to the assessment of the suitability of the HB method for voltage calculations on feeders with significant feeder reactance (high X/R ratios).

Figure 3.3 shows the outcome of a Monte-Carlo simulation for a feeder with connected loads of lagging power factor (pf = 0.8) for different cases of X/R ratios. Simulation shows a gradual decrease in the consumer voltage as the X/R ratio increases. A significant deviation from the result of a purely resistive network model (in red bold trace) is seen with network models of higher X/R ratios. The result is supported by the theoretical expectation of a decrease in consumer voltage as the voltage drop across the reactance element increases proportionally to its magnitude.

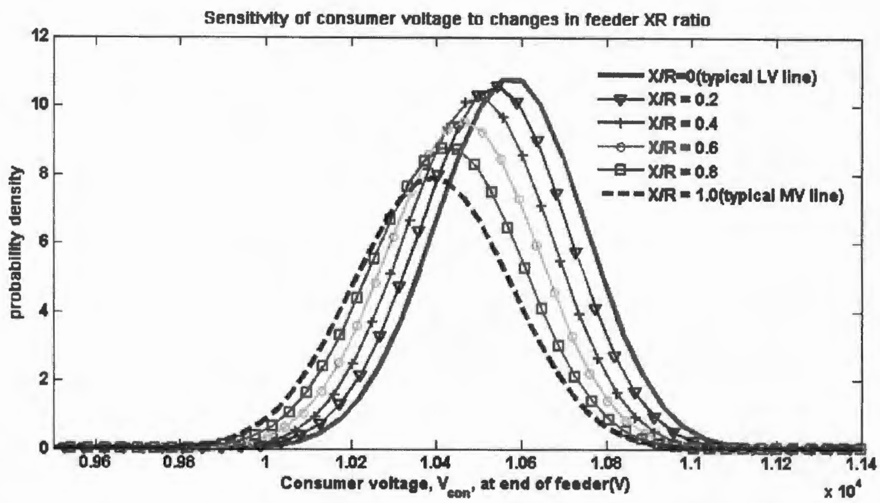

Figure 3.3: Variation of consumer voltage with feeder X/R ratios

NB. The plot given above is a beta pdf with a scaled x-axis. It should be noted that beta distribution functions usually obtain probability densities greater than 1 unlike other distributions like the normal. However, the integral over the distribution does give the expected summated probability of 1. Throughout the report, beta distribution plots will continually be used to represent voltage spreads.

Another plot, Fig. 3.4, shows the changes in voltage drop as a result of increased X/R ratios. It can be noted that voltage drop increases with X/R ratio. In this case, a change of voltage drop from 5.9% to 7.7% is observed between the cases of zero and unity X/R ratios.

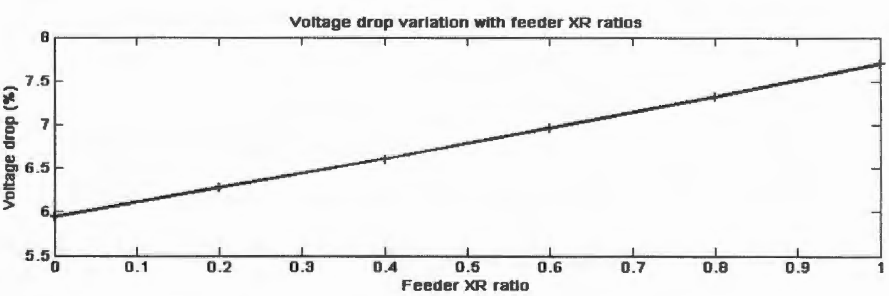

Figure 3.4: Variation of voltage drop with X/R ratios

The non-inclusion of reactance in the voltage calculation would in this case cause an error equivalent to a 2% voltage drop. This error size is unacceptable since the rejection criterion for consumer voltages is 5% voltage drop.

3.5.2. Variation of consumer voltage with load power factor

In a similar investigation approach to that done in the preceding section, the variation of consumer voltage with load power factor is explored. In this case, the feeder X/R ratio is kept constant whilst the

power factor of the connected loads is varied incrementally from 0.8 to unity. Result from the Monte-Carlo Simulation resulted in the plots given in Fig. 3.5 and 3.6 given below.

Plots in Fig. 3.5 reveal a substantial drop in consumer voltages with power factor. This finding agrees with theoretical expectations of lagging power factors to cause increased current flow in power networks resulting in increased voltage drops along feeders. If the assumption of unity power factor is applied here, an over estimation of voltages would result. This is illustrated in the given plots in Fig. 3.5; there are significant differences in the distribution and range of voltages between the unity power factor case (red continuous, bold trace) and the deviant cases of power factor.

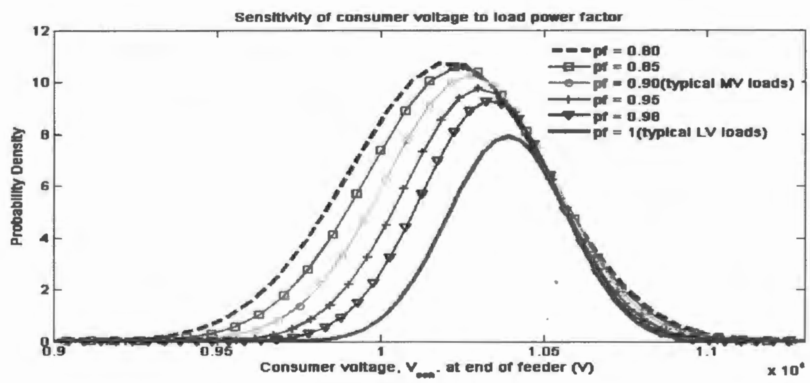

Figure 3.5: Variation of consumer voltage with load power factor

In order to quantify the error that may result with the assumption of load unity power factor in voltage calculations on MV feeders, a plot of load power factors and the associated voltage drops is made. In this plot, given in Fig. 3.6, voltage drop is seen to decrease with increase in power factor. The differences in the values of voltage drop when compared to the unity power factor case increase as power factor values get increasingly lagging.

If the HB algorithm without adjustments is applied in this case, the differences noted in the values of voltage drop between the variant cases of power factor and that of unity are translated into voltage error.

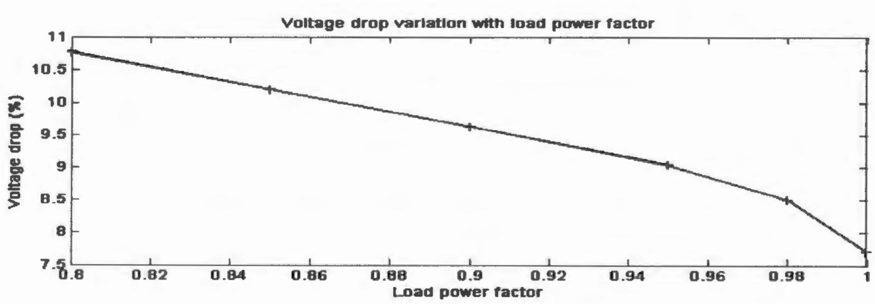

Figure 3.6: Variation of consumer voltage drop with power factor

For power factors closer to unity, the relative error (expressed as a percentage of the nominal voltage) is less than that noted at lower power factors. At a power factor of 0.8, the voltage drop error is about 3% if the assumption of unity power factor were applied in the voltage calculation method. This result points to the inaccuracy of this assumption when applied to MV feeders.

3.6. Concluding Remarks

The presentation of the Herman-Beta algorithm and the contrast between the LV and MV networks done in this chapter shed light on the following:

1. There is a distinct difference in the network parameters for LV and MV networks. MV networks, as compared to LV networks, have more significant feeder reactance values and connected loads are usually of lagging power factor.
2. Differences in parameters appear in feeder voltage equations for MV. Sensitivity tests have shown a notable variation of consumer voltage with these parameters.
3. From the results of sensitivity tests, it is concluded that there is need to compensate for both non-unity power factors and non-zero feeder X/R ratios in voltage calculations on MV feeders using the HB algorithm.

Before the investigations on the approaches for the compensation of sensitive parameters is embarked on, it is important to first develop the necessary tools required for the task. This work forms the objective of the proceeding chapter.

Chapter 4

4. TOOLS FOR VOLTAGE DROP COMPUTATION AND ANALYSIS

The objective of this chapter is to develop the programming tools necessary for voltage computation and analysis in the scope of the project. The Herman-Beta algorithms for voltage calculation in passive and active LV feeders are translated into MATLAB code. Tests are subsequently done to check for errors in the code. The error-free software is then validated against the Monte-Carlo counterparts programs.

4.1. Programming Software

The programming platform used in this study is MATLAB, a product from MathWorks. MATLAB provides a high-level technical, numeric and scientific computing environment for algorithm development, data analysis and numeric computation, with ease of handling large matrices. MATLAB covers a lot of engineering fields in its range of applications and toolboxes. One application that we will take to our advantage is a statistical tool, the Probability Distribution Function Toolbox. With this toolbox and other related functions that involve probability distribution functions, we will be able to fit voltage arrays into intended distribution functions (Beta in our case) and perform analysis on the output pdfs. MATLAB also provides visualization through 2D and 3D pictorials. This will be essential in the validation of statistical methods through comparison.

Besides the provision of engineering tools that are highly useful in handling vectors and matrices, MATLAB is generally faster than most programming languages. It is object oriented and has graphical interfaces that are interactional allowing users to customize functions and nurture tools to their intended functionality. This is also the case with the Probability Distribution Function Toolbox.

The HB algorithm as presented in Chapter 3 is transferred into MATLAB code. Another program for voltage computation, the Monte Carlo method, is also developed and used to validate the HB algorithm. This common environment in MATLAB will allow meaningful comparisons between the two methods.

4.2. The Monte Carlo Simulation method

4.2.1. General Discussion

The Monte Carlo method is a powerful mathematical tool used for solving complex problems characterised by stochasticity, multiple input combinations and uncertainty. In power systems, the Monte Carlo Simulation (MCS) method has been widely used for power flow computation and system reliability analysis. In power flow computations, the MCS method uses a randomly sampled input variable in a deterministic computation to arrive at system output variables. This process is done iteratively such as to cover a wide range of possible inputs. In this way, the method can be used in probabilistic computations which have inputs described by probability distribution functions. The main attribute of the MCS method lies in the sampling of random numbers simulating variables in the pool of possible inputs. This means that a number y drawn randomly from a closed interval $[0,1]$ can be used to represent a random sample from a stochastic variable Y described by a particular probability density function.

Since the MCS method is literally an iterated deterministic calculation, it is usually more accurate than most probabilistic methods used for voltage calculations in power systems. However, the iterations make the method computationally rigorous and slow. For this cause, the MCS method is mainly used to validate other computational methods in Power System Analysis [24].

The correct and effective use of the MCS method is mainly governed by two aspects, namely,

1. Random variable sampling
2. Number of iterations

Random variable sampling

As previously mentioned, random number sampling is required to represent a possible input from the distribution function of the stochastic input variable. In programming, random number generators are mostly used for probabilistic sampling. These generators depend on seed values for initialisation. A seed value when used in iteration results in the same sequence of 'random' numbers. Therefore, to ensure equal chance on the randomly drawn numbers, the random generator function should be controlled so as not to repeat a seed value. In this work, a beta pdf customised random generator function, ***betarnd***, is used. This function is an appropriate tool as it ensures the sampling of random numbers with equal chance through the random, non-repeated use of seed values.

Number of iterations

Since the MCS is characterised by repetitive input variable sampling. The number of iterations done is a direct measure of the input sample size covered and therefore a measure of possible error in the calculation. The error in the results from a MCS is inversely proportional to the square of the iterations performed. This would mathematically mean that the greater the number of iterations the smaller the resultant error. However, performing a large number of iterations is computationally straining to machines and consequently results in a slow process. Besides these draw backs, it has also been found that the continual increase in iterations may sometimes not necessarily decrease the error in some cases. In this study, a compromise value of 15000 iterations is used. This value does not result in much computational strain and obtains an acceptable accuracy in calculations.

4.2.2. MCS algorithm as used in voltage computations

The following is a brief discussion on how the MCS is used in this work for voltage calculations. An in-detail discussion is given in Appendix B.

In the computation of voltage drop or conversely consumer voltage on distribution feeders using the MCS, the following steps are taken:

1. Using the betarnd function, a random number between 0 and 1 is drawn from a given probability distribution function describing the customer load currents. This number represents the fraction of the circuit breaker current that a consumer draws.
2. Using the sampled load current, voltage drop is calculated using appropriate electric circuit theory.
3. From the sending end voltage and the voltage drop in step (2), consumer voltage is calculated.
4. Steps 1-3 are iterated 15000 times; storing the voltage results in an array after an iteration run.
5. With the obtained voltage array, a beta pdf is plotted using a MATLAB function, *dfittool ()*.
6. On the voltage pdf, the required risk level, conversely a confidence interval on the output pdf is applied to get the percentile voltage.

The steps discussed above are translated into MATLAB code and the resulting MCS algorithm based on the passive network equations in Section 3.3.2 is denoted $MC_{p\text{-}LV}$. This software will be used to assess the accuracy of the HB method on voltage computations on passive networks. Adjustments to the voltage equations on which the MCS is based on will allow the extension of the algorithm to LV active networks and also to MV feeders.

4.3. Test Network Configuration and parameters

Network Topology

The network topology used in the series of tests in this study is that of a 3-phase 4-wire LV feeder. The feeder impedance is assumed to be purely resistive with no reactance element. The phase load impedance represents all the connected customers at a particular node. These loads are assumed to be drawing real power thus of unity power factor at the time of maximum demand. Fig 4.1 shows the network model used.

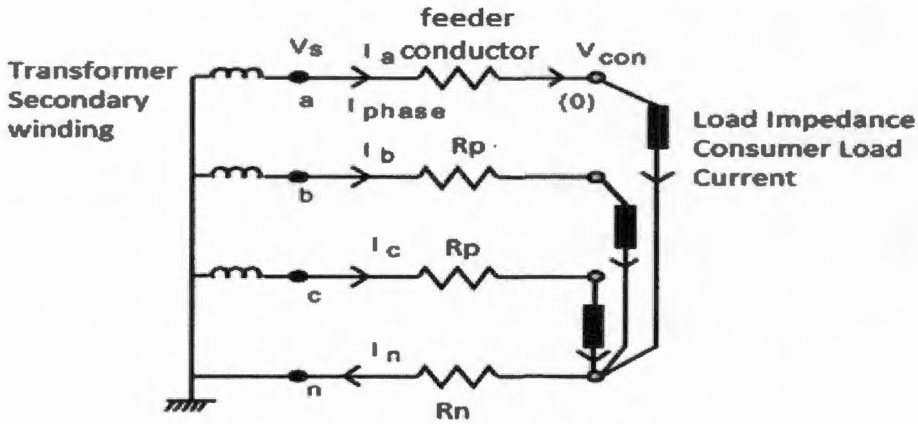

Figure 4.1: Feeder Network Model for LV systems [1]

The network equations on the model given are discussed in the preceding chapter. Both the MCS and the HB methods are formulated based on them. The input parameters to these equations are given in the section that follows.

Network Parameters

The network properties for the test network for LV feeders are given in Table 4.1.

Table 4-1: Network Parameters for Test Feeder

FEEDER PARAMETER	PARAMETER VALUE
Sending Voltage, V_s	230V
Number of nodes	2
Inter-nodal distance	200m
Load Current pdf parameters	α = 1.5
	β = 4.0
	C_b= 60 [circuit breaker size]
Temperature [^{0}C]	T_1= 20
	T_2= 40
Conductor type	Copper Conductor, 35mm^{2}Cu

A simplified model of the feeder as shown in Fig 4.2 can be used for illustration of power flows and the general layout of feeder connections.

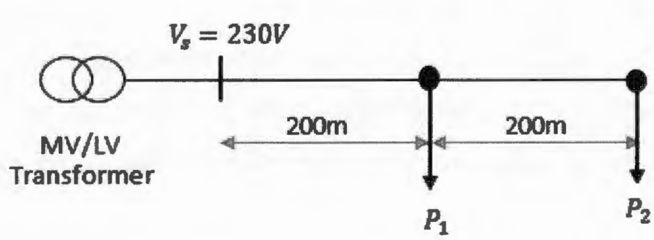

Figure 4.2: One line diagram for LV test network

In the tests conducted here and further in the report, various phase assignment methods will be used. In some tests, where consistent voltage drop calculation across the phases is to be verified, the balanced phase allocation denoted by *bal*xxx will be used. The *cosxxx* and the *cycxxx* methods are also used; mainly to demonstrate distinct calculation of feeder voltages under balanced and unbalanced load conditions. The effects of different connection types on feeder voltages are however not covered in this study.

Table 4.2 is a revisit of the already discussed (refer to Chapter 2) methods of phase assignment.

Table 4-2: Phase Connection Patterns

Phase assignment Method	Configuration
Balanced (Bal111)	Equal load (customer) assignment on phases
Cyclic (cyc)	R, W, B, R, W, B...
Cosine (cos)	R, W, B, B, W, R, R...

4.4. HB MATLAB code generation and testing

The HB algorithm as presented in the previous chapter is translated into MATLAB language. The resulting code is then used for voltage calculations on the LV network with parameters and feeder configuration detailed in section 4.3 above. The code generation process is briefly discussed as follows.

Firstly, equations based on a single node feeder are written into code. A loop structure is then implemented to extend calculations to subsequent nodes. This part of the program matches the superposition step in the HB algorithm. At the end of the feeder, summated nodal quantities are used to calculate beta parameters of the consumer voltage pdf. Using the generated pdf, the percentile voltage at the required risk level is calculated. This developed software based on the HB algorithm for passive feeders is denoted $HB_{p\text{-}LV}$. On this software, error-check tests are done to confirm the correct presentation of the algorithm in code. The description of the tests along with the obtained results is presented in the proceeding section.

4.4.1. Comparison of HB MATLAB code with Excel based algorithm

The purpose of this test is to confirm the correct representation of the HB algorithm in MATLAB software. The procedure involves the calculation of feeder voltages on the test network using the two representations of the algorithm, $HB_{p\text{-}LV}$ and the excel spreadsheet version, $HB_{p\text{-}LV\text{-}Excel}$. A comparison of the voltage outcomes from the two methods is then done to verify the identical calculation of voltages.

NB. The excel form of the algorithm, $HB_{p\text{-}LV\text{-}Excel}$, is an open-source material readily available to LV network designers for use. This material can be accessed at Eskom's website.

The description of the tests conducted to confirm the correctness of $HB_{p\text{-}LV}$ is given below:

Test 1: Consistency of code in voltage drop calculations across phases

The purpose of this test is to ensure that the voltage drop algorithm is correctly applied to all phases on the feeder. To test this, a bal111 assignment method is used on both nodes on the feeder. Under such balanced loading, identical voltage results are expected in all the phases and these should also match those from $HB_{p\text{-}LV\text{-}Excel}$.

Table 4.3 below shows the test results obtained. The beta pdf parameters and the percentile voltage at 90% confidence ($Vcon_{90\%}$) are used as test variables.

Table 4-3: Validation of MATLAB code with Excel Spreadsheet Outcomes

Feeder type	Phase	Test Variables	$HB_{p\text{-}LV}$	$HB_{p\text{-}LV\text{-}Excel}$	|Relative Error|
LV feeder 3ph-4wire Bal111 assignment	A	α	15.8903	15.8903	0.00
		β	11.6907	11.6907	0.00
		$Vcon_{10\%}$	217.1089	217.1089	0.00
	B	α	15.8903	15.8903	0.00
		β	11.6907	11.6907	0.00
		$Vcon_{10\%}$	217.1089	217.1089	0.00
	C	α	15.8903	15.8903	0.00
		β	11.6907	11.6907	0.00
		$Vcon_{10\%}$	217.1089	217.1089	0.00

Tabulated results show identical values for beta parameters as well as percentile voltage across all phases. This result confirms consistency in voltage calculations across the phases. The exact matching of test variables for each phase between $HB_{p\text{-}LV}$ and $HB_{p\text{-}LV\text{-}Excel}$, suggests the correct implementation of algorithm into MATLAB software. To further test the correctness of the software, an investigation to confirm correct voltage calculations under different phase loading is done.

Test 2: Distinct voltage drop calculations for different phase loading conditions

The previous test ensured that $HB_{p\text{-}LV}$ was consistently applied to the three phases such that under balanced loading the same voltage results are obtained. In order to reinforce this result, another test is conducted. The purpose of this test is to ensure that the voltage drop algorithm is correctly applied to all phases such that under unbalanced loading, distinct voltage results in the phases are obtained. The same feeder configuration and parameters as outlined earlier will continue to be used. The phase assignment used in this test is such that phase A and phase B are loaded whilst phase C is unloaded.

Table 4.5 shows the results of the comparison made between the $HB_{p\text{-}LV}$ and $HB_{p\text{-}LV\text{-}Excel}$ using the test variables α, β and $V_{con10\%}$

Table 4-4: Results for consistency check of algorithm across phases

Feeder type	PHASE	Test Variables	$HB_{p\text{-}LV}$	$HB_{p\text{-}LV\text{-}Excel}$	|Relative Error|
LV feeder 3ph-4wire Customer assignment - 110 (node 1,node 2)	PHASE A (loaded)	α	11.9995	11.9995	0.00
		β	7.0595	7.0595	0.00
		$V_{con10\%}$	214.38	214.38	0.00
	PHASE B (loaded)	α	11.9995	11.9995	0.00
		β	7.0595	7.0595	0.00
		$V_{con10\%}$	214.38	214.38	0.00
	PHASE C (unloaded)	α	6.6521	6.6521	0.00
		β	17.6389	17.6389	0.00
		$V_{con10\%}$	233.32	233.32	0.00

From the results obtained for $HB_{p\text{-}LV}$, it is seen that the voltage in the unloaded phase (C) is greater than that in the loaded phases A and B; where voltages in A and B are the same. These values together with the beta parameters for all phases agree with those obtained using the $HB_{p\text{-}LV\text{-}Excel}$. The differences in phase voltages between the loaded and unloaded phases agree with electric circuit theory. The zero relative error in the results between $HB_{p\text{-}LV}$ and $HB_{p\text{-}LV\text{-}Excel}$ confirms the correct implementation of the algorithm to all phases in the developed software.

Test 3: Reverse Power Flow Test

In order to assess the HB algorithm for the correct formulation in line with electric circuit theory hence the correct calculation of voltage drops, a reverse power flow test is performed. In this test, a reverse computation of voltages from the receiving end to the sending end is done. The voltage values at the receiving end of the feeder as calculated in section 4.4.1(1) are used as the 'supply voltages'. The loads connected to the two nodes on the feeder are negated in order to reverse power flow. Figure 4.3 below shows the one-line diagram of the test network.

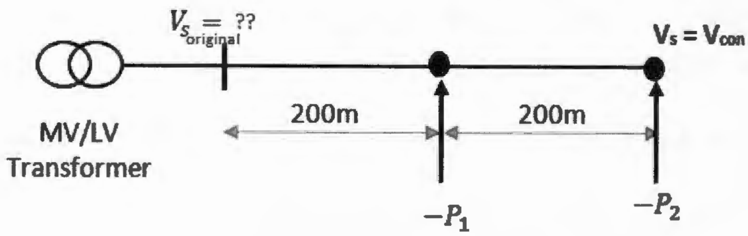

Figure 4.3: One line diagram for test network - reverse power flow

As shown in Fig. 4.3 above, the test network as was used in the previous tests is maintained only with changes in power flow as seen by the negative loads, P_1 and P_2.

Table 4-5: Results for reverse power flow test

Feeder type	Customer Phase Assignment	Test Variable	Forward Power Flow	Reverse Power Flow	|Relative Error|
3ph-4wire	Bal111 (node 1,Node 2)	V_s	230.00	229.689	0.14%

Results in Table 4.5 show a small value of error in the computation of the sending end voltage using the reverse power flow method. The error is explained by the fact that the consumer voltage at the end of the feeder (that simulates the role of a sending voltage) was calculated within a frame of a 10% design risk. This affects the computation of the voltage as that risk is carried through in the calculation. We can conclude that the value arrived at reflects that the algorithm agrees with electrical theory based voltage drop calculations

4.4.2. NRS034 Benchmark Tests

Test Description

Benchmark tests are used to validate HB-based software using different network parameters and conditions. The NRS034 details the test protocols to be used and also the test results expected from such. Parts of these tests are performed here so as to test the validity of the MATLAB encoded software, $HB_{p\text{-}LV}$, for voltage computation on LV feeders.

It should be mentioned that the NRS034 contains errors in the details of the benchmark tests. These errors would result in false negative testing results. The following amendments were done so as to correct the test information:

1. The design temperature T_2 is changed from 20° to 22° and 60° to 64.5° depending on the test parameters.

2. The type of cable used in the tests is a 70mm^2 copper conductor of 100metres inter-nodal length.

Tests 13-24 which apply to three phase systems and therefore the ones relevant to this work are covered.

Results

Table 4.6 shows the comparison of voltage drop results between the MATLAB software and the NRS034 for the benchmark tests conducted.

In the results shown, the voltage drop at the end of the feeder is the same for both the NRS034 and the MATLAB software under all the investigated conditions. This result confirms the correct implementation of the HB algorithm in software. We are therefore confident that there is no misrepresentation of the HB algorithm done.

However, the correct implementation of the algorithm is not adequate reason for method adoption. There is need to investigate the validity of this voltage drop computation tool before considering adoption to MV feeders. This is done using a renowned tool, the Monte-Carlo simulation.

Table 4-6: Benchmark Test Results

Test No.	NETWORK PARAMETERS						END FEEDER %VOLTAGE DROP						RESULT STATUS
	LOAD PARAMETERS			DESIGN PARAMETERS			NRS034			HB MATLAB			
	Alpha	*Beta*	*C*	*Risk*	*Temp*	*Ratio k*	*R*	*Y*	*B*	*R*	*Y*	*B*	
13	1.65	7.37	60	10	22	1	8.02	8.02	8.02	8.02	8.02	8.02	✓
14	0.60	0.491	10	10	22	1	16.51	-	-	16.51	-	-	✓
15	1.65	7.37	60	10	22	1	6.44	6.16	6.01	6.44	6.16	6.01	✓
16	1.65	7.37	60	10	22	1.4	7.05	6.73	6.56	7.05	6.73	6.56	✓
17	1.65	7.37	60	10	22	1	3.09	6.18	9.29	3.09	6.18	9.29	✓
18	1.65	7.37	60	10	64.5	1	3.58	7.19	10.79	3.58	7.19	10.79	✓
19	1.65	7.37	60	10	22	1	6.27	6.20	6.16	6.27	6.20	6.16	✓
20	3.5	2.86	20	10	22	1	4.95	4.91	4.89	4.95	4.91	4.89	✓
21	0.60	0.491	10	10	22	1	3.06	3.03	3.01	3.06	3.03	3.01	✓
22	1.65	7.37	60	10	22	1	6.30	6.23	6.09	6.30	6.23	6.09	✓
23	1.65	7.37	60	20	22	1	5.36	5.32	5.22	5.36	5.32	5.22	✓
24	0.60	0.491	10	10	22	1	12.83	-	-	12.83	-	-	✓

4.5. Validation of HB_{p-LV} using the Monte-Carlo simulation

Validation test description

In this test, the network as described earlier in section 4.3 is used. The bal222 phase assignment method used on both nodes on the feeder. The MCS method for passive feeders, MC_{p-LV}, and the generated code for HB, HB_{p-LV}, are both used to compute voltages on the described network.

Validation is then concluded through a comparison of results between the two methods. The MCS serve as the base of comparison.

Test Results

Table 4.7 below gives details of the results of the validation test. The expected value of the consumer voltage, E(Vcon) and the 10% percentile voltage, $Vcon_{10\%}$ are used as test variable in the validation exercise.

Table 4-7: Validation test results

TEST VARIABLES		VALUES
$E(V_{con})$	$MC_{MV\text{-}PF}$	218.89
	$HB_{MV\text{-}PF}$	218.98
	Error (V)	0.09
$Vcon_{10\%}$ *(V)*	$MC_{MV\text{-}PF}$	208.59
	$HB_{MV\text{-}PF}$	208.59
	Error (V)	0.00
$\%V_{drop}$ error		0.00

The tabulated results show a very low error in the calculation of feeder voltages using $HB_{p\text{-}LV}$. The slight error noted evolves from the calculation of the expected value of consumer voltage. This error is only approximately 9mV which translates to a 0.08% error when calculated as a percentage of the nominal voltage. The results for percentile consumer voltage are identical (zero error). This shows high agreement between the two methods of voltage computation. A clearer analysis can be done by looking at the voltage pdfs at the end of the feeder.

Figure 4.4 shows the consumer voltage pdfs obtained through the two methods under comparison. It can be seen from the plot that the two pdfs are nearly identical. The $HB_{p\text{-}LV}$ trace follows the $MC_{p\text{-}LV}$ trace with great accuracy. There are only a few areas in which the $HB_{p\text{-}LV}$ trace slightly deviates from the $MC_{p\text{-}LV}$ trace. This can be explained by the fact that the HB analytical method is based on a worst case approach and it would require a large number of iteration in the MCS in order to exhaust the worst case scenarios. Therefore this error can be seen to vanish with an increased number of iteration towards infinite sampling.

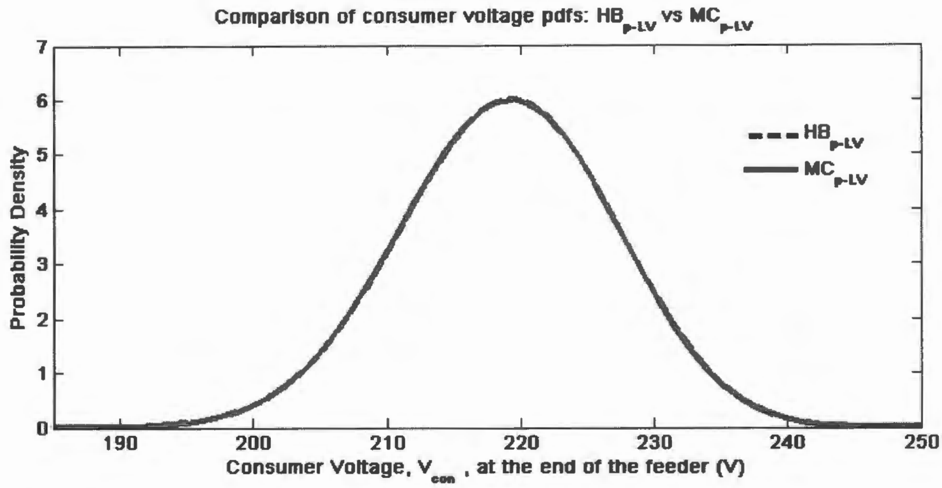

Figure 4.4: Comparison of consumer voltage pdfs, HB_{p-LV} vs. MC_{p-LV}

Based on the results obtained from the investigations undertaken thus far, we can conclude that the HB algorithm for passive networks is valid. It is now required that the same series of tests and validation be done for the algorithm for active feeders. This is undertaken in the section that follows.

4.6. HB algorithm for LV feeders with DG

The HB method for LV active feeders, HB_{a-LV} will be used in this study to develop a voltage calculation tool for MV feeders through modification. To avoid the carry-over of error, we need to develop HB_{a-LV} and test it for errors through comparison with the excel-based algorithm. After that, validation with the Monte-Carlo will be done.

4.6.1. Feeder configuration and parameters

The network configuration as presented earlier in Section 4.3 is used. However, in addition a generator node is included. The one-line model used in the investigation is as given below.

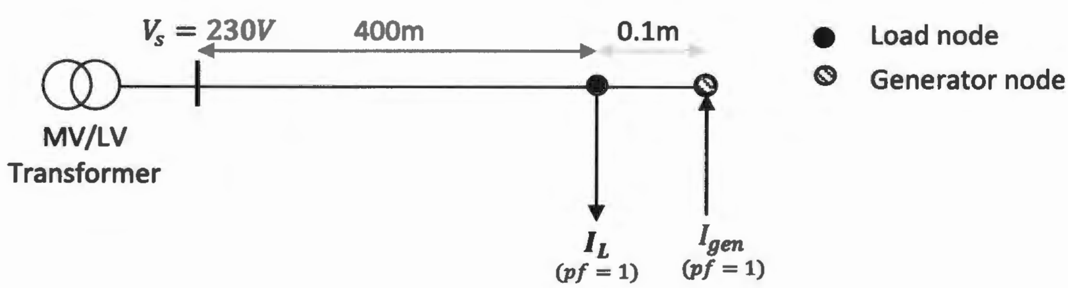

Figure 4.5: One-line test network for active LV feeder

The following network parameters are used for the tests conducted. The values given are common to all methods used for voltage calculations unless changes are otherwise stated.

Table 4-8: Test feeder parameters for LV active network

FEEDER PARAMETER	PARAMETER VALUE	
Sending Voltage, V_s	230V	
Number of nodes	2	
Customer Phase Assignment	Node 1(**Load**)	6 4 2
	Node 2(**Generator**)	-1 -1 -1
Inter-nodal distance	0.1m Load-Gen separation,	
Load Current pdf parameters	Generator Node	Load Node
	$\alpha = 1.5$	$\alpha = 1.5$
	$\beta = 4.0$	$\beta = 4.0$
	C_b= 60 A[circuit breaker size]	
Conductor type	Copper Conductor, $35mm^2$Cu	
	Temperature	$T_1 = 20°$
		$T_2 = 40°$
Feeder Impedance, X/R ratio	0	

In the table above, it should be noted that the generator connections are represented as negatives. This is in-line with the modifications done to the algorithm for incorporation of DG as explained in the previous chapter. If these values are entered as positives then the generator will act as a normal load consuming power rather than supplying the utility grid.

4.6.2. $HB_{a\text{-}LV}$ MATLAB code generation and testing

The changes as outlined in Chapter 3 for inclusion of DG in the HB algorithm are implemented in the code and compiled. The resulting code, $HB_{a\text{-}LV}$ is tested for errors before it is validated using the Monte-Carlo simulation. The following tests are conducted.

Test 1: Comparison test with excel-spreadsheet based HB algorithm

This test serves to establish the correctness in the translation of the algorithm from its formulae into software. The coded algorithm $HB_{a\text{-}LV}$ is used to calculate voltage drops on the test network. The Excel-based algorithm is then used for the same calculations and results are compared. Since the representation of the algorithm in software is not done with any simplifications, the results from the two methods should be identical.

Test 2: Consistency of code in voltage calculations across the phases

The purpose of the test is to ensure that the code is correctly implemented in all three phases. The same test feeder applies but some changes to the parameters are done. The customer assignment in

this test is such that there is balanced loading across the phases. In this way it is simple to determine if errors exists in the code or not. A balanced phase assignment method bal666 is used for the loads whilst the generators are kept the same.

Test Results

Table 4.9 below shows the results for error checks run on the HB algorithm written in MATLAB code. The test statistics reveal agreement of outcomes between the MATLAB based algorithm and the Excel spreadsheet. All the test variables show a zero relative error.

Table 4-9: Test 1 results for error checks on MATLAB code for HBa-LV

Test Variable		HB$_{a\text{-}LV}$(MATLAB)		HB$_{a\text{-}LV}$(Excel sheet)		|Relative Error|
V_{max} (phase A)		298.6V		298.6V		0.00
V_{min} (phase A)		54.0V		54.0V		0.00
Beta parameters of Vcon (phase A)		α	47.9665	α	47.9665	0.00
		β	32.0579	β	32.0579	0.00
Consumer Voltage $\|Vcon_{90\%}\|$	A	217.62		217.62		0.00
	B	234.31		234.31		0.00
	C	249.20		249.20		0.00
Feeder voltage Drop %	A	5.38		5.38		0.00
	B	-1.87		-1.87		0.00
	C	-8.35		-8.35		0.00

The test results for consistency in voltage calculations across the phases are given in Table 4.10. The results show identical outcomes in the test variables in all phases. This result reflects that the same algorithm is used in the three phases. Hence, consistency is observed.

The positive results for Test 1 and 2 indicate a correct translation of algorithm into code. At this point we trust that the excel-spreadsheet is correctly programmed. This assumption can be detrimental to the success of the outcomes of the investigations based on this algorithm. There is a need to validate the algorithm before modifications on it are done.

Table 4-10: Test results for consistency of voltage calculation across phases using $HB_{a\text{-}LV}$

Test Variable		Phase A	Phase B	Phase C	|Relative Erro
V_{max}		338.3 V	338.3 V	338.3 V	0.00
V_{min}		54.0 V	54.0 V	54.0 V	0.00
Beta parameters of Vcon	α	60.6624	60.6624	60.6624	0.00
	β	48.7265	48.7265	48.7265	0.00
$Vcon_{90\%}$		228.9V	228.9 V	228.9 V	0.00
Voltage Drop %		0.48	0.48	0.48	0.00

*NB. The maximum and minimum voltages V_{max} and $V_{min}$are worst case voltages used in the HB algorithm as explained in section 3.3.5 earlier. These values may at times be impractical since they are calculated under the worst loading conditions on the feeder. However, they are essential in the calculation of voltages.

4.6.3. Validation of $HB_{a\text{-}LV}$ using the Monte-Carlo method

Validation test description

The Monte-Carlo Simulation algorithm for passive feeders is modified to include generators. This is done by negating the phase currents for generator node calculations. The modified code is denoted $MC_{a\text{-}LV}$ for easy reference.

Using $MC_{a\text{-}LV}$, voltage calculations on the test feeder with parameters detailed in Table 4.9 are done. For validation, a comparison of the $HB_{a\text{-}LV}$ results with those from $MC_{a\text{-}LV}$ on the same network is done.

Test Results

The validation test investigation yielded results detailed in Table 4.11. With regards to nodal voltage, the calculation of percentile voltages using the HB algorithm obtained slightly higher values, only by 0.47V. This difference, expressed as a percentage of the nominal voltage, only comes to approximately 0.2% which indicates high accuracy in the calculation.

Table 4-11: Validation test results, $HB_{a\text{-}LV}$ vs $MC_{a\text{-}LV}$

Test Variables		Values
$E(V_{con})$	$MC_{MV\text{-}PF}$	200.69
	$HB_{MV\text{-}PF}$	200.62
	Error (V)	0.07
$Vcon_{10\%}$ *(V)*	$MC_{MV\text{-}PF}$	217.15
	$HB_{MV\text{-}PF}$	217.62
	Error (V)	-0.47
$\%V_{drop}$ error		0.20

The test results given also show high agreement in the expected values of consumer voltage. An insignificant error of 7mV is noted in this regard. To have a better analysis of the performance of HB_{a-LV}, the resulting consumer voltage pdfs from both methods are plotted on the same axis.

Figure 4.6 below shows a good alignment of pdfs only with slight error. The quantitative analysis of error done using the tabulated results agrees with this plot. Slight error is seen at the base of the distribution plot and also at its peak. It seems as if the HB plot is slightly widened at the bottom thus pulling its crest a little lower. A plausible explanation to this is similar to that given for the passive feeder results. The HB analytical method is based on a worst case approach and it would require a large number of iteration in the MCS method in order to exhaust the worst case combinations. Therefore, this error can be seen to reduce with an increased number of iteration towards infinite sampling.

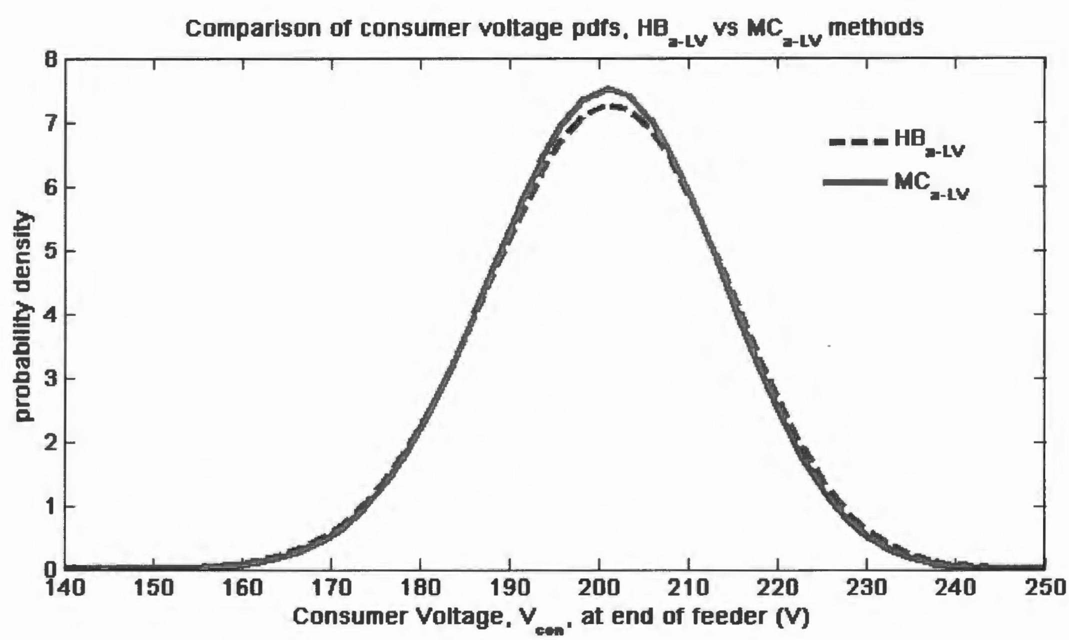

Figure 4.6: Comparison of consumer voltage pdfs, HB_{a-LV} vs MC_{a-LV}

Based on the plots in Fig. 4.6, it can be concluded that the HB algorithm for active feeders, HB_{a-LV}, is an acceptably accurate method for voltage calculations in LV feeders with DG.

4.7. Concluding Remarks

In this chapter the necessary tools required in this study were developed; the Monte-Carlo simulation together with the HB software were generated and thoroughly tested. The results gathered affirm the validity of the HB method as a tool for voltage calculation in both passive and active LV feeders using beta distributed currents as loads. The tests also confirm correct coding of the HB algorithm and MCS into MATLAB software. These tools having been validated in this section of work can be confidently used in further investigations in the research.

In proceeding chapters, the HB methods, $HB_{p\text{-}LV}$ and $H_{a\text{-}LV}$, will be used as foundation to the development of a tool for voltage computation in MV systems.

Chapter 5

5. USING ABSOLUTE VALUE OF IMPEDANCE TO CATER FOR REACTANCE IN MV VOLTAGE DROP CALCULATION

It has been established that the effects of reactance in voltage drop calculations in MV networks cannot be ignored. Errors in network power flow analysis would arise leading to uneconomical and incorrect network planning and design decisions. This chapter attempts to avoid such errors through modifying the input parameter for resistance to include the effects of reactance. This is done using the absolute value of impedance in place of resistance in the HB algorithm. Tests are then done to assess the accuracy of the method through the MCS.

5.1. Overview of proposed method

Tests conducted in the previous chapter have shown the importance of inclusion of line reactance in power flow equations as the consumer voltage is dependent on it. Deterministic methods and probabilistic methods based on DLF correctly model network parameters with the inclusion of reactance. Elements like power factor and line reactance can easily be factored in the calculations without increase in complexity. This is however not the case with analytical probabilistic methods which often would result in tedious mathematical calculations and in many cases, complexity.

To avoid such, an approximate modelling of the feeder's complex impedance through its absolute value is done. This approach attempts to compensate for the effects of reactance in the calculation of voltages on the feeder. The following procedure is used in the approach:

1. Modify the input parameter, R_p in the HB algorithm through substitution with the modulus value of feeder impedance.

$$|Z_p| = \sqrt{R_p^2 + X_p^2} \tag{5.1}$$

2. Effect input parameter modification on the HB software.
3. Test correctness of modified approach by running network test with $X_p = 0$; correlating to the same algorithm for LV feeder with zero X/R ratios. Under this reactance condition the calculations should result in the same voltage drops.
4. Modify the MCS algorithm so that it is based on equations in section 3.4.1 (these equations make provision for voltage calculations on feeders with complex impedance). Denote the resulting algorithm as MC_{MV}.

5. Using both methods, the MCS and the HB with modified inputs, perform voltage drop computation on MV feeder for various values of reactance.
6. Use results to validate the proposed method and draw conclusions.

5.2. Compensation for feeder reactance using $|Z_p|$

From the literature review covered, MV distribution feeders have been found to have significant values of reactance. For these feeders, the impedance value Z_p is a complex function described by orthogonal pairs R_p and X_p. A vector pictorial in Fig. 5.1 shows these relations.

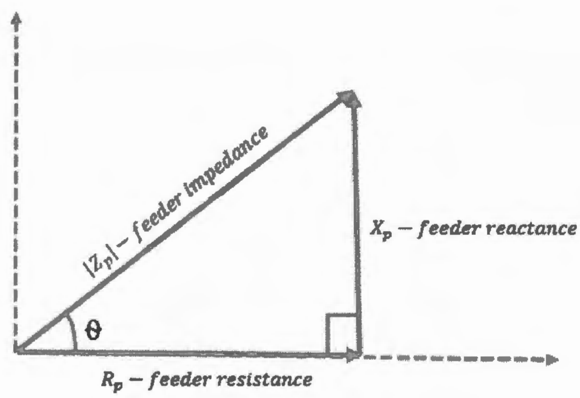

Figure 5.1: Vectorial representation of complex impedance

Mathematically, the impedance vector Zp can be expressed in terms of the feeder resistance and reactance as below.

$$\boldsymbol{Z_p} = R_p + jX_p \tag{5.2}$$

Another acceptable representation of the complex impedance is through phasor notation as follows:

$$\boldsymbol{Z_p} = |Z_p|\angle\theta \tag{5.3}$$

$$where\ |Z_p| = \sqrt{R_p^2 + X_p^2}\ \ and\ \theta = \tan^{-1}\left(\frac{X_p}{R_p}\right)$$

In the investigation carried out in this chapter, the approximation of feeder impedance by its absolute value without its phasor angle is used. This is done so as to avoid the modification of the HB algorithm beyond the input parameters (Rp in this case); the inclusion of the imaginary component or the phasor angle will require the re-formulation of the algorithm which is a complex task beyond the scope of this work.

Using |Zp|, the effects of reactance are partly incorporated in the calculation of voltages. This is expected to achieve comparable results with the calculation of voltages using the MCS with the exact parameters.

The changes expected in the algorithm are merely the substitution of line resistance, R_p with absolute value impedance $|Z_p|$. The new network equations with the modified parameter at node i are given by:

$$dV_{i-R} = I_a|Z_p|(1+k) - \frac{1}{2}(I_b + I_c).k.|Z_p| \tag{5.4}$$

$$dV_{i-I} = \frac{\sqrt{3}}{2}(I_b - I_c).k.|Z_p| \quad ;where\ k = \frac{|Z_p|}{|Z_n|} \tag{5.5}$$

The magnitude of consumer voltage at that node is given by equation 5.6 below.

$$V_{con} = \sqrt{(V_s - dVR_i)^2 + dVI_i^2} \tag{5.6}$$

The modification to the input parameter as explained above does not affect the HB algorithm equations beyond the substitution of Rp with |Zp|. Therefore, only this substitution to all equations of the algorithm is required in order to fully implement the new approach to voltage calculations. In coding, this could be simply achieved through a few lines of code as follows;

```
Xp = k2 * Rp;              %where k2 is the feeder X/R ratio
Rp = sqrt(Rp^2 + Xp^2);%inflated Rp represents |Zp|
```

The resulting MATLAB code based on the described modifications is denoted $HB_{MV-|Z|}$ for future referencing. This code is to be tested for errors and then validated using the MCS. The test protocol is described in the preceding sections.

5.3. MV test network parameters and configuration

In this section, the test network on which voltage calculations are to be done is described. The network parameters used in the test are also given.

5.3.1. Network configuration

A three-phase feeder with 3 nodes is used in the tests that follow. Fig. 5.2 shows the network model for a typical MV feeder. As with the model in Fig. 3.1, the load impedance shown is purely resistive as loads are considered to be of unity power factor. On the other hand, the assumption of a purely resistive feeder is dropped as reactance is factored in.

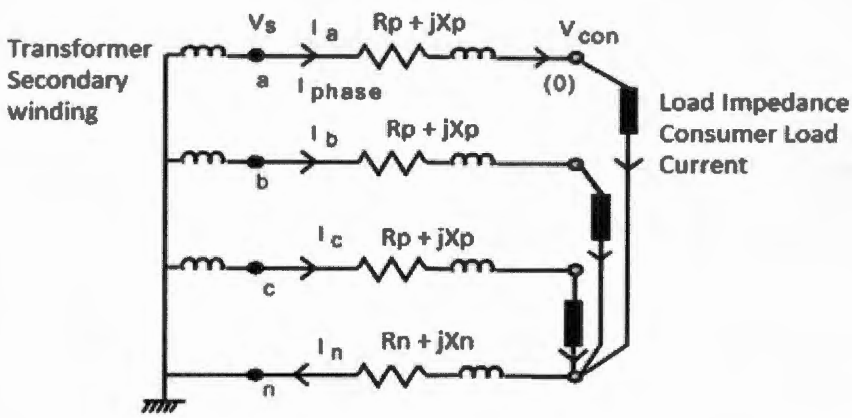

Figure 5.2: Feeder network model for MV network with simplified impedance

A one-line network diagram can be used to illustrate the network model depicted in Fig. 5.2 for power flow analysis. The one line diagram expands the network model to three nodes as shown below:

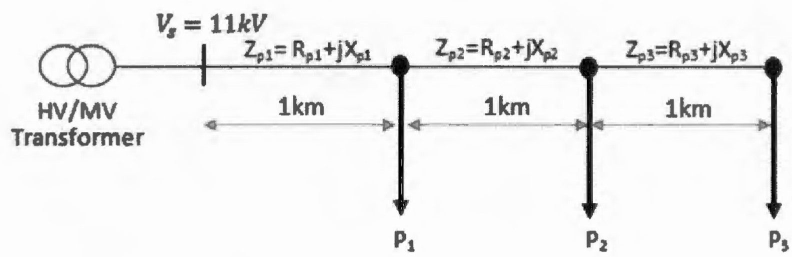

Figure 5.3 : One line test network model for MV feeder with inclusion of reactance

As noted in the diagram above, the feeder sections are now represented by complex impedance as per adopted MV network model. However, connected consumers only draw real power denoted by quantities P_1, P_2 and P_3.

5.3.2. Network Parameters

Table 5.1 shows the network parameters used in the tests to be conducted. The loads are at unity power factor and are assigned to the phases using the cos330 method. The customer load distribution parameters shown in the table are assumed values since no real network data was available at the time of testing. The data is however sufficient for testing the effectiveness of the method being developed since the data is common to both the MCS and the HB method.

Table 5-1: Test network parameters for passive MV feeder

FEEDER PARAMETER	PARAMETER VALUE	
Sending Voltage, V_s	11 kV	
Number of nodes	3	
Customer Phase Assignment	Node 1	3 3 0
	Node 2	0 3 3
	Node 3	3 0 3
Inter-nodal distance	1 km	
Load Current pdf parameters	$\alpha = 1.5$	
	$\beta = 4.0$	
	Load power factor = 1	
	C_b= 100 [circuit breaker size]	
Temperature [^{0}C]	T_1= 20	
	T_2= 40	
Conductor type	Copper Conductor, 35 mm^{2}Cu	
	Temperature	$T_1 = 20°$
		$T_2 = 40°$
Feeder Impedance, X/R ratios	0 – 1 (in steps of 0.2)	

5.4. Testing the $HB_{MV-|Z|}$MATLAB software for errors

The generated software based on the modified HB algorithm, $HB_{MV-|Z|}$ is first checked for errors before it is used. This is essential as it prevents false negatives in the process of validation. Two tests are done here, one that checks for errors in $HB_{MV-|Z|}$ based on the source algorithm, HB_{p-LV} and another that checks for consistency of voltage drop code across the phases.

5.4.1. Test 1: Voltage drop calculation comparison with HB_{p-LV} for condition X/R = 0

The purpose of this test is to check and rectify any errors in $HB_{MV-|Z|}$ that may have evolved from the modification of input parameters. To do this, a special case $X_p = 0$ which matches the impedance characteristic in LV feeders is used. The HB_{p-LV} software developed in Chapter 4 can then be used to assess the correctness (not validity) of $HB_{MV-|Z|}$ in the transferal of changes into code.

To conduct this test, voltage calculations on the feeder are done using the two methods for the described test condition. Following this, voltage results reflected in selected test variables are compared. The results from the two methods are expected be identical since they are based on the same network model and algorithm as well.

5.4.2. Test 2: Consistency of voltage drop calculation across the phases

The purpose of this test is to check the consistency of $HB_{MV-|Z|}$ in voltage drop calculations across phases. This is done using the test feeder with a balanced load assignment, Bal 333 and the impedance condition $X_p/R_p = 0.2$. The non-zero X/R ratio used allows the use of the modified part of the input parameter formulation. This ensures that the modification applied does not introduce error in this regard. All the other test network parameters are kept constant except for those highlighted in Table 5.2.

Table 5-2: Modified test network parameters for Test 2 on $HB_{MV-|Z|}$

FEEDER PARAMETER	PARAMETER VALUE	
Customer Phase Assignment	Node 1	3 3 3
	Node 2	3 3 3
	Node 3	3 3 3
Feeder X/R ratio	0.2	

Under balanced loading, the voltage drop in all the phases is expected to be the same. This would demonstrate consistent voltage calculations across the phases.

If any of the 2 tests described above are negative then errors are tracked for correction. Positive results in the two tests will confirm correct implementation (not validity) of the proposed method in software.

5.4.3. Test Results

Table 5.3 shows the results for Test 1. The test statistics reveal agreement of outcomes between HB_{P-LV} and $HB_{MV-|Z|}$ in all the test variables with zero relative error.

Table 5-3: Test 1 results for error checks on MATLAB code for $HB_{MV-|Z|}$

Test Variable		$HB_{P-LV}(V_s = 11kV)$		$HB_{MV-|Z|}(X_P = 0)$		|Relative Error|
V_{max} (phase A)		11.680kV		11.680kV		0.00
V_{min} (phase A)		9.646kV		9.646kV		0.00
Beta parameters of Vcon (phase A)		α	43.6965	α	43.6965	0.00
		β	32.3044	β	32.3044	0.00
Consumer Voltage |Vcon| (percentile)	A	10.668kV		10.668kV		0.00
	B	10.819kV		10.819kV		0.00
	C	10.534kV		10.534kV		0.00
Feeder voltage Drop %	A	3.02		3.02		0.00
	B	1.64		1.64		0.00
	C	4.23		4.23		0.00

The identical results in the test parameters confirm that the modification to the formulation of the input parameters does not introduce error in the HB algorithm.

Further tests for consistency of voltage drop calculations across the phases after modification to include reactance in the impedance yielded the results as given in Table 5.4.

Table 5-4: Test 2 results for consistency of voltage calculation across phases in $HB_{MV-|Z|}$

Test Variable		Phase A	Phase B	Phase C	|Relative Error|
V_{max}		12.035kV	12.035kV	12.035kV	0.00
V_{min}		8.929kV	8.929kV	8.929kV	0.00
Beta parameters of Vcon	α	69.9346	69.9346	69.9346	0.00
	β	51.5111	51.5111	51.5111	0.00
Consumer Voltage $\|Vcon\|$ (10%)		1.0539kV	1.0539kV	1.0539kV	0.00
Feeder voltage Drop %		4.19	4.19	4.19	0.00

The test variables between the phases as shown in Table 5.4 are identical, implying zero error. These results confirm a consistent application of the voltage drop algorithm across the phases. The results from both tests summed together give confidence in the software $HB_{MV-|Z|}$ developed for calculation of voltage feeders on MV feeders. However, the validity of the proposed method still has to be tested against the MCS. This forms the objective of the proceeding section.

5.5. Validation of $HB_{MV-|Z|}$ for voltage drop calculation on MV feeders

Investigations on the variation of consumer voltage with X/R ratios on MV feeders in Chapter 3 revealed the correlation between consumer voltage and feeder reactance. The consumer voltage was seen to decrease significantly with increases in X/R ratios. The original algorithm, HB_{P-LV} on the other hand has a null variance of consumer voltage with changes in X/R ratio. This accrues from the assumption of purely resistive feeders applied in the algorithm. The developed and tested approach, $HB_{MV-|Z|}$, attempted to compensate for reactance through the modification of input parameters.

This suggested approach is now validated in this section.

5.5.1. Test 1: Variation of consumer voltage with increasing X/R ratio

In this test, $HB_{MV-|Z|}$ is used to compute voltages on the MV test feeder with X/R ratios varied from 0 to 1. The resulting consumer voltage pdfs are plotted and analysed. A positive test is characterised by the gradual decrease of consumer voltages as X/R ratios increase. This result would confirm some level of compensation of the effects of reactance in the voltage calculation. The quantitative analysis on how well the noted variation in voltages compares to the expected variation is covered in Test 2.

5.5.2. Test 2: Validation of $HB_{MV-|Z|}$ using the MCS

Test 1 serves as a quick test to check the functionality of the proposed method. The achievement of the expected variation of voltages suggests the validity of the tested method without quantifying accuracy. The objective of Test 2 is to quantify the accuracy of the method through comparison with MCS voltage results on the same test network.

The procedure taken involves the computation and comparison of feeder voltages, for different cases of X/R ratios, on the test network using $HB_{MV-|Z|}$ and MC_{MV}. The variation of X/R ratios is from 0 to 1 in steps of 0.2 inclusively.

5.6. Results – Validation of proposed approach to voltage computation on MV feeders

Test 1: Variation of consumer voltage with reactance

Figure 5.4 below shows the outcome of voltage computations on the test network using the HB algorithm with modified inputs for different ratios of X/R. Simulation shows a gradual decrease in consumer voltage as the reactance increases with X/R ratios. This can be seen in the diagram by the stretch of consumer voltage pdfs towards the right.

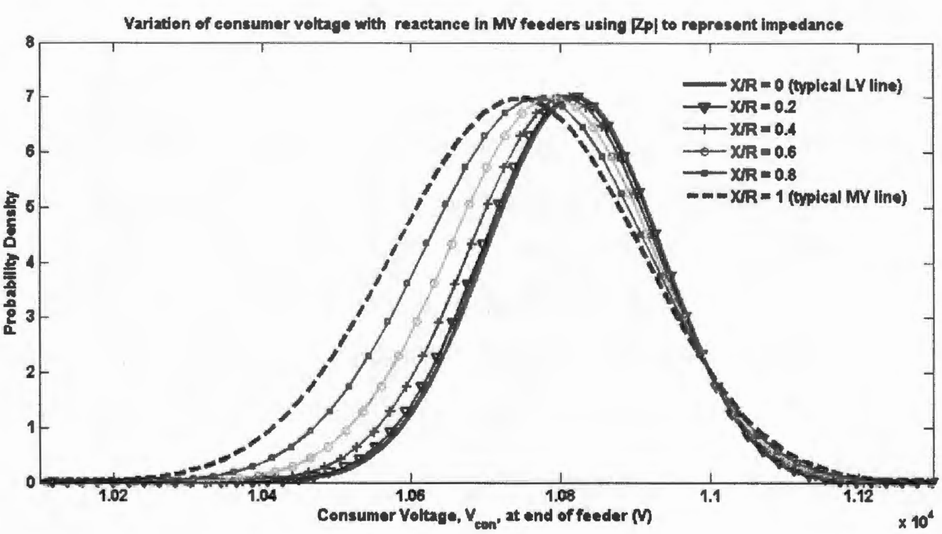

Figure 5.4: Variation of Consumer Voltage with reactance on MV feeder using |Zp| to represent impedance

The variation of consumer voltage with changes in X/R ratios is consistent with the expected decrease in consumer voltage as voltage drops across the reactance element increase with X/R ratios. The results suggest that the effects of reactance on voltage computations are in some way compensated through the use of |Zp| in place of Rp.

In order to quantify the accuracy of the proposed approach, there is need to quantitatively compare the voltage results using $HB_{MV-|Z|}$ with those obtained using the MCS. This investigation is explored in validation test 2.

Test 2: Comparison of voltage drop calculations between $HB_{MV-|Z|}$ and MC_{MV}

Voltage drop calculations as per the described procedure outlined in section 5.5.2 were done and results tabulated as shown in Table 5.5.

Table 5-5: Test 2 results: $HB_{MV-|Z|}$ vs MC_{MV} for voltage computation in MV feeders

Test Variables		Case 1 X/R = 0.00	Case 2 X/R = 0.20	Case 3 X/R = 0.40	Case 4 X/R = 0.60	Case 5 X/R = 0.80	Case 6 X/R = 1.00
$E(V_{con})$ (kV)	MC_{MV}	10.816	10.799	10.784	10.766	10.752	10.736
	$HB_{MV-\|Z\|}$	10.816	10.812	10.802	10.785	10.764	10.740
	Error	0.00	-0.013	-0.018	-0.019	-0.012	-0.004
$Vcon_{10\%}$ (kV)	MC_{MV}	10.670	10.655	10.638	10.617	10.601	10.579
	$HB_{MV-\|Z\|}$	10.668	10.661	10.642	10.612	10.574	10.530
	Error	0.002	-0.006	-0.004	0.005	0.027	0.049
$\%V_{drop}$ error		0.02	0.05	0.04	0.05	0.25	0.45

The results obtained generally show low error margins in the calculation of voltages using the new approach. For the test variable E(Vcon), error values do not seem to have a fixed trend with X/R ratios. The maximum relative error noted in this regard when compared to the expected values from the MCS is only 19 V. Similarly, errors in percentile voltages are quite low. However, with this test variable, a trend in error size is noted. The errors increase with X/R ratios. Still, the highest relative error recorded is only 49 V which translates to 0.45% voltage error (when expressed as a percentage of the nominal voltage). The acceptable errors noted in the calculations suggest the validity of the new approach $HB_{MV-|Z|}$ for voltage calculations on MV feeders with insignificant feeder reactance.

In order to verify the correct depiction of the distribution of consumer voltages, the resulting pdfs from the voltage calculation results obtained were plotted; Figure 5.5 shows these plots.

It can be noted from the plot in Fig. 5.5 (a) that the spread of consumer voltage is perfectly obtained when X/R is zero. This confirms the accuracy of the HB algorithm for LV feeders since the condition under this case is that of a purely resistive feeder. The accuracy in spread is nearly maintained for low values of X/R as seen in Fig. 5.5(b) and (c). However, the error builds up further with higher reactance values. In Fig. 5.6(c) – (e), the $HB_{MV-|Z|}$ traces are misaligned with those of MC_{MV}. This error should be as a result of incorrect maximum and minimum voltage values in the normalization process; step 8 of the algorithm (see Appendix A pg.136). This argument is based on the fact that the magnitude of errors

in the calculation of E(Vcon) as given in Table 5.5 suggests a great agreement between $HB_{MV-|Z|}$ and MC_{MV}. This is however in contradiction to the misalignments noted in the graphs in Fig. 5.5. Since the distribution parameters are obtained from the normalized statistical moments, it is reasonable to conclude that the incorrect scaling voltages (used for normalization) added substantial error to the spread of voltages. Nonetheless, the distribution of consumer voltages depicted by $HB_{MV-|Z|}$ is still acceptable as it still tracks the MC_{MV} trace even though it does this with some errors. The nearly even distribution of misalignments on either side of the MC_{MV} trace makes the calculation of the percentile voltage a little less than expected.

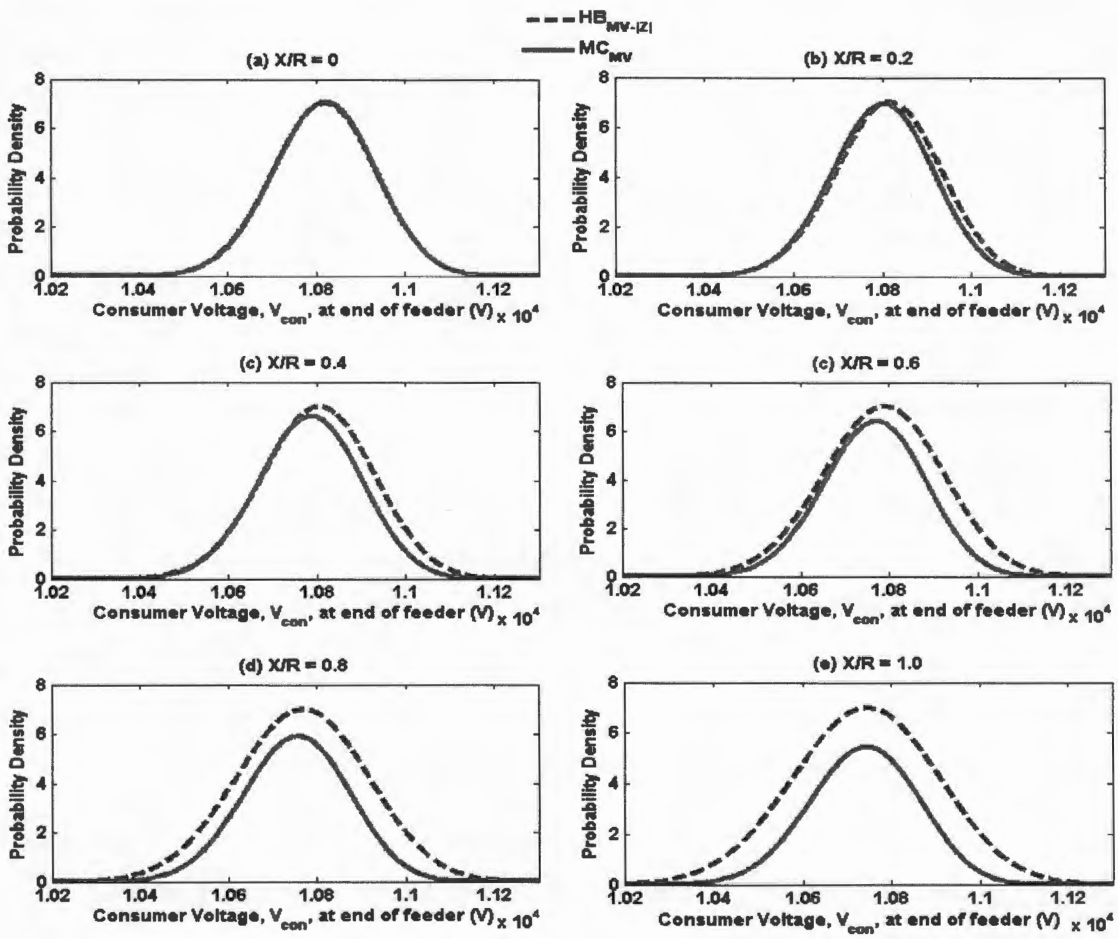

Figure 5.5: Spread of consumer voltages - $HB_{MV-|Z|}$ vs MC_{MV} for cases 5.6(a) – X/R = 0; 5.6(b) -X/R = 0.2; 5.6(c) – X/R = 0.4; 5.6(d) – X/R = 0.6; 5.6(e) – X/R = 0.8 and 5.6(f) – X/R = 1

5.7. Concluding Remarks

The modification of inputs to include effects of feeder reactance in the computation of voltages has been successfully accomplished. The results obtained from the investigation led to the following conclusions regarding the simplification of representing complex impedance as an absolute value:

- The proposed method, $HB_{MV-|Z|}$, calculates the percentile consumer voltage along MV feeders within an acceptable low margin error. On the other hand, the spread of consumer voltage is not accurately depicted. The omission of the impedance vector angle in the calculation of voltage drop affects this result.
- The limitation and error in the original HB algorithm as a result of the omission of reactance in voltage calculations on MV feeders is satisfactorily addressed by the use of absolute value of impedance in place of resistance ($|Zp|$ in place of Rp).
- If better accuracies are sought for, the feeder impedance angle has to be incorporated in the computation of voltages. In other words the impedance has to be represented as a complex variable without simplification. However, this would require a complete new derivation of the HB algorithm.

In the investigation just completed, it has been found that adjustments to the resistance input parameter to compensate for line reactance are sufficient with acceptable error for voltage calculations on MV feeders. However, this investigation is not sufficient as a stand-alone since voltage calculations are dependent on both reactance and load power factor. The next chapter dwells on the compensation of non-unity load power factor in the HB algorithm.

Chapter 6

6. EXTENSION OF VOLTAGE DROP ALGORITHM TO INCLUDE VARYING POWER FACTOR EFFECTS IN MV SYSTEMS

The previous chapter adequately dealt with the inclusion of line reactance in voltage drop calculations on MV feeders using the Herman-Beta approach. However, the algorithm still suffers a limitation being for loads of unity power factor. Unfortunately, the MV system is mainly characterised by non-unity power factor as discussed in literature. This calls for an extension of the developed algorithm to include effects of varying power factor.

This chapter therefore involves the modification of input parameters in the previously adjusted algorithm, $HB_{MV-|Z|}$, to include the effects of non-unity power factor loads. Following development, the algorithm will be tested for errors and validation will be done through comparison with voltage calculations using the Monte-Carlo simulator.

6.1. Introduction

An investigation reported earlier on in Chapter 3 reveals the dependency of voltage drop calculations on load power factor. The assumption of unity power factor is valid for LV systems in which residential loads tend to unity power factor at the instant of maximum demand [1], [4], [17], [24]. However, the simplification or assumption of unity power factor loads cannot be extended to MV feeders owing to the nature of consumers in the distribution network. Such a simplification would result in incorrect voltage drop calculations which lead to uneconomical network design and planning decisions. To avoid such predicaments, voltage drop calculations should be done without such simplifications and/or assumptions.

In many MV distribution networks, the power factor is found to range between 0.8 and unity [7], [42], [55]. Lower power factors in power systems mostly result in increased voltage drops and power losses. This often leads to the need for larger transformers and cables in the network unless reactive power compensators are put in place to avoid the transmission of reactive power. An inclusion of power factor in voltage drop and power loss computations is therefore an important task that cannot be avoided. Under-estimation of voltage drops and losses would result if the power factor is not considered. This potentially leads to the violation of the permissible voltage limits and also deteriorates power quality in the network.

6.2. Monte-Carlo method for voltage calculation on MV feeders with non-unity power factor

The MCS method, MC_{MV} developed in the previous sections for testing proposed algorithms for voltage computation had a condition of unity power factor. In order to use the same method as a validation tool in this section, a modification needs be done to include the effects of power factor in the calculation of voltage drop.

The cases considered in earlier chapters dealt with consumers drawing real power without reactive power. This meant that the nodal load currents were real variables with no imaginary components. This however changes for cases in which the power factor is non-unity. Consumers draw both real and reactive power which results in complex nodal currents. In the work presented by Celli *et al.* [23], real and reactive power variables drawn from customer pdfs were divided by the nominal voltage. V_{nom} to obtain complex nodal currents as illustrated below:

$$\boldsymbol{S} = P + jQ \tag{6.1}$$

$$\boldsymbol{S} = I^{*}V_{nom} \tag{6.2}$$

$$I^{*} = I_R - jI_I = \frac{P+jQ}{V_{nom}} \tag{6.3}$$

Where S, P and Q represent the apparent, real and reactive power consumed by loads

I_R and I_I are the real and imaginary load (or nodal) currents drawn by the loads

Though their method is based on load power modelling, it indirectly uses load currents to estimate parameters of nodal voltages along the feeder. Mean and variance parameters of the complex nodal currents were then used in the determination of voltage parameters through a simple voltage drop equation:

$$\boldsymbol{V} = \boldsymbol{IZ} \tag{6.4}$$

In a similar way, in this research load currents are drawn from a customer probability density function with given distribution parameters. The drawn values are considered as the real components of the nodal current I_R . Then, to enforce the power factors under investigation, we assume all customer loads are at the same power factor (characteristic of the substation power factor). This assumption allows the projection of the drawn current I_R onto the imaginary axis to obtain the quadrature component in the following manner:

$$I_I = I_R.\tan\emptyset \qquad ;where\ \emptyset\ is\ the\ power\ factor\ angle \tag{6.5}$$

This equation comes as a result of algebraic manipulations on the complex current equation given previously.

$$I^* = I_R - jI_I = \frac{P+jQ}{V_{nom}} = \frac{P+j(Ptan\emptyset)}{V_{nom}} \quad (6.6)$$

$$I^* = I_R - jI_R.\tan\emptyset \quad (6.7)$$

The voltage drops along the feeders are then calculated using the same Kirchhoff's Law based equations and the new expressions for nodal currents. This modified method is denoted as $MC_{MV\text{-}PF}$ for easy reference.

6.3. Modification of HB-algorithm to include power factor variations

In the preceding section, the derivation of Load-Flow equations for a feeder with loads of non–unity power factor resulted in complex nodal currents. Using the HB algorithm, which is dependent on the statistical distribution of load currents, complex nodal currents would lead to complex random variables which are difficult to deal with. This poses a computational challenge in the incorporation of power factor in the statistical voltage drop tool.

$$I_{nodal} = I_R + jI_I \quad (6.8)$$

$$I_{nodal} = C_b.[(X_1 + X_2 + \cdots + X_{ma}) + j(Y_1 + Y_2 + \cdots + Y_{ma})] \quad (6.9)$$

Equations 6.8 and 6.9 above illustrate the problem of complex statistical variables that is introduced with non-unity power factor loads. The random variables X and Y represent the individual consumer real and reactive current components drawn at an arbitrary node with *ma* connected consumers.

In other work, Celli *et al.* [23] used expected and standard deviation values of both the real and imaginary components of the nodal currents in the computation of voltage drop. This approach requires the re-formulation of statistical moments and network constants in the HB algorithm which is beyond the scope of this work.

An alternative way around this would be to compensate for the effects of power factor on voltage calculations in a similar way done in the previous chapter. To do this, we need to find out the direct effects of power factor on network quantities.

Power factor variation has a direct effect on customer load current. The phase load current, I_L, increases as power factor decreases. This is quantitatively illustrated by an equation relating power factor with current as follows:

$$I_L = \frac{P}{Vcos\emptyset} \quad (6.10)$$

- ***Where P and V are phase quantities denoting real power consumed and bus (or nodal) voltage respectively.***

Considering the phase quantities P_L and V to be constant, a low power factor as depicted by $cos\emptyset$ would result in a higher current than usual in the network. This causes increased voltage drops across electric components. To explain this, let us consider the current equation for a load drawing real power (unity power factor), P_L; we denote this current as I_{L-old}.

$$I_{L-old} = \frac{P_L}{V} \tag{6.11}$$

If the real power and voltage are considered constant, the nodal current I_{L-new} due to a change of power factor from unity to $cos\emptyset$ is given by:

$$I_{L-new} = \frac{P_L}{Vcos\emptyset} \tag{6.12}$$

I_{L-old} can be then substituted into equation 6.12 to obtain a relationship between the two load current variables.

$$I_{L-new} = \frac{I_{L-old}}{cos\emptyset} \tag{6.13}$$

Equation 6.13 describes a scaling function for the load current using load power factor. This means that low values of power factor lead to the inflation of the load current. In the proposed approach presented here, the input parameters for load current are modified through inflation with power factor to include the effects of non-unity power factor loads. The implementation of this approach is discussed in the section below.

Software implementation

The proposed approach to modify the current input parameters can easily be implemented through the inflation of the circuit breaker (or current scaling factor, C) magnitude. In so doing, all drawn load currents are higher than expected therefore simulating the increased current under lower power factors. Similarly, the statistical moments of load currents could be inflated with the power factor. In this way, a new distribution with higher current values is indirectly created.

MATLAB code to express the changes described above is given in the code snippet below:

```
pf = [0.8 0.85 0.9 0.95 0.98 1];% matrix of power factors under test
    … %declaration of other parameters and other code falls here
for index = 1:6   % loop used in the study of different pf scenarios
    C_b = C_b/pf(index);     % inflation of circuit breaker current
```

```
                                        % to simulate increase in load current
                                        % with power factor
```

OR

```
G = (alpha/(alpha+beta))/pf(index);
H = (((alpha*(alpha+1))/((alpha+beta)*(alpha+beta+1))))/pf(index)^2;
% scaling of statistical moments of customer load current to simulate
% increase in customer load currents with power factor.
```

The changes in the algorithm as indicated above are effected and the new algorithm compiled in preparation for testing. From here onwards the newly developed software will be referred to as HB_{MV-PF}. This software will be tested for errors and then validated through a comparison voltage drop calculation with the MCS software.

6.4. Testing the HB_{MV-PF} MATLAB software for errors

In this section, the HB software with input parameter adjustments, HB_{MV-PF}, is tested for coding errors. A similar test routine using the test network as described in Chapter 5 is used (cos330, 3 nodes, 1 km separation). The following changes are effected to the network parameters:

1. The conductor X/R ratio is unity for all cases under testing. This is so as to as to confine the investigation to typical MV feeder characteristics.
2. The consumer load power factor is unity for Test 1 and then set to 0.8 for Test 2 in the investigation of consistent voltage drop calculation across feeder phases.

The description of the tests conducted to test the newly generated software for errors follows.

6.4.1. Test 1: Voltage drop calculation comparison with $HB_{MV-|Z|}$

The first test checks for possible errors brought about by the new formulation of input parameters. The test is conducted through comparison of voltage calculations with $HB_{MV-|Z|}$ at consumer unity power factor load and X/R ratio. Under this condition, HB_{MV-PF} and $HB_{MV-|Z|}$ are expected to give the same voltage results since the network configurations and parameters are common. Identical results will demonstrate a correct modification of $HB_{MV-|Z|}$ without introducing errors in the code.

6.4.2. Test 2: Consistency of voltage drop calculation across the phases

Test 2 checks the consistency of HB_{MV-PF} in voltage drop calculations across all phases. To do this, an arbitrary case of $pf = 0.8$ is used for voltage computation on the feeder under a balanced load assignment, Bal 333. In this case, the voltage drop across the phases is expected to be the same.

6.4.3. Test Results

Table 7.1 below shows the results for the test 1. The test statistics reveal agreement of outcomes between HB_{MV-PF} and $HB_{MV-|Z|}$ in all the test variables with zero relative error.

Table 6-1: Test 1 results for error checks on MATLAB code for HB_{MV-PF}

Test Variable		$HB_{MV-\|Z\|}(X/R = 1)$		$HB_{MV-PF}(pf = 1)$	|Relative Error|
V_{max} (phase A)		11.964 kV		11.964 kV	0.00
V_{min} (phase A)		9.086 kV		9.086 kV	0.00
Beta parameters of Vcon (phase A)		α	43.5028		0.00
		β	32.2007		0.00
$V_{con_{10\%}}$	A	1.0530 kV		1.0530 kV	0.00
	B	1.0744 kV		1.0744 kV	0.00
	C	1.0341 kV		1.0341 kV	0.00
Voltage drop (%)	A	4.28		4.28	0.00
	B	2.32		2.32	0.00
	C	5.99		5.99	0.00

The correct calculation of voltages in agreement with $HB_{MV-|Z|}$ at unity power factor suggests that the modification to include variation of power factor was done without any alteration of the general voltage drop formulae. This however does not imply the modifications were principally correct. Another test for the validation of the modified HB algorithm has to be done to prove the accuracy of the proposed method. This validation will be done against a Monte-Carlo simulation as done in previous investigations.

Though the test results discussed above confirm correct implementation of voltage drop formulae in all three phases, it is necessary to further test the software for consistency of voltage drop calculations across the phases for a case of non-unity load power factor. This test at non-unity power factor (0.8 in this case) allows testing of HB_{MV-PF} with the utilisation of the modified part of the software. Table 6.2 shows the results for the test of consistency of voltage calculations across the phases using HB_{MV-PF} under a non-unity load power factor.

Table 6-2: Test results for consistency of voltage calculation across phases using HB_{MV-PF}

Test Variable		Phase A	Phase B	Phase C	|Relative Error
V_{max}		12.795kV	12.795kV	12.795kV	0.00
V_{min}		7.411kV	7.411kV	7.411kV	0.00
Beta parameters of Vcon	α	69.5045	69.5045	69.5045	0.00
	β	51.1800	51.1800	51.1800	0.00
$V_{con_{10\%}}$		1.0200kV	1.0200kV	1.0200kV	0.00
Feeder voltage Drop %		7.27	7.27	7.27	0.00

A zero relative error as obtained across all test variables confirms the correct implementation and consistency of the modified algorithm into code for the three phases.

Through performing these two tests we have gathered confidence in the correct representation of the intended voltage calculation approach in the code. To confirm validity of the proposed voltage calculation tool, voltage calculations on the MV test network are done and compared against results from $MC_{MV\text{-}PF}$ on the same network. The description of such tests follows.

6.5. Validation of $HB_{MV\text{-}PF}$ for voltage drop calculations on MV feeders

Earlier on in this report in Chapter 3, we established the need for inclusion of power factor in the assessment of voltage drop on MV feeders. This was motivated by the observation of variation of consumer voltage with load power factor. The consumer voltage was noted to decrease with power factor as load current increased. This sort of variation could not be achieved with the HB approach as voltage calculations are independent of load power factor. The new approach to voltage calculation on MV feeders discussed in this chapter attempts to solve that inadequacy.

This approach is now validated in this section. The test protocols are detailed as follows.

6.5.1. Test 1: Variation of consumer voltage with power factor

In this test, $HB_{MV\text{-}PF}$ is used to compute voltages on the MV test feeder with load power factors varied from 0.8 to unity. The resulting consumer voltage pdfs obtained from the different scenarios are plotted and analysed. A positive test is characterised by the gradual increase of consumer voltages as power factor values tend to unity. This result would confirm an appreciable level of compensation of the effects of non-unity power factor on voltage drop. The quantitative analysis on how well the noted variation in voltages compares to the expected variation is covered in Test 2.

6.5.2. Test 2: Validation of $HB_{MV\text{-}PF}$ using the MCS

Test 1 serves as a quick test to check the functionality of the proposed method. The achievement of the expected variation of voltages suggests the validity of the tested method without quantifying accuracy. The objective of Test 2 is to quantify the accuracy of the method through comparison with MCS voltage results on the same test network.

In this test, the results for voltage calculation performed on the test network are tabulated and compared. The calculation of relative error between the results from the two methods will allow the drawing of conclusions regarding the validity of the proposed approach.

6.6. Validation Results

6.6.1. Test 1: Variation of consumer voltage with load power factor

In order to confirm the significant compensation of power factor in voltage calculations, the variation of consumer voltages with power factor was tested. The expected variation according to the Monte-Carlo method is shown in Fig. 6.1 below.

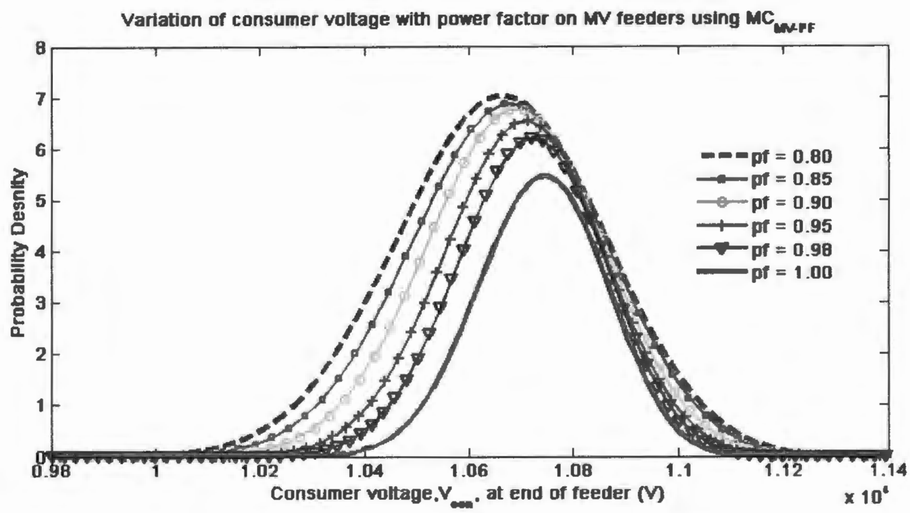

Figure 6.1: Variation of consumer voltage with power factor using MC_{MV-PF}

Figure 6.2 shows the outcome of voltage drop computations using HB_{MV-PF} on the test network for different values of load power factor. The plot shows a gradual increase of consumer voltage with power factor. Low consumer voltages are experienced under low power factor loads whilst high power factors result in better consumer voltages.

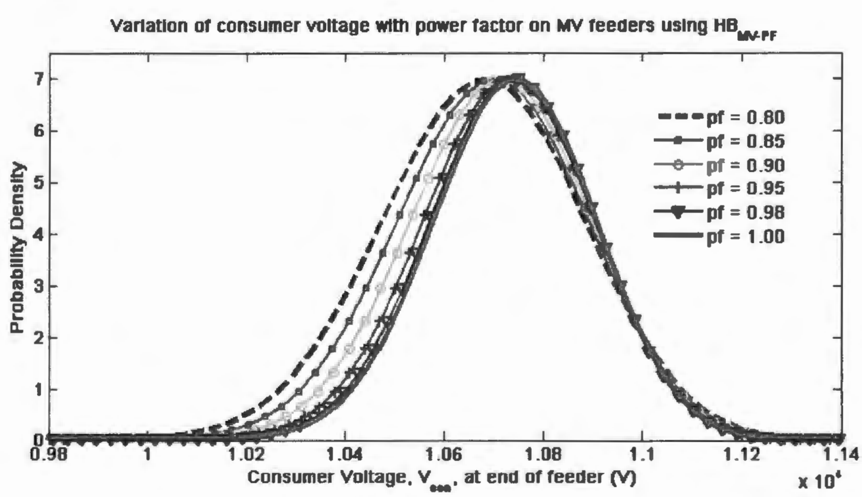

Figure 6.2: Variation of consumer voltage with power factor using proposed method HB_{MV-PF}

The variation of consumer voltage with power factor is consistent with the expected increase in voltage drop with falling power factor. However, as can be noted in the contrast between Fig. 6.1 and

2, the plots for $HB_{MV\text{-}PF}$ maintain the same height whilst the ones for $MC_{MV\text{-}PF}$ get shorter with the increase in power factor. This is an error on the distribution of voltages. Power factor changes are seen to cause much notable pdf transformations with $MC_{MV\text{-}PF}$ than $HB_{MV\text{-}PF}$. It is certain that the proposed approach successfully achieves the variation of voltages with power factor. However, it is a question as to how well it accomplishes this. To quantify its accuracy, a comparison of the voltage pdfs for the investigated cases was done.

6.6.2. Test 2: Comparison of voltage drop calculations between $HB_{MV\text{-}PF}$ and $MC_{MV\text{-}PF}$

Voltage drop calculations as per the described procedure outlined in section 6.5.1 were done and results tabulated as shown in Table 6.3.

Table 6-3: Voltage drop calculation comparison between $HB_{MV\text{-}PF}$ and $MC_{MV\text{-}PF}$ for different load power factors

Test Variables		Case 1 Pf = 0.80	Case 2 Pf = 0.85	Case 3 Pf = 0.90	Case 4 Pf = 0.95	Case 5 Pf = 0.98	Case 6 Pf = 1.00
$E(V_{con})$ (kV)	$MC_{MV\text{-}PF}$	10.659	10.670	10.684	10.703	10.715	10.737
	$HB_{MV\text{-}PF}$	10.675	10.694	10.711	10.726	10.735	10.740
	Error (V)	-16	-24	-27	-23	-20	-3
$Vcon_{10\%}$ (kV)	$MC_{MV\text{-}PF}$	10.404	10.436	10.471	10.508	10.537	10.580
	$HB_{MV\text{-}PF}$	10.412	10.446	10.477	10.505	10.520	10.530
	Error (V)	-8	-10	-6	3	17	50
$\%V_{drop}$ error		-0.07	-0.09	-0.05	0.03	0.15	0.45

The results for the expected value of consumer voltage show under-calculation errors with $HB_{MV\text{-}PF}$. The error margins are from as little as 3 V up to 27 V. The errors reflect the differences in the spread of the voltage pdfs from the two methods. The case of unity power factor results in the least error whilst all the other cases have an average error of about 20 V.

The percentile consumer voltage errors are generally lower than those observed with $E(V_{con})$ in all cases of power factor except unity. The differences in nodal voltages fall in the range 3-50V. This reflects a voltage drop calculation error of the range 0.03-0.45 % respectively. The unity power factor case obtains the greatest error. The error band shows that the method obtains a good estimation of the consumer voltages at different power factors. However, the high differences in the trend of error values between $E(V_{con})$ and the percentile voltages suggest incorrect spreads in the distribution pdfs from $HB_{MV\text{-}PF}$. This is analysed through comparing the output pdfs from the two methods for all the cases investigated. These plots are shown in Fig. 6.3.

With regards to the distribution of voltages, the method under test, $HB_{MV\text{-}PF}$ follows the MC_{MV} trace in a similar manner to that observed with X/R ratios in the previous chapter. At the lowest power factor, Fig. 6.3(a), the plots are well aligned only with slight error. As power factor increases, the $HB_{MV\text{-}PF}$ trace is seen to stretch right and upward, as shown in Fig. 6.3(b) and (c). This results in over-estimation of percentile voltages. This trend reverses in the case pf = 0.90. The $\text{HB}_{\text{MV-PF}}$ trace starts to stretch left and upward pulling the percentile voltage with it. The result of these transformations is a larger pdf centred on the $\text{MC}_{\text{MV-PF}}$ trace; as seen in Fig. 6.3(f) for the unity power factor case.

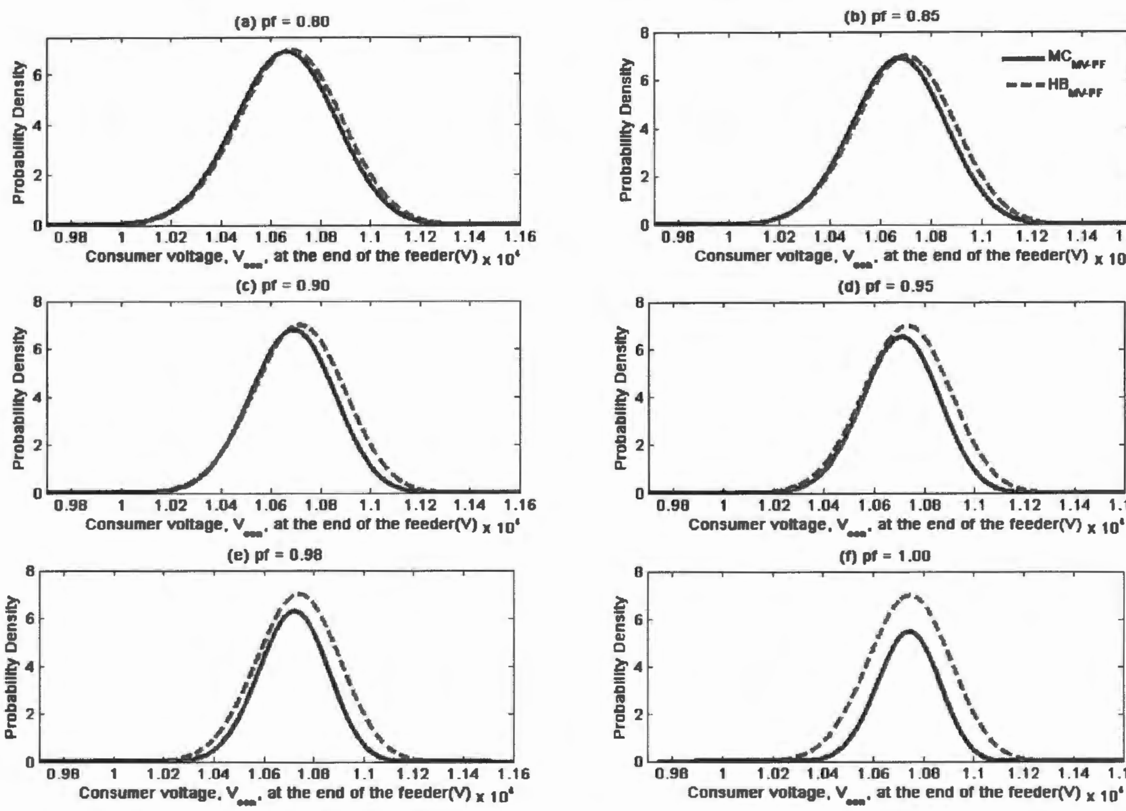

Figure 6.3: Spread of consumer voltages – HBMV-PF vs. MCMV for cases 7.2(a) pf = 0.80; 7.2(b) pf = 0.85; 7.2(c) pf = 0.90; 7.2(d) pf = 0.95; 7.2(e) pf = 0.98 and 7.2(f) pf = 1.00

Generally, it can be concluded that the distribution errors are acceptable since the tracking of the $\text{MC}_{\text{MV-PF}}$ is still accomplished. The misalignments when measured in volts are at most about 60V in the case of unity power factor in plot (f). This error could be as a result of over-estimation of worst case scenario voltages used to obtain the beta parameters of the voltage pdfs. Regardless of the misalignments of the $\text{HB}_{\text{MV-PF}}$ plots from the $\text{MC}_{\text{MV-PF}}$ ones, the percentile voltage error is still kept within acceptable limits.

6.7. Concluding remarks

Based on the findings from the investigation on the inclusion of the effects of power factor, the following conclusions can be made:

- The method of inflation of load current reasonably modelled the effects of lagging power factor on consumer voltages.

- The approach taken in this chapter proves to obtain appreciable accuracy in the calculation of feeder voltages, especially the resultant percentile voltages. However, the overall distribution of voltages builds up errors as load power factor increases towards unity. This is because the effects of lagging power factor on voltage drop becomes much less than that achieved through current inflation.
- There is need for advanced techniques in the modelling of non-unity power factor for a more accurate depiction of customer voltages.
- Reactive power loads (as modelled through the drawing of more current by non-unity power factor loads) result in increased voltage drops in the network. This is an undesired effect that potentially leads to poor power quality issues in the power system. Reactive power compensation is therefore an important area that deserves looking into.
- In the investigation being concluded here, a common power factor associated with a substation has been used to depict customer reactive current load profiles. This is so because load data is not that available for MV loads. If the power factors associated with each load are given, then the inflation of load current would be done for each load calculation. This does not alter the method presented here in any way.

Chapter 7

7. THE HB ALGORITHM AS A VOLTAGE CALCULATION TOOL ON MV ACTIVE FEEDERS

The previous chapters saw the successful adoption of the HB algorithm for voltage calculations on passive MV feeders. This was done through the modification of input parameters to include the effects of feeder reactance and non-unity power factor loads.

This chapter will cover the application of similar adjustments to the HB algorithm for LV active feeders to make it suitable for MV feeders. The performance of the resulting method on voltage calculations for MV feeders is assessed through comparative studies with the Monte-Carlo Simulation. Validity is then concluded based on the findings.

7.1. Introduction

As reflected in literature, the interconnection of distributed generators to distribution networks is ever increasing. The resultant active network with current injections differs from the classic network in which power flows only in one permissible direction. Current or power injections are useful in supplementing power generation for consumption by loads during periods of high demand. However, under extreme conditions troubles arise.

Under minimal loading and maximum DG generation, cases of over-voltages and the breach of branch thermal limits are likely to occur. Minimum generation under maximum loading would also result in an undesirable case of under voltages. Besides these two cases, the general intermittent and varied power generation nature of DGs may introduce rapid voltage changes in the network. All these cases require sensitive monitoring in order to avoid violation of stipulated voltage and current regulatory levels.

The tools applicable to passive networks consequently become inadequate in the assessment of voltage and current conditions in the network. Appropriate probabilistic tools are required in the assessment of these conditions in order to ensure power system reliability and quality of supply. As such, the HB method for active feeders, $HB_{a\text{-}LV}$, is adjusted to include the effects of feeder reactance and non-unity power factor.

7.2. Methodology

The investigations in this chapter merely involve the replication of modifications done to the HB algorithm for passive feeders to that for active feeders. This will then allow voltage calculations on active MV feeder using the HB method.

In the development of this new approach, the following assumptions and/or theories are carried through:

- **DG units only generate real power without reactive power generation or consumption.**
- **Generation units can be modelled using negative customer currents as supported in literature [56]. The beta distribution function can be used in the modelling of these currents.**
- **Connection of DG is done through separate nodes in order to maintain algebraic identity. The generator node is spaced 0.1 m from the load node.**
- **The presentation of DG as negative currents is implemented through assignment of generation units as a 'negative number of customers'.**
- **The complex feeder impedance will be approximated through its absolute value, $|Z_p|$.**
- **The loads are assumed to be of varied power factor. The current inflation method as presented in Chapter 6 for inclusion of non-unity power factor loads is maintained.**
- **A 10% design risk is used in the calculation of consumer voltages. For active feeders, a 90% confidence interval is used to extract the percentile voltage that resembles the risk.**

In the light of the above, the HB method for active LV feeders, $HB_{a\text{-}LV}$, is adjusted accordingly to obtain its MV translate, $HB_{a\text{-}MV}$. The following procedure is used in the testing of the developed algorithm.

1. **Algorithm with modified parameters, $HB_{a\text{-}MV}$ is tested for errors through a voltage calculation on a network with in-service generators, purely resistive feeders $(X_p = 0)$ and unity power factor loads $(pf = 1)$. Comparison against $HB_{a\text{-}LV}$ with $V_s = 11\ kV$ would show errors or tampering with the original HB voltage equations.**
2. **$HB_{a\text{-}MV}$ is tested for consistency in voltage drop calculations on typical MV feeder with unity X/R ratio, non-unity power factor loads and in-service generators. A balanced load and generator phase assignment method is used.**
3. **Negative results from procedures 1 and 2 are used to correct the algorithm. With each correction made, the test procedures are repeated again until passed.**
4. **After corrections and verifications, the algorithm is ready for validation. The Monte-Carlo Simulation performed on the test feeder is used to validate $HB_{a\text{-}MV}$. In the MCS, no**

assumptions or simplifications are done to the representation of feeder parameters or network elements.

7.3. Active MV test network configuration and parameters

7.3.1. Network Configuration

The same three-phase network which has been used in preceding chapters is maintained. However, in addition to the connected loads, generators are also connected to the feeder. Generator nodes are separated from the load nodes by a small distance of 0.1m. This is relevant in the modelling of customers with generators on site (same point as utility connection of load), be it industrial CHP or wind farms. The distance is however not fixed; it can be changed to any value as long as it is separated from the load nodes.

Fig. 7.1 below shows a simple 2-node network with lagging power factor loads, a complex impedance feeder and online generators.

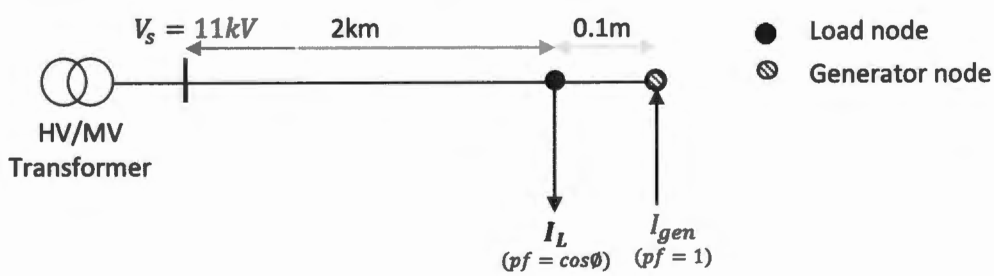

Figure 7.1: One line test network model for MV active feeder

In the diagram above, the power injection from installed generators is shown as a current source, I_{gen}. This is consistent with the model adopted as discussed earlier.

7.3.2. Network Parameters

A description of the network properties for the test network is given in Table 7.1. Some parameters will be varied in some tests but this will be done without changing the configuration of the test network.

It should be noted that the term 'customers' is being used to refer to both the number of connected loads and generators. This emanates from the consideration of generators as 'negative customers'. As has been highlighted before, under the list of assumptions and theories, the specification of the number of connected generators per phase should be given as a negative number.

The beta parameters for both loads and generation are assumed values (not network collected). Since the values are common to both the MCS and HB algorithms, the objectives of the investigations are still served.

Table 7-1: Network parameters for test network - active MV feeder

FEEDER PARAMETER	PARAMETER VALUE	
Sending Voltage, V_s	11kV	
Number of nodes	2	
Customer Phase Assignment	Node 1(**Load**)	4 4 4
	Node 2(**Generator**)	-1 -1 -1
Inter-nodal distance	0.1m Load-Gen separation,	
Load Current pdf parameters	Generator Node	Load Node
	$\alpha = 1.5$	$\alpha = 1.5$
	$\beta = 0.$	$\beta = 0.5$
	pf = 1.00	pf= 0.80
	C_b= 100 A[circuit breaker size]	
Conductor type	Copper Conductor, 35mm^{2}Cu	
	Temperature	T_1 = 20°C
		T_2 = 40°C
Feeder Impedance, X/R ratio	1	

The table above also shows that the circuit breaker size is common to both loads and generators. We assume that the generator maximum current is also 100A. This is not a restriction though; there can be a different specification to this scaling value depending on the connections of DG on the network. In the same way, the current pdf parameters can be differentiated from those of the loads without effect on the algorithm.

7.4. Algorithm changes to incorporate DG in MV feeder voltage calculations

7.4.1. Monte-Carlo Simulation

The Monte-Carlo method for passive MV feeders with complex impedance and non-unity power factor loads, $MC_{MV\text{-}PF}$ is modified to include generator nodes. This change only involves a sign change on the currents for generation. With this change, $MC_{MV\text{-}PF}$ is changed to $MC_{a\text{-}MV}$ where the subscript 'a' denotes active.

7.4.2. Modification of input parameters in the HB-algorithm

In order to adopt the HB algorithm for active LV feeders for calculation of voltages on MV feeders, the compensations done in Chapters 6 and 7 are carried over. These modifications are again given here for easy reference.

- Substitution of R with $|Z_p| = \sqrt{R_p^2 + X_p^2}$ for both load and generator node calculations
- Inflation of load currents with power factor in order to simulate the effects of non-unity power factor on feeder voltages. This is done through the inflation of the current scalar C_b for load nodes only (the injection or consumption of reactive power by generators is beyond the scope of this research).

$$C_{b-pf} = \frac{C_b}{pf} \tag{7.1}$$

The above listed changes are effected to the software for active LV feeders $HB_{a\text{-}LV}$. The resulting software is denoted $HB_{a\text{-}MV}$.

7.5. Error tests on $HB_{a\text{-}MV}$ MATLAB software

In this section, $HB_{a\text{-}MV}$ is tested for coding errors. The same test routine as presented in previous experiments is performed.

7.5.1. Test 1 – Comparison of $HB_{a\text{-}MV}$ with $HB_{a\text{-}LV}$ under LV conditions

Test involves error checking in the translation of the modified algorithm into MATLAB code through comparison of voltage calculations with $HB_{a\text{-}LV}$ for the condition $pf = 1 \; and \; \frac{X}{R} = 0$ (unity power factor loads on a purely resistive feeder). Under this condition, $HB_{a\text{-}LV}$ (with supply voltage V_s = 11kV) and $HB_{a\text{-}MV}$ are expected to give the same voltage drop results since the network configurations and parameters are common. Identical results will demonstrate correct adjustments to $HB_{MV\text{-}PF}$ without introduction of errors in the code.

7.5.2. Test 2 – Consistency of $HB_{a\text{-}MV}$ on voltage calculations across phases

This test checks the consistency of $HB_{a\text{-}MV}$ in voltage drop calculations across the phases. To do this, typical MV parameters ($pf_{loads} = 0.8 \; and \; \frac{X}{R} = 1$) are used. Customer assignment for both loads and generators is done using a balanced phase assignment method ($444L - 111DG$). Voltage calculations are done on the network and phase results compared. In this case, the voltage drop across the phases is expected to be the same. Identical results would confirm a consistent algorithm across the phases on the feeder.

7.5.3. Results for Error Tests on $HB_{a\text{-}MV}$

Test 1 Results

Table 7.2 shows the results for error checks run on the new software $HB_{a\text{-}MV}$. The test statistics reveal agreement of outcomes between $HB_{a\text{-}MV}$ and $HB_{a\text{-}LV}$ in all the test variables with zero relative error. The results confirm non-deviation from the voltage calculation methodology as used in the original algorithm.

Table 7-2: Test 1 results for error checks on MATLAB code for $HB_{a\text{-}MV}$

Test Variable		$HB_{a\text{-}MV}$ $(pf = 1, X/R = 0)$		$HB_{a\text{-}LV}$ $(V_s = 11kV)$		|Relative Error|
V_{max} (phase A)		11.677 kV		11.677 kV		0.00
V_{min} (phase A)		9.985 kV		9.985 kV		0.00
Beta parameters of Vcon (phase A)		α	43.6541	α	43.6541	0.00
		β	36.3671	β	36.3671	0.00
$V_{con10\%}$	A	11.028 kV		11.028 kV		0.00
	B	11.028 kV		11.028 kV		0.00
	C	11.028 kV		11.028 kV		0.00
Feeder voltage Drop %	A	-0.25		-0.25		0.00
	B	-0.25		-0.25		0.00
	C	-0.25		-0.25		0.00

The zero relative error in the test variables under the test conditions shows that the modifications done were with no error. The results on percentile voltage and voltage drop across the phases give confirmation of an error-free modification across the phases.

Though the test results discussed above confirm correct implementation of voltage drop formulae in all three phases, it is necessary to further test the software for consistency of voltage drop calculations across the phases for typical MV feeder parameters. This test with conditions of non-unity power factor loads and complex impedance feeder $\left(pf = 0.8; \frac{X}{R} = 1\right)$ allows testing of $HB_{a\text{-}MV}$ with utilisation of the modified parts of the software. The test results are given below.

Test 2 Results

Table 7.3 shows the results for the test of consistency of voltage calculations across the phases using $HB_{a\text{-}MV}$. Zero relative errors obtained in all test variables confirm the correct implementation and consistency of $HB_{a\text{-}MV}$ in voltage calculations in the three phases.

Table 7-3: Test results for consistency of voltage calculation across phases using $HB_{a\text{-}MV}$

Test Variable		Phase A	Phase B	Phase C	|Relative Error
V_{max}		12.117 kV	12.117 kV	12.117 kV	0.00
V_{min}		9.245 kV	9.245 kV	9.245 kV	0.00
Beta parameters	α	43.5589	43.5589	43.5589	0.00
	β	35.5479	35.5479	35.5479	0.00
$\|Vcon\|$ (10%)		11.031 kV	11.031 kV	11.031 kV	0.00
% voltage Drop		-0.28	-0.28	-0.28	0.00

Through performing these two tests we have gathered confidence in the correct representation of the intended algorithm in code. To confirm validity of the proposed voltage tool, voltage calculations on the MV test network are done and compared with results from $MC_{a\text{-}MV}$ on the same network. The description of such tests follows.

7.6. Validation of $HB_{a\text{-}MV}$ for voltage drop calculation on MV feeders

7.6.1. Test 1: DG only feeder

In this test, $HB_{a\text{-}MV}$ is used to calculate voltage drops on a feeder with DG connections only. DGs are then disconnected, and the same number of loads at unity power factor connected instead. The loads are at unity power factor just like the generators so that meaningful comparison can be made. Voltage calculations on the resulting feeder are done using $HB_{a\text{-}MV}$ at a confidence level of 10% (for passive feeders). A comparison of results from the two cases is done to ensure the algorithm is modified correctly to accommodate DG.

7.6.2. Test 2: Variation of consumer voltages with increased DG penetration

This validation test investigates the variation of consumer voltage with increased DG penetration on the feeder. DG penetration is varied uniformly through increasing the number of connected generators from zero to a value slightly above the load. The load remains constant in all test runs. For every case, $HB_{a\text{-}MV}$ and $MC_{a\text{-}MV}$ are used to compute feeder voltages. Comparison of the results is done quantitatively and graphically using output pdfs.

7.7. Validation results

7.7.1. Test 1

Voltage drop calculation results on the feeder for the tested cases described in Test 1 are given in Table 7.4. From the results, it is seen that the 'DG only' feeder obtains a voltage rise approximately equal to the value of voltage drop in the 'load only' feeder.

Table 7-4: Test results on correct DG modelling in $HB_{a\text{-}MV}$

Test Variables	$HB_{a\text{-}MV}$ 444L-000DG	$HB_{a\text{-}MV}$ 000L-444DG
α	36.1052	26.8961
β	26.5918	36.4853
$Vcon_{90\%}$ (kV)	10.672	11.327
V_{drop} (%)	2.9782	-2.9753

The slight difference in the results is because the generator node is 0.1 metres further on the feeder than the load node. The difference is therefore accounted for by the drop across the small length of feeder separating the nodes. The result confirms the correct modelling of DG as a negative load.

7.7.2. Test 2

The effects of increasing DG penetration on feeder voltages as analysed by $MC_{a\text{-}MV}$ are shown in Fig. 7.2. The concept of voltage rise is demonstrated in the plots given as voltage pdfs are pulled along the positive x-axis with the increase in DG penetration.

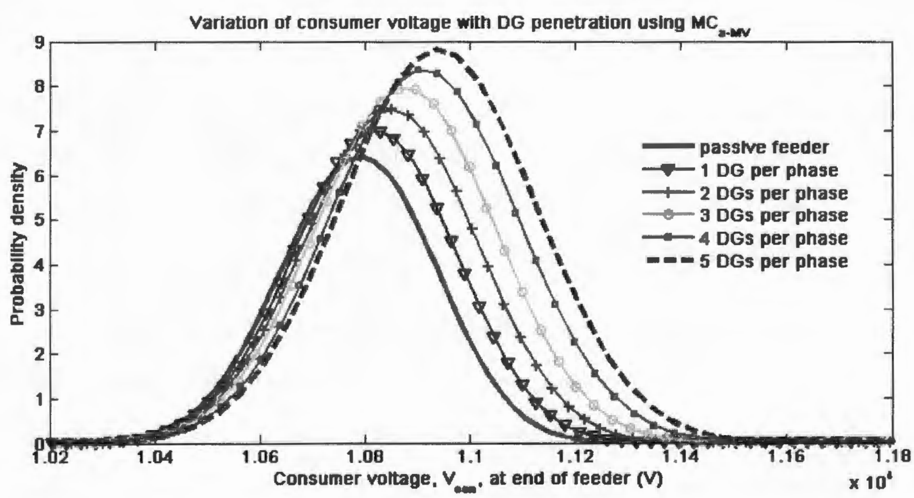

Figure 7.2: Variation of consumer voltage with DG penetration using $MC_{a\text{-}MV}$

The results agree with theoretical expectations of voltage regulation through DG. Since the DG injects current into the feeder, it is expected that voltages will increase. To check if the proposed approach is valid, the same investigation was conducted using $HB_{a\text{-}MV}$. The variation of voltage with DG penetration was plotted as shown in Fig. 7.3.

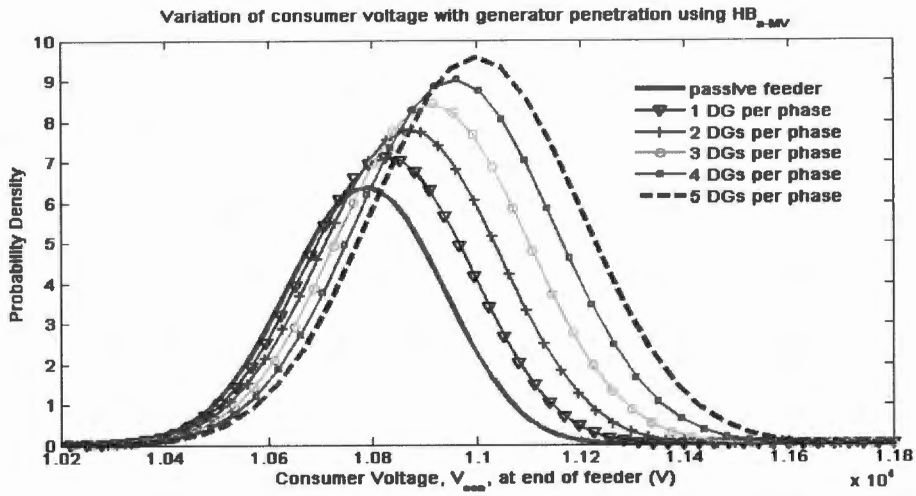

Figure 7.3: Variation of consumer voltage with DG penetration using $HB_{a\text{-}MV}$

The expected variation in consumer voltage is achieved as shown. However, the increase in voltages from case to case seems higher than that observed in Fig. 7.2 with $MC_{a\text{-}MV}$. The bases of the pdfs also look slightly pulled to the right in Fig. 7.3 compared to Fig. 7.2. This can be seen clearly in the last case (blue dashed line). In the $HB_{a\text{-}MV}$ results, the trace touches the x-axis at point x = 11.6 kV whilst it does the same at about x = 11.5 kV for $MC_{a\text{-}MV}$. It can be concluded that the test result is positive but levels of accuracy need to be determined. To do this, a quantitative analysis of the results is done.

Test results on the variation of consumer voltage with DG penetration are given in Table 7.5. The results show similar voltage values between the two methods for both test variables $E(V_{con})$ and $V_{con90\%}$. The relative error noted in the results increases with DG penetration. The maximum error of 79V (for percentile voltages) is noted in Case 6. This error is small since it corresponds to a voltage drop error of 0.72% only.

Table 7-5: Voltage drop calculation comparison between $HB_{a\text{-}MV}$ and $MC_{a\text{-}MV}$ for different DG penetration cases

Test Variables		Case 1 444L-000DG	Case 2 444L-111DG	Case 3 444L-222DG	Case 4 444L-333DG	Case 5 444L-444DG	Case 6 444L-555DG
$E(V_{con})$	$MC_{a\text{-}MV}$	10.783	10.814	10.847	10.877	10.909	10.941
	$HB_{a\text{-}MV}$	10.783	10.826	10.870	10.913	10.957	11.001
	Error (V)	0	-12	-23	-36	-48	-60
$Vcon_{90\%}$ (kV)	$MC_{a\text{-}MV}$	10.972	11.013	11.055	11.093	11.138	11.176
	$HB_{a\text{-}MV}$	10.973	11.031	11.088	11.145	11.200	11.255
	Error (V)	1	-18	-33	-52	-62	-79

The results also show greater error values in the percentile voltages than in the expected values (means) of voltage. This is because of the differences in skewness of the voltage pdf from the two methods. These differences as seen in the results are quite small. In order to observe the accuracy of the proposed method, voltage pdfs for the different cases are plotted and comparisons between the two methods made.

Plots in Fig. 7.2 show a stretch transformation to the right on the $HB_{a\text{-}MV}$ plots. The plots are pinned to the same base point on the left side but the base increases to the right with DG penetration. Hence the pdfs get more misaligned, as shown in Fig. 7.4 below. The misalignment error, as reflected from the quantitative analysis, is not much when expressed as a voltage difference. Its correlation to DG penetration is however worrying. This error should be as a result of the approximation of the complex feeder impedance with |Zp| for the DG nodes. This is supported by the fact that load quantities are kept constant throughout the investigation. Therefore, the noted errors should be from the voltage calculations for the DG nodes. A further analysis on this is lodged in the subsequent section.

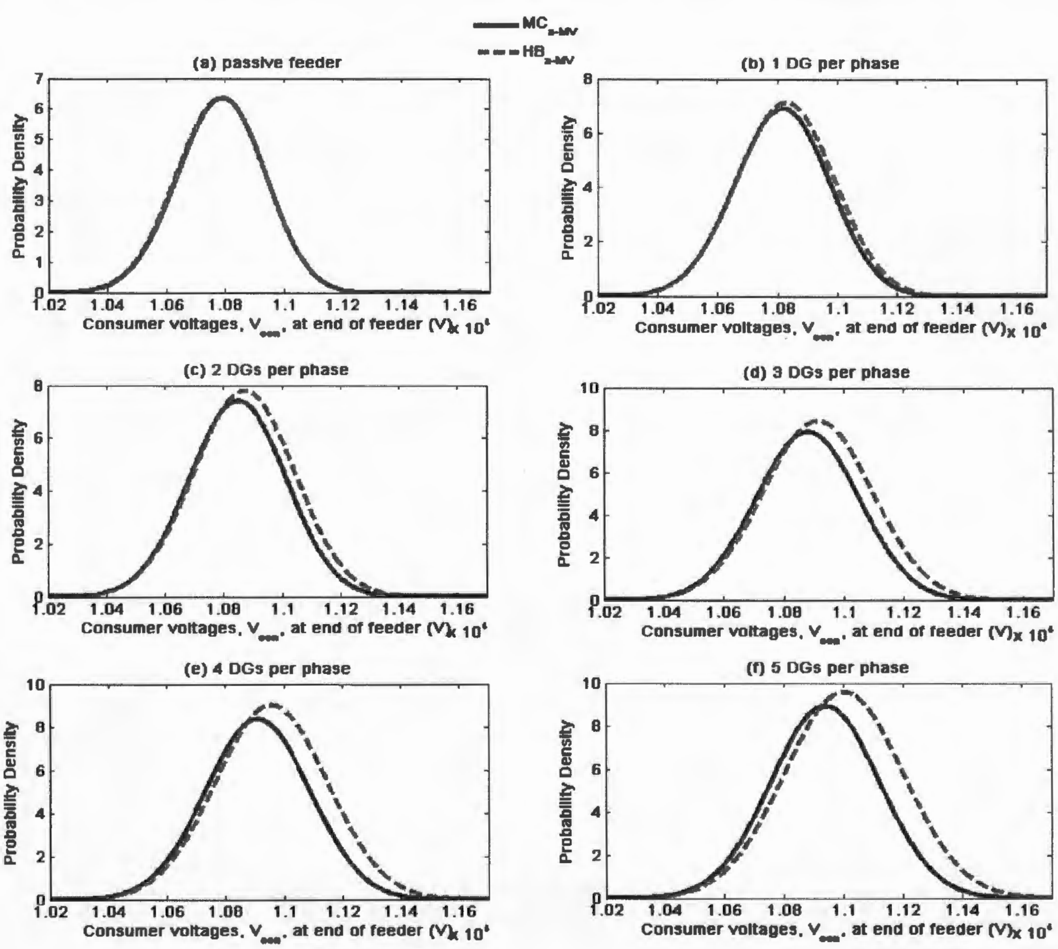

Figure 7.4:Spread of consumer voltage, $MC_{a\text{-}MV}$ vs. $HB_{a\text{-}MV}$ for cases (a) passive feeder;(b) 444L-111DG (c) 444L-222DG; (d) 444L-333DG; (e) 444L-444DG and (f) 444L-555DG

7.8. Improvement of $HB_{a\text{-}MV}$

The increase in error in the calculation of voltages, seen in the preceding section, is as a result of the over-estimation of voltage drops due to the connected generators. These generators are supplying real power and therefore are 'negative loads' at unity power factor. Generally, on a feeder with unity power factor loads, the effects of line reactance on voltage drop are quite insignificant. The assumption of a resistive feeder should hence work better than using the absolute value |Zp|, which would result in substantial increases in voltage drops (or voltage rise in case of DG).

To investigate this, the calculation of voltages on the test feeder was repeated without the compensation of input parameters to include feeder reactance at DG nodes. However, the adjustments made in the calculation of voltages for the load nodes are maintained.

Results

The plots in Fig. 7.5 show a remarkable improvement on the accuracy of the consumer voltage profiles. All subplots show great alignments between $HB_{a\text{-}MV}$ and $MC_{a\text{-}MV}$ traces. The slight errors noted in Fig. 7.5(d) and (e) could be because of the limited iterations in the Monte-Carlo or possibly due to the increased penetration of DG. Nonetheless, these errors are quite small.

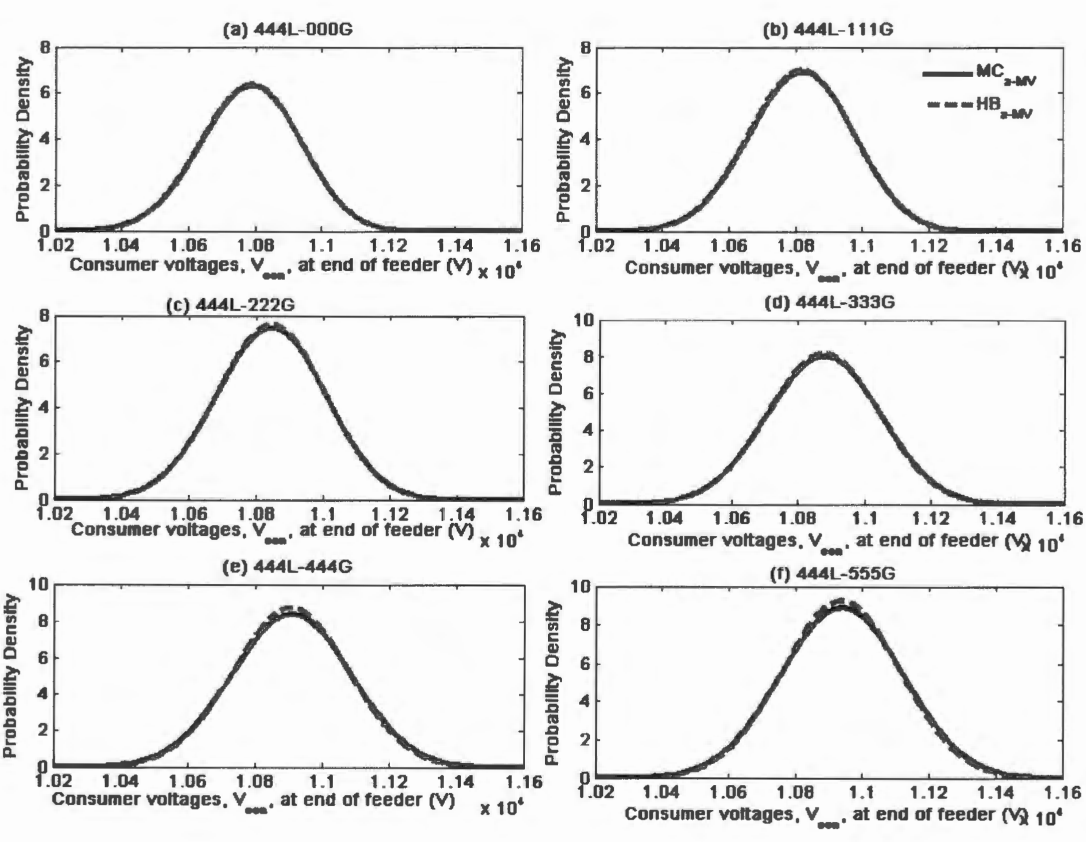

Figure 7.5: Spread of consumer voltage, $MC_{a\text{-}MV}$ vs. improved $HB_{a\text{-}MV}$ for cases (a) passive feeder;(b) 444L-111DG (c) 444L-222DG; (d) 444L-333DG; (e) 444L-444DG and (f) 444L-555DG

The results demonstrate that the inclusion of DG in the calculation of voltages does not introduce notable errors. In other words, the error in the whole calculation of voltages on an active feeder would be largely due to the errors in the calculations for the loads. This of course applies to unity power factor generators. The consideration of non-unity power factor generators, which is beyond the scope of this study, would require the same input parameter adjustments as done for loads. In this case, similar but reversed errors to those found in calculations for the loads would be expected.

7.9. Concluding remarks

The investigations conducted in this chapter led to the following conclusions:

- The approach to the calculation of voltage drops on feeders with DG done in $HB_{a\text{-}LV}$ works well in MV systems.
- Errors initially noted as a result of over-compensation of feeder reactance in voltage drop calculations for DG nodes were eliminated by assuming resistive feeder for DG nodes. This approach works well for unity power factor loads (positive or negative) since the effects of reactance on voltage drop are minimised in such cases.
- The approach of modifying the input parameters at load nodes without altering the parameters for DG nodes works satisfactorily well. The errors seen in the active feeder calculations are indistinguishable to those noted in passive feeders, suggesting that the errors (if any) resulting from including DG are insignificant.

Chapter 8

8. VOLTAGE REGULATION IN MEDIUM VOLTAGE NETWORKS: SHUNT CAPACITORS

Chapter 6 shed light on the effects of reactive power flow in power systems that may be undesirable. The reduction of bus voltages as a result of low power factor loads affects system reliability and quality of supply. Power factor correction, voltage regulation and reactive power compensation are therefore required in the restoration of bus voltages to permissible margins and the improvement of power transmission efficiency in the power system.

This chapter concerns the analysis of voltage regulation techniques in MV networks using the HB algorithm with modified input parameters. The effects of shunt capacitors as voltage regulators on MV radial feeders are explored through nodal voltage analysis. The application of the HB algorithm in the assessment of this network configuration forms the objective of this chapter. The Monte-Carlo Method is used as a validation tool through comparison of voltage calculations in the network.

8.1. Shunt capacitor banks as voltage regulation tools in MV networks

Shunt capacitors are often used in MV networks to supply reactive power requirements by loads thereby reducing reactive power flow in the network. These capacitors are often located near the loads to ensure optimal compensation. The thermal capacity of the network is substantially released as the current flowing in the network is reduced through the VAr compensation effect. The injection of reactive power from the capacitors, Q_C, improves the power factor as apparent power is reduced. Shunt capacitor implementation in power systems has the following advantages:

- Minimisation of system losses
- Improvement of quality of supply as nodal voltages are raised
- Improvement of voltage regulation
- Release of power system thermal capacity

To obtain optimal compensation performance from the capacitor banks, positioning and sizing has to be done carefully with assessment of impacts through load flow studies coupled with optimisation algorithms. In this work, we are interested in the development of the power flow analysis tool in such networks with voltage regulation network elements.

8.1.1. MV network model with inclusion of shunt capacitors

A simple three-node network with lagging power factor loads, a complex impedance feeder and installed shunt capacitor bank as shown in Fig. 8.1 is used.

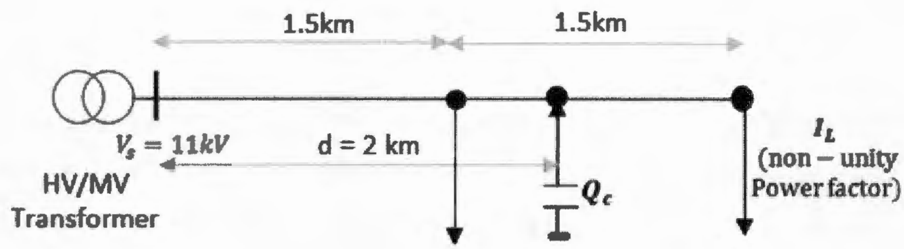

Figure 8.1: One-line network model for MV feeder with shunt capacitor

In the network model illustrated above, the shunt capacitor bank works by injecting reactive power, Q_C into the feeder at a distance, d, from the substation transformer.

8.1.2. Network Parameters

A description of the network parameters for the test network in this investigation is given in Table 8.1.

Table 8-1: Test network parameters for MV feeder with shunt capacitor

FEEDER PARAMETER	PARAMETER VALUE	
Sending Voltage, V_s	11kV	
Number of nodes	3	
Customer Phase Assignment	Node 1(**Load**)	4 4 4
	Node 2(**Shunt Cap.**)	1 1 1
	Node 3(**Load**)	4 3 2
Inter-nodal distance	*(See Fig. 8.1)*	
Load Current pdf parameters	Capacitor node	Load Node
	$I_C = 1.50^*C_b$	$\alpha = 1.5$
		$\beta = 4.0$
		pf= 0.80
	C_b= 100 A[circuit breaker size]	
Conductor type	Copper Conductor, $35mm^2$Cu	
	Temperature	$T_1 = 20°$
		$T_2 = 40°$
Feeder Impedance, X/R ratio	1	

Loads on the first and third nodes are drawing lagging power factor currents modelled by a beta pdf whereas at the second node, capacitor banks injecting a current j1.50p.u are connected.

The placement of the capacitor banks on the feeder is an important task. For a single node, the placement at the same place as the load is most effective as it avoids the flow of reactive power over distances. However with multiple load nodes on the feeder, it is not economical to have capacitors on every node. Hence, optimal positioning of the capacitors is required so as to achieve maximal voltage regulation with fewer capacitors. To do this, optimisation techniques such as genetic algorithms are required. However, for simplicity, a rule of thumb which stipulates placement of capacitor banks at a point 2/3 of the targeted feeder section is adopted [57]. The nodal distances between the capacitor and loads given in Table 8.1 are based on this placement criterion. The separation of the load nodes from the capacitor also helps establish distinct current flow on the feeder and in maintaining algebraic identity when analysing the network.

8.2. Monte-Carlo method for voltage calculation on MV feeders with shunt capacitors

The algorithm for voltage calculations on feeders with non-unity power factor loads, $MC_{MV\text{-}PF}$ is extended to include shunt capacitors. To do this, the capacitive reactive power is added to the inductive reactive power component of the load. Since the reactive power from the capacitor is leading while that drawn by the load is lagging, a negative sign is used to denote this power Q_C. The total apparent power is then given by:

$$S = P + j(Q - Q_C) \tag{8.1}$$

Where:

Q is the load reactive power component

Q_C is the Var rating of the shunt capacitor

The above equation can be used to get nodal currents through division with the nominal voltage as done for the loads. The resulting nodal currents equations are given by:

$$I^* = I_R + j(I_I - I_C) = \frac{P+j(Q-Q_C)}{V_{nom}} = \frac{P+j(Ptan\emptyset-Q_C)}{V_{nom}} \tag{8.2}$$

Where:

I_R is the per unit real component of the load current

I_I is the per unit imaginary component of the load current

I_C is the per unit capacitor current

In the equation above, I_I and I_R are variables described by a beta distribution function. On the other hand, I_C, the capacitor current is a constant variable. This means that, as random variables for the load currents are drawn in iteration, the value of I_C remains the same since it is deterministic. Alternatively, this current could be modelled by a beta pdf with high, equal alpha and beta parameters. However, the representation through a constant value will be used in this study.

If the capacitor banks and loads are not tied to the same node, the equation for nodal currents is simply broken down into two parts as follows:

$$I_{loads} = I_R - jI_I = I_R - jI_R \tan\emptyset \tag{8.3}$$

$$I_{cap} = -(-jI_C) = jI_C \tag{8.4}$$

Using the nodal currents and the impedance of the feeder in, the voltages on the feeder can be determined.

$$\boldsymbol{V = IZ} \tag{8.5}$$

The calculation of voltages for the load nodes is done using the equations implemented in $MC_{MV\text{-}PF}$. The method for voltage calculation for the compensator nodes is discussed below.

Voltage calculation for shunt capacitors

The voltage drop equations for shunt capacitor nodes are derived in the same way as done for consumer loads in Chapter 3, section 4.1. The only difference is that the current in question is a fixed imaginary quantity. The substitution of phase currents with jI_C yields the following equations:

$$dV_{i-R} = -\left[I_{C(a)}X_p(1+k) - \frac{1}{2}kX_p\left(I_{C(b)} + I_{C(c)}\right) + \frac{\sqrt{3}}{2}kR_p\left(I_{C(b)} - I_{C(c)}\right)\right] \tag{8.6}$$

$$dV_{i-I} = I_{C(a)}R_p(1+k) - \frac{1}{2}kR_p\left(I_{C(b)} + I_{C(c)}\right) + \frac{\sqrt{3}}{2}kX_p\left(I_{C(b)} - I_{C(c)}\right) \tag{8.7}$$

$- \textit{where } I_{C(a,b,c)} \textit{denotes the compensator injected current in phase } a, b \textit{ and } c \textit{ respectively}$

The Monte-Carlo software, $MC_{MV\text{-}PF}$, is updated with the latest versions of voltage drop equations (8.6 and 8.7). This newly formulated algorithm is denoted $MC_{MV\text{-}SC}$.

8.3. Using the HB-algorithm to calculate voltages on compensated feeders

8.3.1. Discussion of proposed approach

Shunt capacitors have an effect of voltage rise on feeder buses. The increase in shunt capacitor size increases capacitor leading currents and consequently increases consumer voltages. The effects of capacitors therefore oppose that of loads. This is similar to the DG effect. It would be reasonable to model shunt capacitors as negative loads injecting current into the feeder; except that the current is on the imaginary axis.

In Chapter 6, an approach to the calculation of voltages on feeders with lagging power factor loads was discussed. This approach involved the inflation of load currents in order to compensate for the effects of non-unity power factor on voltage drop. The approximation was necessary since the HB algorithm does not accommodate imaginary currents in its formulation.

Reactive compensators are similar to inductive loads in the sense that they also draw imaginary currents from the network. The difference lies in the sign of this current and the effects they cause. Inductive loads draw negative imaginary currents whilst capacitive loads (compensators in this case) draw positive imaginary currents. Furthermore, inductive loads have the effect of increased voltage drops on the feeder whilst compensators cause voltage rise through their leading currents. Using this analysis, the current inflation method applied to lagging power factor loads can be extended, inversely, to capacitor compensators.

The following procedure explains the manner in which the approach is applied:

1. *Model compensator as 'negative load'*

   Since the effects caused by capacitor banks on voltage drop are opposite to those of loads, consider capacitors as negative loads with a fixed current.
2. *Calculate the imaginary compensator current*

   Calculate the imaginary compensator current. To do this, the rating of the capacitor banks in kVArs together with the nominal phase voltage is used. In order to match the presentation of current quantities in the HB algorithm, the compensator current is expressed in terms of a current scalar, C. This quantity could be assumed to be the same as that used for loads.
3. *Compensate for effects of imaginary current on voltage drop*

   In previous chapters, the effects of lagging power factor were acceptably simulated by the inflation of load current with power factor. Since the inverse effect is sought for, the scaling of load (capacitor) current by the average feeder power factor should be a reasonable approach. This, in the same way as applied to loads, is an approximation of the effects of an imaginary current on voltage drop.

4. *Use algorithm for active feeders, $HB_{a\text{-}MV}$ to calculate voltages*

   The modelling done thus far is similar to that done for generators in the preceding chapter. The only difference is that instead of real power injection, reactive power injection occurs. The last step done to improve $HB_{a\text{-}MV}$ by neglecting feeder reactance for the DG operating at unity power factor is ignored. This is because voltage drops due to feeder reactance are substantial under reactive power flow. In light of this, the compensation of the effects of reactance using $|Z_p|$ is applied to the compensator node (DG node in $HB_{a\text{-}MV}$).

8.3.2. Application of approach

Consider a capacitor bank of size Q_C VArs connected to Phase A. Assuming the nodal voltage at the point of connection is equal to the nominal phase voltage, V_{nom}, the compensator current I_{Cap} is calculated as follows:

$$S = -jQ_C = I_{Cap}^{*} V_{nom} \tag{8.8}$$

$$I_{Cap} = \frac{jQ_C}{V_{nom}} \tag{8.9}$$

Since the imaginary current cannot be represented in the HB algorithm, the inflation method is applied to compensate for the effect of this current on voltage drop.

$$I_C = |I_{Cap}|.\cos\emptyset \tag{8.10}$$

The next step involves the representation of this current in the same way in which current quantities are represented in the HB algorithm. The current is represented as a fraction of the current scalar value C_b as done for loads. The scaling is done as shown in equation 8.11 below.

$$I_C = \sum_{i=1}^{ma} C_b * I_{C_{pu}} \tag{8.11}$$

In the equation above, the variable ma carries a similar meaning as before; in this case, the total number of capacitor banks connected to that phase at the node in question. The variable $I_{C_{pu}}$ is a deterministic (fixed) value which denotes the compensator current as measured in terms of the scalar value C_b. To allow calculation of voltages using the HB method, the first and second order expected values of the capacitor current are required. These are calculated through equations 8.12 and 8.13.

$$G = E\left(I_{C_{pu}}\right) = I_{C_{pu}} \tag{8.12}$$

$$H = E\left(I_{C_{pu}}^{2}\right) = I_{C_{pu}}^{2} \tag{8.13}$$

$$- \, where \, I_{C_{pu}} is \, a \, constant$$

The two values will substitute the G and H values used to describe the distribution of load currents in $HB_{a\text{-}MV}$.

The changes to the input parameters as indicated above are effected on $HB_{a\text{-}MV}$ and the new algorithm compiled in preparation for testing. From here onwards, the newly developed software is referred to as $HB_{MV\text{-}SC}$. This software will be tested for errors and then validated through a comparison voltage drop calculation with the Monte-Carlo software.

8.4. Testing the accuracy of the $HB_{MV\text{-}SC}$ MATLAB software

In this section, the developed algorithm encoded into MATLAB code, $HB_{MV\text{-}SC}$, is tested for coding errors. The same test routine as presented in previous experiments is performed in this section. The tests conditions and/or parameters used in the tests are given below.

i) Tests are based on the test network as described in sections 8.1.1 and 8.1.2 only with deviations as detailed in the points below.
ii) In Test 1, the capacitor banks are switched off $[capacitor \; array - (0\;0\;0)]$.
iii) In Test 2 a balanced load assignment is used. For loads, the Bal 444 is used for both Node 1 and 3. Node 2 remains unchanged.

A further description of the tests is given below:

8.4.1. Test 1: Voltage drop calculation comparison with $HB_{a\text{-}MV}$

This test involves checks if the modification of input parameters to include shunt capacitor banks were done without altering the general voltage drop formulae in the HB algorithm. This is done through comparison of voltage calculations with $HB_{a\text{-}MV}$ (with no DG) for the condition $I_C = 0$ (switched off capacitors). Under this condition, $HB_{a\text{-}MV}$ and $HB_{MV\text{-}SC}$ are expected to give the same voltage drop results since the network configurations and parameters are common. Identical results will demonstrate a correct implementation of the proposed approach without introduction of error in the code.

8.4.2. Test 2: Consistency of $HB_{MV\text{-}SC}$ on voltage calculations across phases

The purpose of this test is to ensure that the voltage drop algorithm is consistently applied across all phases. To do this, the capacitors are switched on drawing a leading current $I_C = j1.50p.u$ (where p.u refers to the expression of this quantity as a fraction of C_b). Voltage computation under a balanced load and capacitor assignment is then done. In this case, the voltage drop across the phases is

expected to be the same. Identical results would confirm a consistent algorithm across the phases on the feeder.

8.4.3. Test Results for error checks on $HB_{MV\text{-}SC}$

Table 8.2 shows the results for Test 1. The test statistics reveal agreement of outcomes between $HB_{a\text{-}MV}$ and $HB_{MV\text{-}SC}$ in all the test variables with zero relative error.

The results confirm that the modifications done to the input parameters to include shunt capacitors were with no error. Table 8.2 also confirms the phase voltage variation expected as a result of the phase assignment pattern. Phase C is seen to have the lowest voltage drop as it has the least load connected to it.

The correct calculation of voltage drops for feeders with off-service capacitors suggests that the modification to include shunt capacitors was done without alteration of the general voltage drop formulae. This however does not imply the modifications were principally correct. Another test for the validation of the $HB_{MV\text{-}SC}$ has to be done to prove the accuracy of the proposed method. This validation will be done against $MC_{MV\text{-}SC}$.

Table 8-2: Test 1 results for error checks on MATLAB code for $HB_{MV\text{-}SC}$

Test Variable		$HB_{a\text{-}MV}$ $(pf = 0.8, no\ DG)$		$HB_{MV\text{-}SC}$ $(Q_C = 0; pf = 0.8)$		|Relative Error|
V_{max} (phase A)		12.349 kV		12.349 kV		0.00
V_{min} (phase A)		7.411 kV		7.411 kV		0.00
Beta parameters of Vcon (phase A)		α	57.6293	α	57.6293	0.00
		β	37.9176	β	37.9176	0.00
Consumer Voltage $\|Vcon_{10\%}\|$	A	1.0070 kV		1.0070 kV		0.00
	B	1.0303 kV		1.0303 kV		0.00
	C	1.0541 kV		1.0541 kV		0.00
Feeder voltage Drop %	A	8.45		8.45		0.00
	B	6.33		6.33		0.00
	C	4.17		4.17		0.00

Though the test results discussed above confirm an expected trend of voltages across the phases, we do not know if the inclusion of capacitors does not affect this. It is therefore necessary to perform another test with uniform loading and in-service capacitors to confirm consistent voltage calculations across the phases.

Table 8.3 shows the results for the test of consistency of voltage calculations across the phases using $HB_{MV\text{-}SC}$ with in service shunt capacitors.

Table 8-3: Test results for consistency of voltage calculation across phases using $HB_{MV\text{-}SC}$

Test Variable		Phase A	Phase B	Phase C	|Relative Error|
V_{max}		13.114 *kV*	13.114 *kV*	13.114 *kV*	0.00
V_{min}		7.2502 *kV*	7.2502 *kV*	7.2502 *kV*	0.00
Beta parameters of Vcon	α	78.4605	78.4605	78.4605	0.00
	β	54.7990	54.7990	54.7990	0.00
Consumer Voltage $\|Vcon_{10\%}\|$		1.0381 *kV*	1.0381 *kV*	1.0381 *kV*	0.00
Feeder voltage Drop %		5.63	5.63	5.63	0.00

A zero relative error obtained across all test variables confirms the correct implementation and consistency of the voltage drop algorithm in the three phases.

Through performing the two tests, we have gathered confidence in the correct representation of the proposed methodology in code. To confirm validity of the proposed voltage tool, voltage calculations on the MV test network are done and compared against results from $MC_{MV\text{-}SC}$ on the same network. The description of such tests follows.

8.5. Validation of $HB_{MV\text{-}SC}$ for voltage drop calculation on compensated MV feeders

8.5.1. Description of Tests

It has been established that consumer voltages (bus voltages) fall with power factor. The result of reactive power compensation is therefore increase in nodal voltages. The increase in shunt capacitor size is expected to decrease voltage drops consequently increasing consumer voltages.

To validate the proposed algorithm, we first check for the expected voltage variation basing on the variation obtained with the Monte-Carlo simulation. Once variation is affirmed, a quantitative comparison of the two methods will provide information on the accuracy of the proposed algorithm. To summarise this, the tests to be performed are:

1. Test 1 – confirmation of the variation of consumer voltage with shunt capacitor size.
2. Test 2 – quantitative comparison of the accuracy of $HB_{MV\text{-}SC}$ with $MC_{MV\text{-}SC}$.

Both tests are based on the test network and parameters as described in sections 8.1.1 and 8.1.2. The only modification is that the shunt capacitor size is varied from 0 – 2.50p.u in steps of 0.5.

8.5.2. Tests results for the validation of $HB_{MV\text{-}SC}$

Test 1: Variance of consumer voltage with shunt capacitor compensation

The effect of VAr compensation using shunt capacitors as investigated through $MC_{MV\text{-}SC}$ is demonstrated in Fig 8.2. The consumer voltage is noted to increase with shunt capacitor size. The variance and distribution of consumer voltages is seen to change with the introduction of compensation on the feeder (purple, box marked trace).

After this, the shape of the distribution seems to remain unchanged. The variation thereafter seems to be a graphical translation on the voltage axis in the positive x direction. The plot shows improvement in voltage regulation on the feeder.

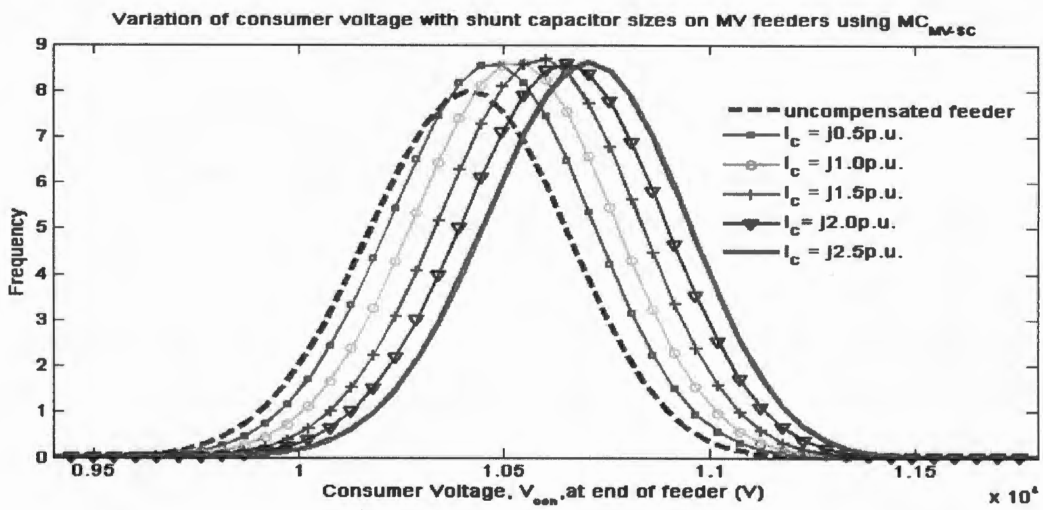

Figure 8.2: Variation of consumer voltage with increases shunt capacitor compensation - Monte-Carlo Method

Voltage computations on the feeder using the developed algorithm, $HB_{MV\text{-}SC}$, obtained a similar variation to that achieved with the Monte-Carlo simulation as shown in Fig. 8.3. Voltage drops on the feeder decrease (consumer voltage increase) with increased compensation from shunt capacitors. A similar change in voltage pdf shape shown with the initial switching on of capacitors is also evident in the purple trace in Fig. 8.3. From this trace, the distribution of voltages is more or less kept constant whilst the trace is shifted positively along the voltage axis. This trend of consumer voltage increase with compensation matches the anticipated variation. However, the traces in Fig. 8.3 are generally slightly taller than the Monte-Carlo ones. This means that the voltages are more concentrated around the mean for $HB_{MV\text{-}SC}$ than they are in $MC_{MV\text{-}SC}$. This is likely to slightly raise the 0.1 percentile voltage value in $HB_{MV\text{-}SC}$.

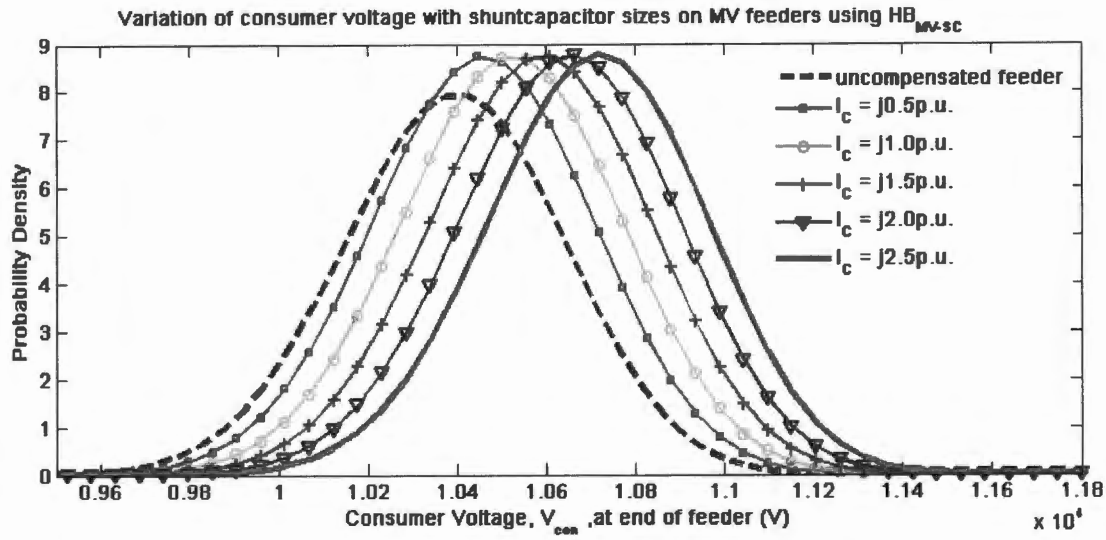

Figure 8.3: Variation of consumer voltage with capacitor compensation using proposed method $HB_{MV\text{-}SC}$

The increase in consumer voltage drop with capacitor compensation is consistent with the discussed theory. The capacitors have an effect of thermal loading reduction on the feeder. Current flow in the feeder is decreased resulting in reduced voltage drops.

The verification of voltage variation with VAr compensation partially confirms the validity of the developed method for voltage calculations on MV feeders with installed shunt capacitors. It is concluded that Test 1's outcome is positive. However, for a full validation Test 2 is necessary.

Test 2: Comparison of voltage drop calculations between $HB_{MV\text{-}PF}$ and $MC_{MV\text{-}PF}$

As motivated under the description of tests, a quantitative comparison of voltage results between $MC_{MV\text{-}PF}$ and $HB_{MV\text{-}PF}$ is necessary in determining the accuracy of the latter. The numeric results of consumer voltage calculations for different capacitor compensation levels are tabulated in Table 8.4. The same test variables as used in preceding experiments in this report are maintained.

Table 8-4: Voltage drop calculation comparison between $HB_{MV\text{-}SC}$ and $MC_{MV\text{-}SC}$

Test Variables		Case 1 $I_C = 0$	Case 2 $I_C = j0.5$	Case 3 $I_C = j1.00$	Case 4 $I_C = j1.50$	Case 5 $I_C = j2.00$	Case 6 $I_C = j2.50$
$E(V_{con})$	$MC_{MV\text{-}SC}$	10.400	10.463	10.519	10.583	10.641	10.699
	$HB_{MV\text{-}SC}$	10.389	10.453	10.517	10.580	10.644	10.708
	Error (V)	11	10	2	3	-3	-9
$Vcon_{10\%}$ *(kV)*	$MC_{MV\text{-}SC}$	10.091	10.148	10.206	10.269	10.324	10.383
	$HB_{MV\text{-}SC}$	10.070	10.135	10.199	10.263	10.327	10.391
	Error (V)	21	13	7	6	-3	-8
$\%V_{drop}$ error		0.19	0.12	0.06	0.05	-0.03	-0.07

Results shown in the table above reflect a good accuracy in voltage calculations using the developed algorithm. Error in the expected values of consumer voltage ranges between 2 and 11 Volts. The greatest errors are noted in Case 1, 2 and 6. There seems to be no fixed trend in the size of error with compensation. However, with increased compensation, the error signs change. The expected voltages in $HB_{MV\text{-}SC}$ become higher than those in $MC_{MV\text{-}SC}$. The size of error is however kept within the usual margins as with positive error.

The error values in percentile voltage lie between 3 and 21 Volts (regardless of sign). These values are a bit higher than those observed with $E(V_{con})$. This is because of the slight differences in the skewness of the voltage pdfs on which the extraction of percentile voltages depend. Since percentile voltage values are used for design, there is interest in the expression of the differences as voltage drop errors. The range of voltage drop error noted is between 0.03 and 0.2%. Such low errors could possibly just be because of the Monte-Carlo's limited input combinations in its calculations of voltages. It can be said that $HB_{MV\text{-}SC}$ has great precision in the calculation of voltages on feeders with shunt capacitors. Its accuracy can also be shown graphically in comparison with $MC_{MV\text{-}SC}$.

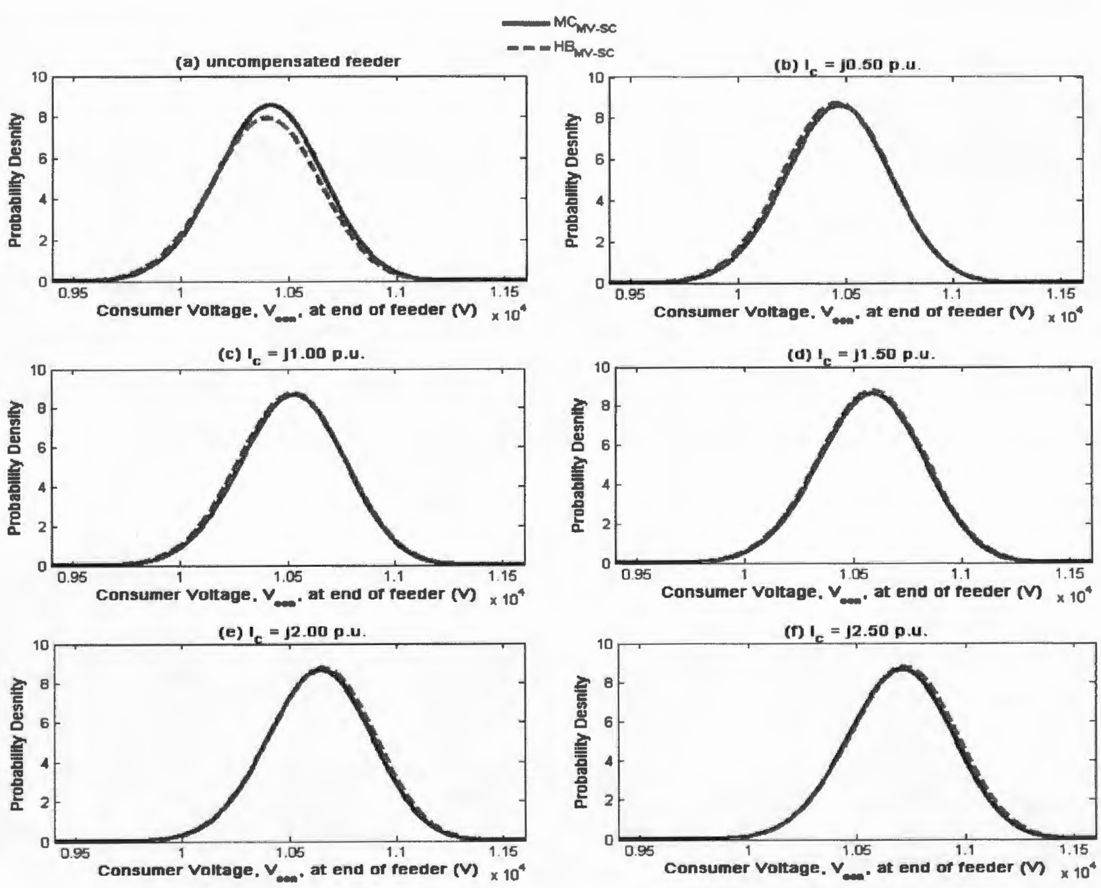

Figure 8.4: Spread of voltages - $HB_{MV\text{-}SC}$ vs. $MC_{MV\text{-}SC}$ for cases 7.4(a) I_C=0.00; 7.4(b) I_C = j0.50; 7.4(c) I_C=j1.00; 7.4(d) I_C=j1.50; 7.4(e) I_C=j2.00 and 7.4(e) I_C=j2.50

The plots in Fig. 8.4 show great alignment of the $HB_{MV\text{-}SC}$ and $MC_{MV\text{-}SC}$ traces with insignificant error. The misalignment noted in Fig. 8.4(a) is not as a result of the modifications applied for shunt capacitors since no capacitors are connected. This is an error from the calculation of voltages on load nodes. The order of error noted in this investigation could merely be as a result of Monte-Carlo simulation variation with sampling. Since the $MC_{MV\text{-}SC}$ algorithm does not exhaust all possible input arguments whilst $HB_{MV\text{-}SC}$ is based on worst case conditions, slight differences in the voltage pdfs are acceptable. Overall, it can be said that the developed algorithm performs plausibly well with good accuracy.

8.6. Concluding remarks

Based on the findings from the investigation conducted, the following conclusions can be made:

- The modelling of shunt capacitors as negative loads satisfactorily simulates their effects on distribution feeders.
- The inclusion of shunt capacitors in the calculation of feeder voltages does not introduce significant error in the overall voltage calculation on the feeder. This means that the error in the calculation of voltages in the uncompensated feeder constitutes the greater part of the error in the calculation.
- Shunt capacitors have notable regulation effects on bus voltages. The inclusion of shunt capacitors in voltage calculations is therefore crucial.
- The ability to incorporate shunt capacitors in voltage calculations on distribution feeders is a good lead to the solution of voltage calculations on feeders with non-unity power factor injections from DGs.

Chapter 9

9. PERFORMANCE ANALYSIS OF MODIFIED HB APPROACH TO THE ORIGINAL HB ALGORITHM

The preceding four chapters have successfully seen the modification of the input parameters in the HB algorithm to include feeder reactance, non-unity power factor loads, shunt capacitors and DG in the calculation. There is however need to assess the level of improvement that these modifications make in comparison to the original unmodified algorithm. In this chapter, different test scenarios are used to assess the performance of the algorithms on the basis of expected results from the MCS.

9.1. Introduction

Through previous investigations undertaken in this study, it has been established that MV feeder voltages are sensitive to reactance and load power factor. The assumptions of unity power factor and negligible reactance made in the HB algorithm for LV consequently became inapplicable with MV feeders. This led to the modification of the application of the HB algorithm in attempts to ensure that voltage variations due to the sensitive parameters are compensated correctly in the formulation.

The modifications applied were however based on approximate modelling since the reformulation of the algorithm to include the new variables is a complex task beyond the scope of this study. Validation tests run on the algorithms with modified inputs reflected the correct variation, within acceptable error margins, of consumer voltage with the parameters under test.

In this chapter, voltage calculations on a series of test cases are done using the original HB algorithm, its modified application approach and the Monte-Carlo Simulation. Comparison of the outcomes from these methods will allow the assessment of the improvement on voltage calculations brought about by the modifications done in this report.

9.2. Methodology

The HB method has been extensively tested and proven to be effective for voltage calculations on purely resistive feeders with unity power factor loads. If MV feeders were of this configuration, the HB algorithm would have worked well without adjustments. To show this, initially a resistive test feeder with unity power factor loads is used. This configuration is regarded as the base case scenario. On this feeder, voltage computations are done using the original HB algorithm, the modified approach and the MCS method. Graphical and quantitative comparisons are then performed. Following this, the load power factor and feeder X/R ratios are varied consequently generating modified representations of MV feeders. The performance of the algorithms for these variant cases is then assessed. The base test network used in the tests is given in Fig. 9.1 below.

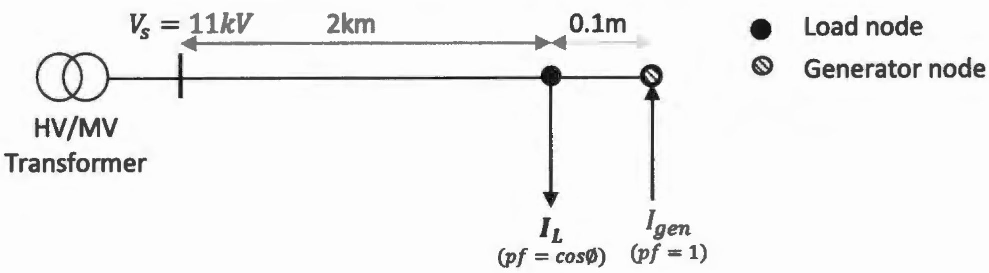

Figure 9.1: Base Case Test network

Though the figure above only shows a single node pair feeder for simplification, the actual test feeder comprises of 6 paired nodes (6 for loads, 6 for DG). In order to expand the feeder to accommodate multiple nodes, subsequent nodes are appended while preserving the nodal distances given in Fig. 9.1. The network parameters for the base case are given in Table 9.1.

Table 9-1: Test network parameters for base case scenario

FEEDER PARAMETER	PARAMETER VALUE	
Sending Voltage, V_s	11kV	
Number of nodes	6	
Customer Phase Assignment	Node 1**(Load)**	Cos 4 0 0
	Node 2**(Generator)**	0 0 0
Inter-nodal distance	0.1m Load-Gen separation,	
Load Current pdf parameters	Generator Node	Load Node
	α = 1.5	α = 1.5
	β = 4.0	β = 4.0
	pf= 1.00	pf= 1.00
	C_b= 100 A[circuit breaker size]	
Conductor type	Copper Conductor, $35mm^2$Cu	
	Temperature	T_1 = 20°
		T_2 = 40°
Feeder Impedance, X/R ratio	1	

For the variant scenarios, network parameters are changed but this is done without altering the network configuration. Generator nodes are used for tests on the active feeder algorithms.

For simplicity, the algorithms used in this investigation are denoted as follows:

- HB for LV passive feeders, used on MV (V_s = 11kV) is denoted $\mathbf{HB_{original\text{-}P}}$

- HB for LV active feeders, used on MV (V_s = 11kV) is denoted **$HB_{original-A}$**
- HB algorithm with modified input parameters for passive MV feeders as presented in Chapter 6, **$HB_{\Delta Inputs-P}$**
- HB algorithm with modified input parameters for active MV feeders as presented in Chapter 7, **$HB_{\Delta Inputs-A}$**
- Monte-Carlo Method for passive and active MV feeders, **MC_{MV-P}** and **MC_{MV-A}** respectively.

9.3. Test Scenarios – Passive feeders

9.3.1. Base Case Scenario

As described previously, the base case scenario involves a resistive feeder with unity power factor loads. In this test 6 nodes are used (without counting the unconnected generator nodes).

Results

Table 9.2 below shows the voltage quantities extracted from the voltage pdfs obtained from the three methods. The percentile voltage (at 10% confidence level, 10% risk) and its voltage drop equivalent are the same for all the three methods. A slight difference is however noted in the expected value of consumer voltage. This value is the same for the HB algorithms but different from that of the MCS method. The size of the relative error expressed as a percentage of the nominal voltage is approximately 0.04% and is a result of the limited iterations performed in the MCS method.

Table 9-2: Base Case Scenario Results

Test Variables	$HB_{original-P}$ Cos400L-000DG	$HB_{\Delta Inputs-P}$ Cos400L-444DG	MC_{MV-P} Cos400L-000DG
$E(V_{con})$ [kV]	10.570	10.570	10.574
$Vcon_{10\%}$ (kV)	10.244	10.244	10.244
V_{drop} (%)	6.87	6.87	6.87

The agreement of the methods in voltage calculations can be depicted through voltage plots as shown in Fig. 9.3 below. The traces of $HB_{\Delta Inputs-P}$ and $HB_{original-P}$ are seen to be identical whilst a slight difference around the peak and the base are noted with MC_{MV-P}. This result confirms that if MV feeders were resistive with unity power factor loads, the HB algorithm would not have required adjustments. The test also confirms the correct coding of $HB_{\Delta Inputs-P}$.

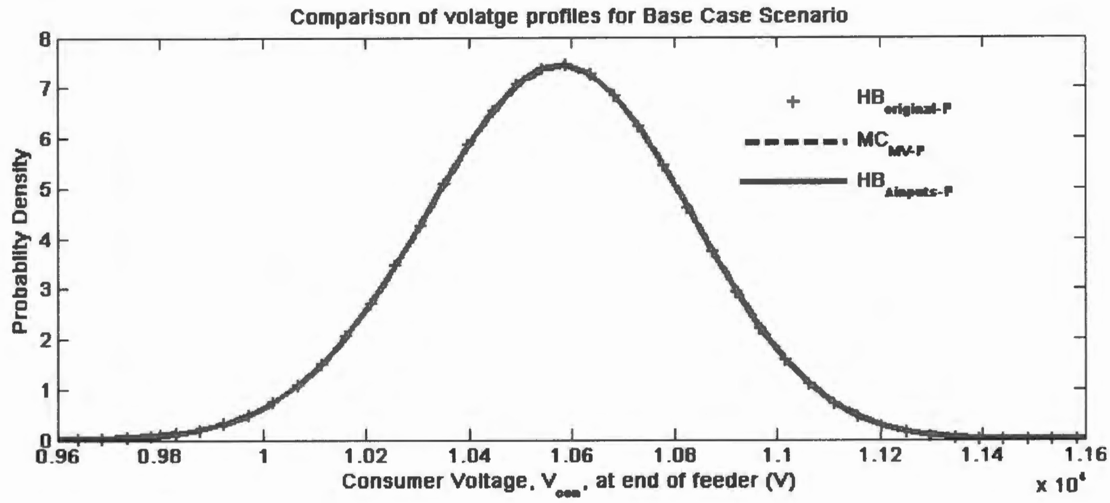

Figure 9.2: Base case scenario results

9.3.2. Case 2 – Feeder impedance variations

To assess the performance of the algorithms on realistic MV feeders, the feeder X/R ratio is varied from 0 to 1.5 whilst the load power factor is kept constant at 0.8 lagging. The effects of the modification applied to cater for reactance on MV feeders can thus be investigated by using the 3 methods to calculate voltages on the feeder. Comparisons of the voltage trend with the variant parameter, voltage values and the spread of the resulting pdfs are conducted.

Results

Figure 9.3 shows the trend of consumer voltages with feeder X/R ratios. In the plots shown, $HB_{original\text{-}P}$ starts off with zero error for condition X/R = 0. However, as feeder reactance increases with the X/R ratio, the error becomes unacceptable.

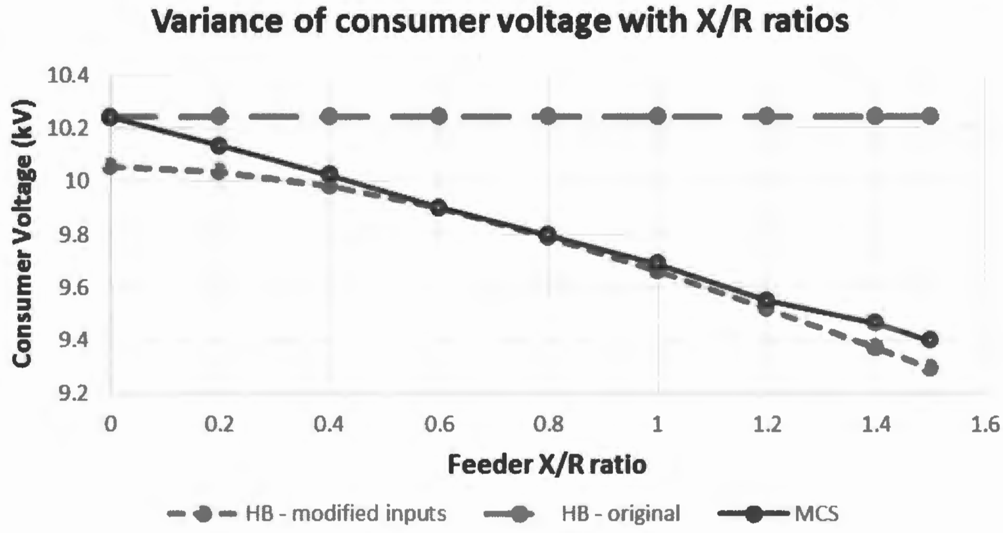

Figure 9.3: Case 2 results - Dependency of voltages on X/R ratios

The modifications in $HB_{\Delta Inputs-P}$ initially result in a slight error for condition X/R = 0. This error stems from the method used to cater for the non-unity power factor (0.8 in this case). This will be further discussed in the section that follows.

This initial error however diminishes with increase in reactance. For X/R ratios greater than 0.4, $HB_{\Delta Inputs-P}$ follows the trend in MC_{MV-P} with greater accuracy. However, slight misalignments are seen as the feeder X/R ratio increases beyond unity.

In order to quantify the accuracy in the methods, the case X/R = 1 is used. Table 9.3 shows voltage values from the output pdfs of the three methods in discussion.

Table 9-3: Case 2 Results - X/R ratio effects

Test Variables	$HB_{original-P}$	$HB_{\Delta Inputs-P}$	MC_{MV}
$E(V_{con})$ [kV]	10.570	10.241	10.249
$Vcon_{10\%}$ (kV)	10.244	9.663	9.690
V_{drop} (%)	6.87	12.15	11.91

These results show a great miscalculation of voltages using $HB_{original-P}$. This is depicted by the large differences in both the percentile and expected consumer voltage values. On the other hand, $HB_{\Delta Inputs-P}$ obtains voltage values with approximately 99.93% accuracy. This is illustrated graphically in Fig. 9.4.

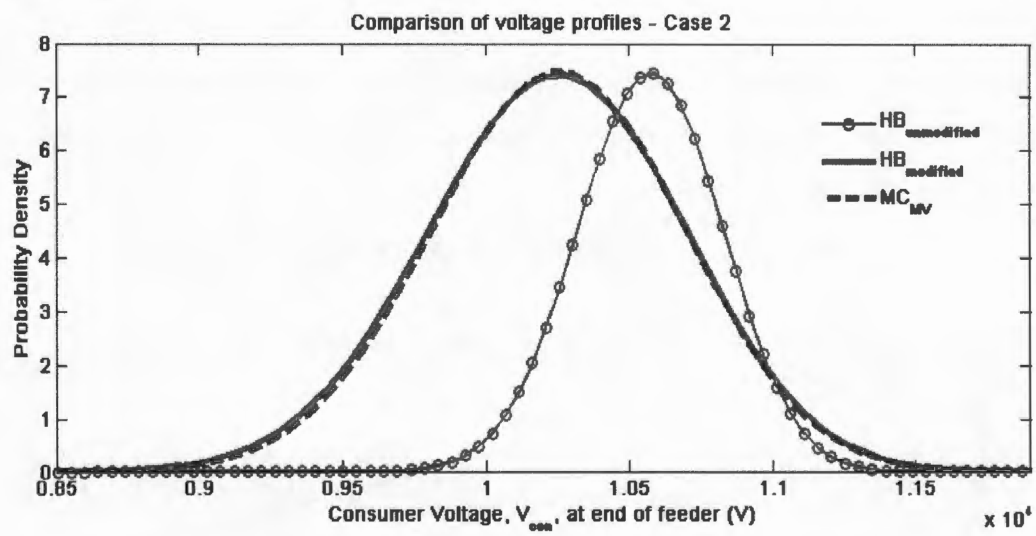

Figure 9.4: Test Case 2 Results - Voltage spread results for unity X/R ratio

The $HB_{\Delta Inputs-P}$ and MC_{MV-P} traces are seen to be matched only with slight error whilst the $HB_{original-P}$ fails to track the distribution of voltages entirely.

9.3.3. Case 3 – Load power factor variations

In this investigation, the modification for lagging power factor loads is assessed. The feeder in the descriptions earlier is maintained. The X/R ratio is kept constant at unity whilst load power factor is varied from 0.8 to unity. Voltage computations are done using the three methods under study and the relevant comparisons made.

Results

The plots given in Fig. 9.5 show the variation of consumer voltages with power factor as obtained through the 3 methods. $HB_{original-P}$ again results in great miscalculations as load power factor strays further away from unity. This is because the method gives the same voltage results for all cases of load power factor since they are assumed to be unity.

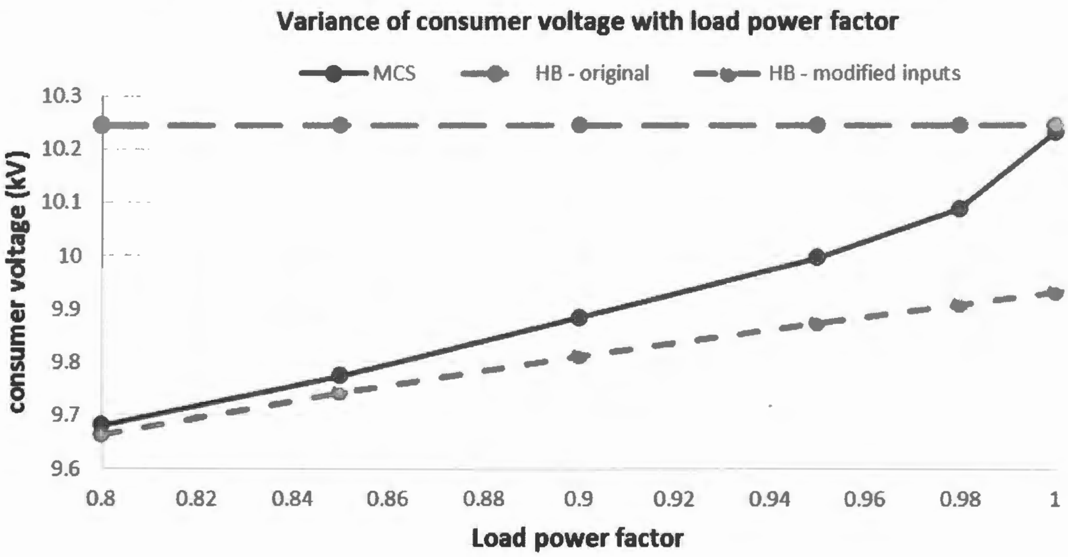

Figure 9.5: Case 3 results - Dependency of voltages on load power factor

The modified algorithm, shown by the blue-short-dashed trace, obtains an improved alignment with the MC_{MV-P} trace. Better accuracies are noted at low power factors whilst the error close to unity power factor is greater than that seen in $HB_{original-P}$. This is because $HB_{\Delta inputs-P}$ overestimates voltage drops for unity power factor loads on a feeder with unity X/R ratio. This suggests inconsistency in the accuracy of the method across case combinations of power factor and X/R ratios.

In order to demonstrate the improvements done to the HB algorithm with regards to modelling the effects of load power factor variation, a non-unity power factor of 0.9 is used. The voltage results are shown in Table 9.4 below.

Table 9-4: Case 3 Results - power factor effects

Test Variables	$HB_{original\text{-}P}$	$HB_{\Delta Inputs\text{-}P}$	MC_{MV}
$E(V_{con})$ [kV]	10.570	10.325	10.257
$Vcon_{10\%}$ (kV)	10.244	9.812	9.880
V_{drop} (%)	6.87	10.23	10.17

Results given above show an improvement in the calculation of voltages using $HB_{\Delta Inputs\text{-}P}$. The spread of voltages achieved through this method attempts mimicking $MC_{MV\text{-}P}$ as illustrated in Fig. 9.6 below.

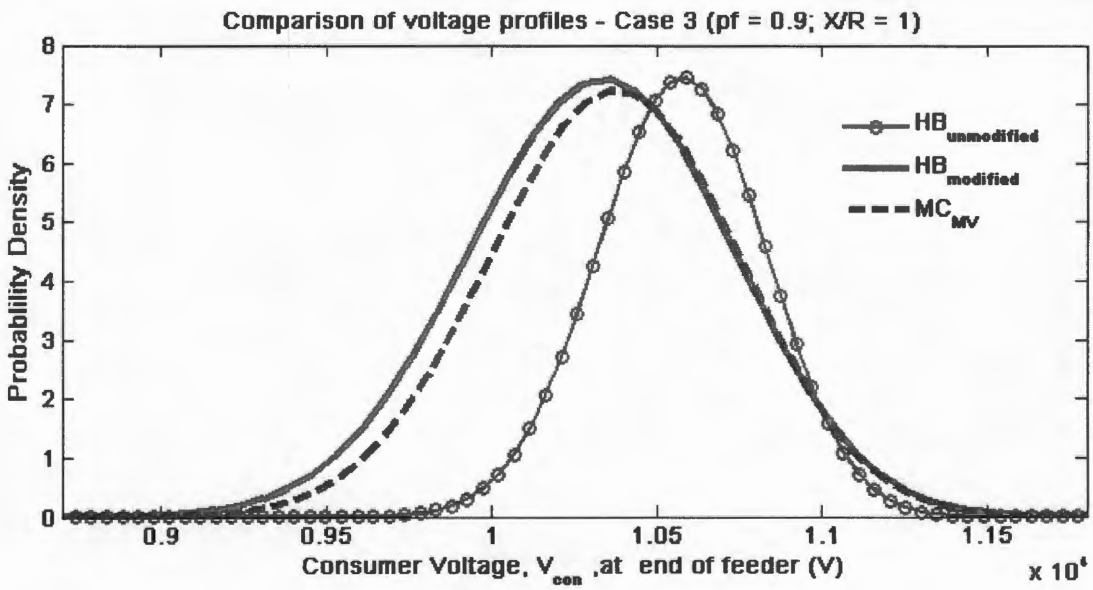

Figure 9.6: Comparison of voltage profiles - Case 3

There seems to be a lot of improvement achieved in voltage calculations through the input modifications applied. However, it has been noted that there could possibly be some inconsistency in the outcomes across combinations of power factor and X/R ratios. A correlation of errors from the two modifications (to include reactance and power factor) could possibly exist. There is need to investigate the variation of error in the voltage calculations with combinations of power factor and X/R ratios.

9.3.4. Variation of voltage error with combinations of power factor and X/R ratios

The purpose of this test is to establish consistency of the modified algorithm in performing voltage calculations for diverse conditions of load power factor and feeder X/R ratios. In the test, load power factor is varied from 0.8 to unity whilst feeder X/R ratio is constant. In each case, voltage computations

on the feeder are performed and recorded. The process is repeated using different values of X/R ratio until all values in the closed interval [0: 1.5] are used. Comparisons of outcomes between $HB_{\Delta Inputs-P}$ and MC_{MV-P} are used to get percentage relative voltage error (expressed in terms of the nominal voltage, V_S) in the calculation by $HB_{\Delta Inputs-P}$. Using the numeric results, a mesh plot is constructed in Excel.

Results

The mesh plot given in Fig. 9.7 below shows the variation of error in the calculation of voltages on the test feeder using $HB_{\Delta Inputs-P}$. The shape of the plot shows non-uniformity of the error across combinations of power factor and feeder X/R ratios. This finding implies that the accuracy of the method is inconsistent.

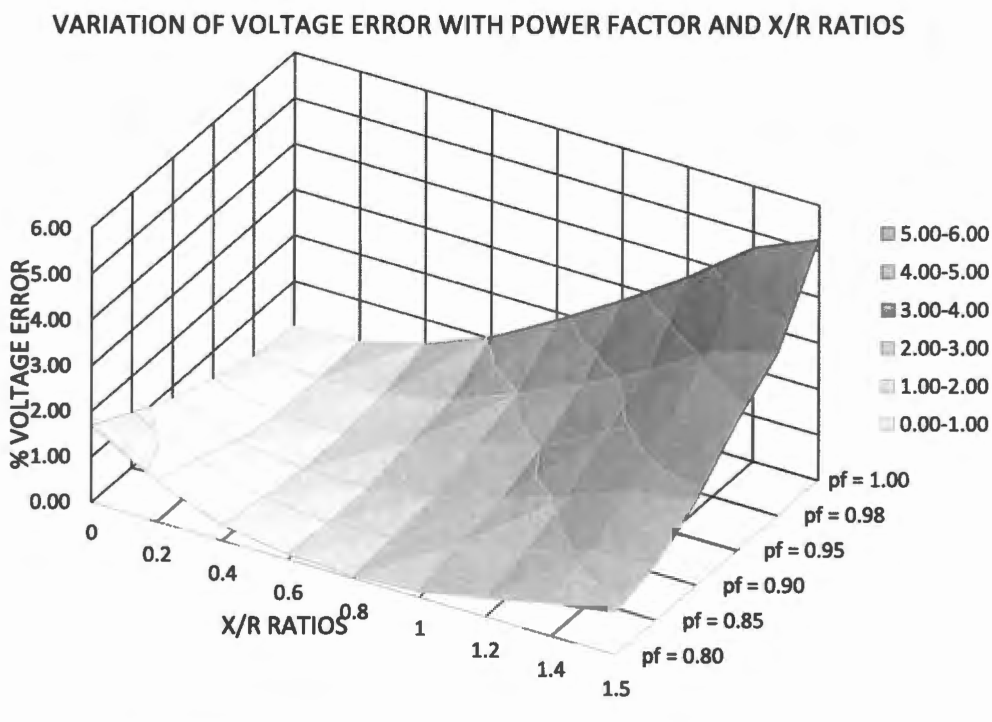

Figure 9.7: Variation of voltage error with XR ratios and power factor - $HB_{\Delta Inputs-P}$

Looking at the distribution of error, it is seen that the majority of the points on the surface given above correlate to errors less than 1% (most faint shade, between 1st and 2nd contour lines). The areas with errors greater than this are mainly as a result of the following combinatory conditions:

- Feeder X/R ratio greater than 1 across power factors greater than 0.85
- Unity power factor loads across X/R ratios greater than 0.8
- X/R ratio of zero with power factors 0.8 and 0.85

The average error seen in the above listed combinations is approximately 2.5%. The majority of these errors are as a result of the over-estimation done by $HB_{\Delta Inputs-P}$ as explained below.

- Voltage drops caused by non-unity power factor loads on a purely resistive feeder are much smaller than those caused by the inflated load current. The proposed method is therefore poor under these circumstances.
- Voltage drops as a result of reactance on a feeder with unity power factor loads are also smaller than those projected by the use of the absolute value of the impedance, $|Z_p|$. This also is a region of poor performance of the algorithm with modified inputs.

To illustrate the improvement in voltage calculations as a result of the modifications applied to input parameters, the errors in voltage calculations due to the $HB_{original-P}$ and $HB_{\Delta Inputs-P}$ are compared. Since the MV feeder X/R ratio is in most cases close to unity, the X/R ratio range [0.8:1.2] is used in the analysis. Fig. 9.8 shows error plots in the calculation of voltages using the two approaches, $HB_{original-P}$ and $HB_{\Delta Inputs-P}$.

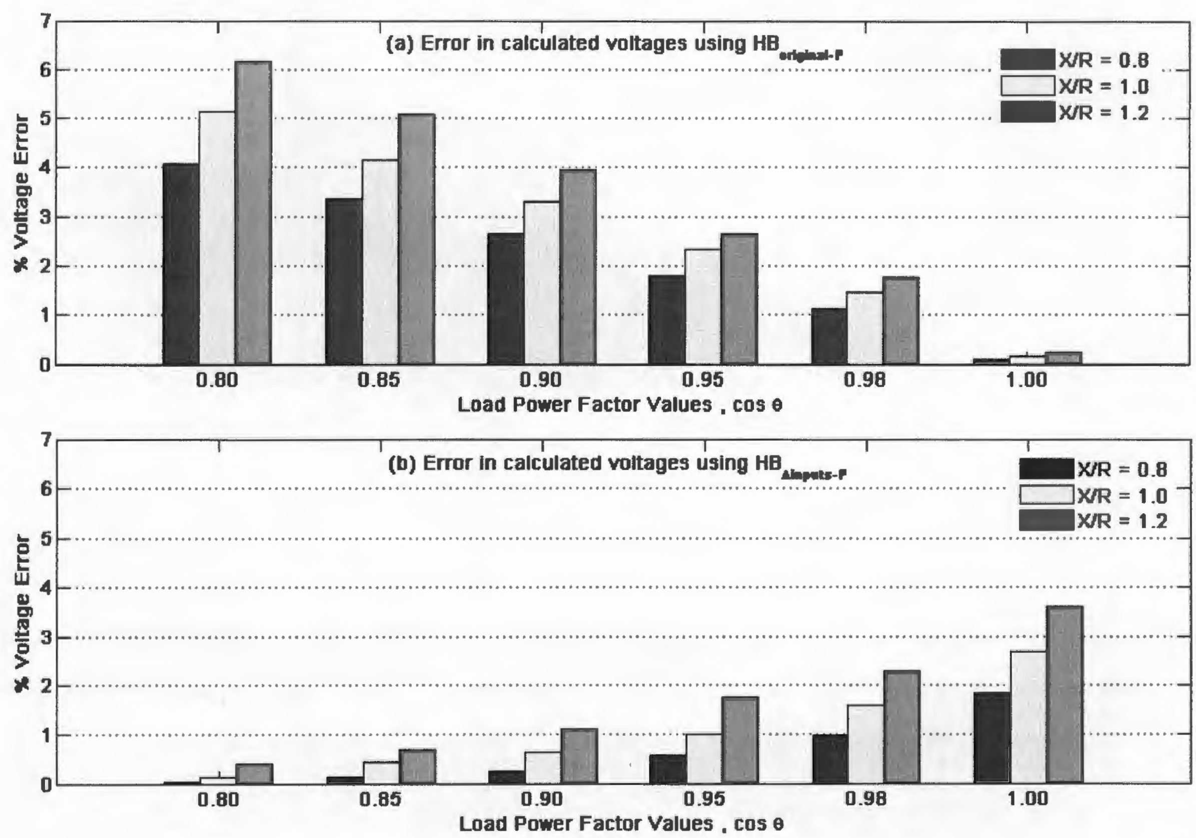

Figure 9.8: Comparison of error in voltage calculations - $HB_{\Delta Inputs-P}$ vs. $HB_{original-P}$

The bar graphs given in Fig. 9.8 confirm an appreciable reduction in error in the calculation of voltages on MV feeders characterised by the given power factors and X/R ratios. For power factor cases 0.80 - 0.95, the original algorithm without adjustments results in voltage drop errors ranging between 3 and 6%. This is quite a large error corresponding to voltages of about 330-660V. Since the voltage rejection criterion in the design process of MV feeders is 5% voltage drop, an error of 3-6% is quite misleading and costly.

With modification of input parameters, the error in this range of power factors and X/R ratios is reduced mostly to values below 1%. However, as the load power factor gets closer to unity, the error noted with $HB_{\Delta inputs\text{-}P}$ increases. At unity power factor, $HB_{original\text{-}P}$ obtains much less error than the algorithm with modified input parameters. The relative error improvement obtained through $HB_{\Delta inputs\text{-}P}$ is shown in the bar plot in Fig. 9.9.

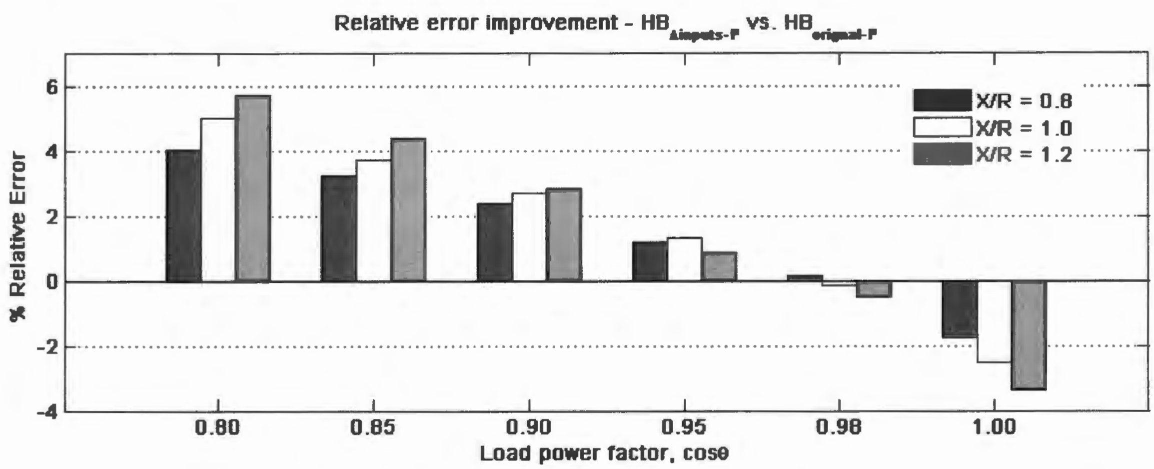

Figure 9.9: Improvement in the calculation of feeder voltages using $HB_{\Delta inputs\text{-}P}$

It can be concluded that on MV feeders, the modified method works better than the unmodified approach for power factors below 0.95. For values between 0.95 and unity, the original algorithm without adjustments offers better approximations to voltages. However due to the linear approximate modelling done for Z_p and I_{load}, this conclusion is limited to the test feeder especially with regard to the size of the load. An investigation on this aspect is vital to determine if the accuracy demonstrated above is consistent with variations in load size.

9.3.5. Variation of voltage error with total customer connections at a node

The purpose of this investigation is to determine the effect of increased customer connections or load current on the accuracy of the developed method. The effects of the approximate modelling of load current for non-unity power factor loads will then be put to test.

Using the test feeder, all variables except the customer assignment pattern are kept constant. The customers are assigned using the cosine approach as before. However, the number of connected customers will be increased from 1 - 6 in single sized steps. With each increase, voltage calculations are done and recorded. The results are used to perform a comparison of the performance of $HB_{\Delta Inputs-P}$ based on the outcomes of $HB_{original-P}$ and MC_{MV-P}.

Results

Fig. 9.10 below depicts the variation of error in voltage calculations with the total number of customers connected at a node. The error is seen to increase with customer connections in an approximately linear fashion.

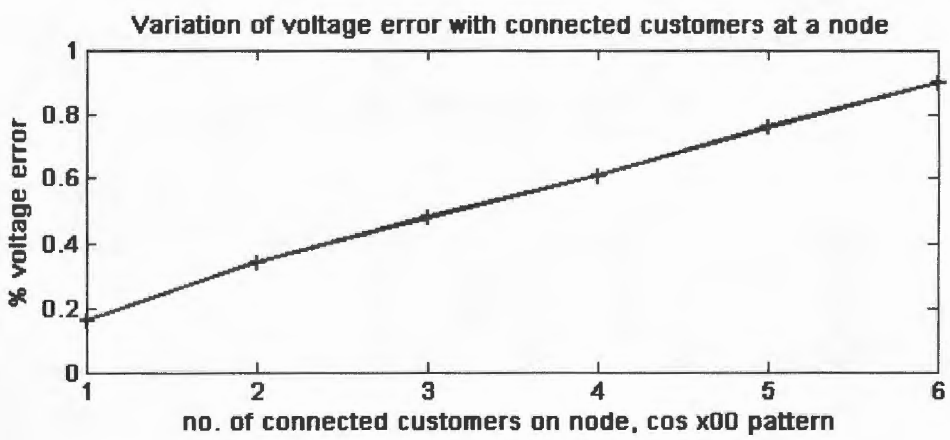

Figure 9.10: Variation of voltage error with connected customers at a node

The results obtained meet expectations since the approximate modelling of the feeder impedance results in an error dependent on the load current. This can be illustrated mathematically.

If an approximation is done on the impedance variable, Z, an error , ΔZ results such that the expected voltage drop can be written in terms of the approximation quantity Z_{approx} and the corresponding error as follows.

$$\Delta V_i = I_{load}.(Z_{approx} + \Delta Z) \tag{9.1}$$

The expansion of the voltage drop equation gives:

$$\Delta V_i = I_{load}.Z_{approx} + I_{load}.\Delta Z \tag{9.2}$$

In equation 9.2, the quantity $I_{load}.Z_{approx}$ is the approximate calculation of voltage drop on the feeder using the modified HB algorithm. Equation 9.2 can be therefore expressed as:

$$\Delta V_i = \Delta V_{HB_{\Delta Inputs-P}} + I_{load}.\Delta Z \tag{9.3}$$

The error in the calculation of voltage drop can then be arrived at by taking the difference of the approximated voltage drop from the accurate voltage drop.

$$\Delta V_i - \Delta V_{HB_{\Delta Inputs-P}} = I_{load}.\Delta Z \quad (9.4)$$

$$\Delta V_{error} = I_{load}.\Delta Z \quad (9.5)$$

The resulting error, found using the mathematical approach, agrees with that shown in the plot in Fig. 9.10. This nature of error is undesirable as it is another element of inconsistency.

9.4. Test Scenarios –Active feeders

The preceding section dwelled on the comparative analysis of the HB algorithm with modified input parameters to that without modifications and to the MCS method. This section attempts to extend this analysis to active feeders, including the installation of shunt capacitors on feeders. However, the original HB algorithm was not formulated for feeders with shunt capacitor installations. Hence, there is no basis for comparison with the algorithm developed in this study. The comparisons made in Chapter 8 on the performance of the extended algorithm (HB_{MV-SC}) are thus sufficient for drawing necessary conclusions regarding the method. This section will therefore dwell on assessing the performance of the modified application for active feeders, $HB_{\Delta Inputs-A}$.

The test scenarios will however exclude variation of power factor and X/R ratios as these have been covered in the assessments done for passive feeders. This is supported by the fact that active feeders are essentially passive feeders with connected DG. The only relevant test worth investigating is the variation of error with increased DG penetration.

9.4.1. Variation of voltage error with DG penetration

The purpose of this test is to investigate the performance of the developed algorithm, $HB_{\Delta Inputs-A}$, on voltage calculations on active feeders as DG penetration increases. The DG nodes on the test feeder are now used in this case. The separation of DG nodes from load nodes is 0.1m as shown in Fig. 9.1. A 6-node feeder comprising of 3 load nodes and 3 generator nodes is used. All the other parameters in the test feeder outlined in Table 9.1 are conserved.

The test procedure will involve the variation of DG penetration from bal111 to bal666 whilst loads are kept at constant power factor (0.9) and size (cos444 assignment applies). The feeder X/R ratio will also be kept at a constant value of 1. For each case, voltage calculations on the feeder are performed and following that, comparisons on the accuracy of $HB_{\Delta Inputs-A}$ to that of $HB_{Original-A}$ are made. The Monte-Carlo method is used as the benchmark.

9.4.2. Results

Voltage calculations were done on the feeder for conditions within the typical MV domain of load power factor (0.9) and feeder X/R ratios (unity). In the plots given in Fig. 9.11(a), a reduction in voltage errors is noted with the $HB_{\Delta inputs\text{-}A}$ method for all cases of penetration.

This trend in error reduction is expected since for unity power DG connections, the reactance of the feeder is ignored as explained in the preceding chapter. This means that the calculation for DG is similar to that in the unmodified algorithm. The error differences between $HB_{\Delta inputs\text{-}A}$ and $HB_{original\text{-}A}$ mainly arise from the errors in the presentation of load power factor and X/R ratios.

Fig. 9.11(b) shows a plot of the actual values of error, other than absolute error as shown in plot (a). Plot (b) reveals an approximately linear error in the calculations of voltages on the active feeder using $HB_{\Delta inputs\text{-}A}$. This trend in error is similar to that depicted in the preceding test results on increased load current effects. Both results portray a linear voltage error rise with increased current on the feeder; in this case current injection as opposed to drawings by loads.

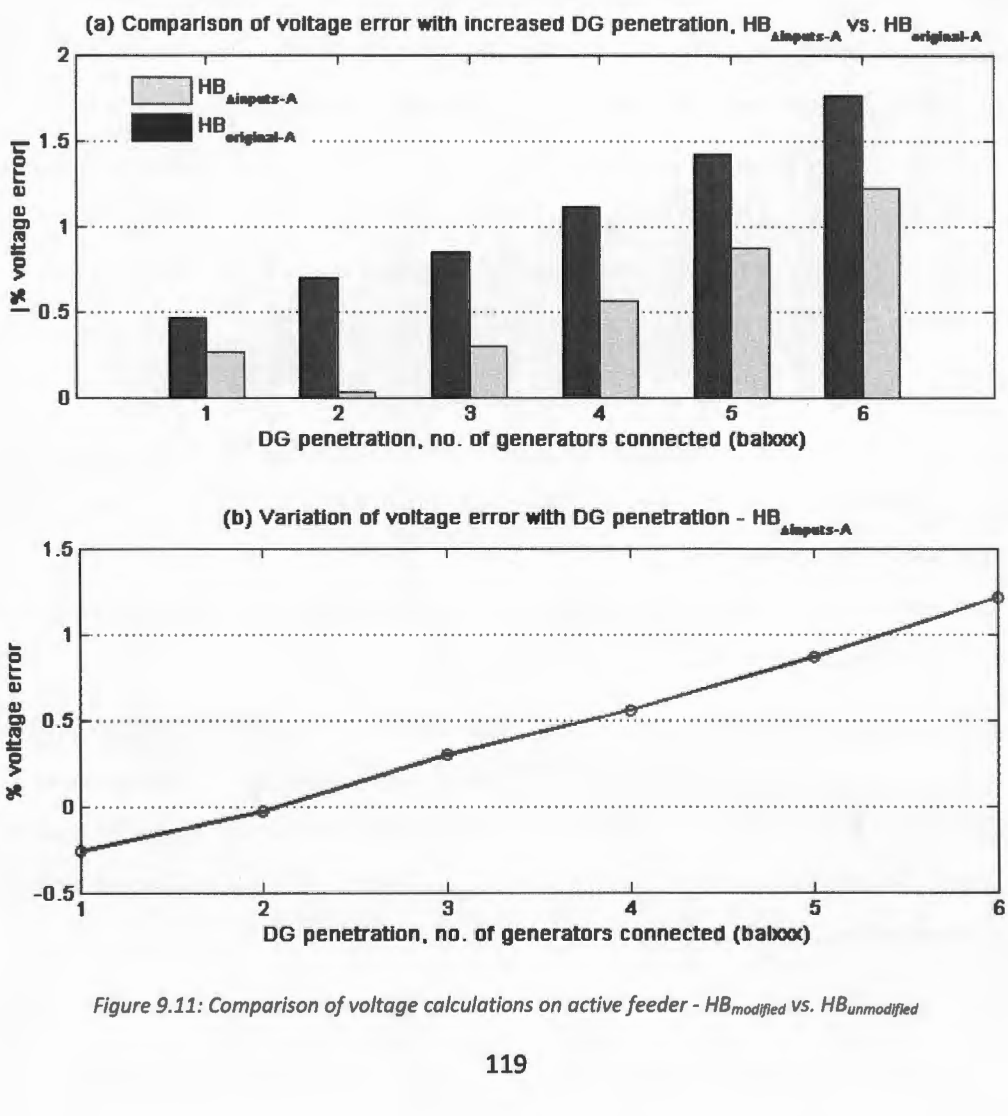

Figure 9.11: Comparison of voltage calculations on active feeder - $HB_{modified}$ vs. $HB_{unmodified}$

9.5. Implication of results

The rigorous testing of the modified algorithm in this chapter generally indicates that the modifications of the input parameters for the HB algorithm to accommodate feeder reactance and non-unity power factors make notable improvements on the accuracy of the HB method. There are however a few cases in which the original HB algorithm works better than the modified approach. In this regard, investigations have shown that for load power factors near unity (greater than 0.95) and zero X/R ratio, the modified approach results in considerable errors mainly due to the over-estimations of voltage drop. The assumptions of unity power factor and negligible reactance offer better results in these cases.

Further tests on the performance of $HB_{\Delta Inputs\text{-}P}$, which included the variation of load power factor and feeder X/R ratios, revealed linear-type errors. The increase in error with customer connections as noted for both passive and active feeders is undesirable. This means that though the modified algorithm was shown to be better than the HB algorithm without adjustments, its accuracy in comparison to renowned tools such as the Monte-Carlo cannot be easily quantified. The dependency of the error on load currents (positive or negative) and combinatory conditions of power factor and X/R ratios makes it inconsistent.

With regards to shunt capacitor calculations, the approach of regarding connections as negative loads with 'generator effects' is a tool worth adopting in power system analysis. This approach is essential in preserving the radial structure of the network since power injections cannot be modelled as power sources in parallel to the utility source. However, the simulation of the injected reactive power as a real quantity scaled by the feeder average power factor may be misleading and also lead to inconsistency in accuracy.

In summation, the results from the investigations done in this chapter show that the HB algorithm with modified input parameters is a better tool for voltage calculations on MV feeders than the HB algorithm without adjustments. However, the accuracy of the method cannot be clearly quantified as it varies with the magnitude of nodal currents (both load and DG) and the combinations of feeder parameters.

Chapter 10

10. CONCLUSIONS AND FUTURE WORK

The objective of the research conducted was to develop a voltage drop calculation tool for use on both passive and active MV feeders. The algorithm was to be developed through the modification of the application of the Herman-Beta algorithm for LV feeders. Once developed, the method would be extended to include the effects of shunt capacitors in its formulation. The intended algorithm was developed and tested. This chapter presents relevant findings and conclusions made from the research.

10.1. Answers to Research Questions

This research has been aimed at the testing of the hypothesis stated at the beginning of this report. The hypothesis was quoted as follows:

"The Herman-Beta algorithm can be adopted for voltage calculation on Medium Voltage (MV) feeders through inclusion of line reactance and power factor variations in the formulation of the input parameters. Following validation of this new approach with a Monte-Carlo simulation, it is possible to further extend the application for voltage calculation on feeders with shunt capacitor compensation."

Through literature search and the investigations conducted, the research questions posed at the beginning of the study can be answered. The following is the list of questions along with a summary of the insights brought about through this study.

- ***What are the key components of an MV network, its configuration, topologies and parameters? How is it different from the LV network?***

The MV distribution system stems from the transmission system and leads to the LV distribution system. In South Africa, its voltage classification range is between 1kV and 44kV. The main implemented technologies are the 3-phase 4-wire, 3-phase 3-wire, single phase and the Single Wire Earth Return systems. Most feeders are of radial type and are relatively shorter than LV feeders. Besides the higher voltages and shorter feeders, the MV network differs from the LV in that its feeders are characterised by higher X/R ratios usually close to unity.

The compatible voltage levels for MV networks according to the NRS048 standard is that power delivered at the consumer terminals be within ±5% of the declared nominal voltage. For LV networks this value is 10%. The guide on voltage limits stipulates a maximum deviation from the standard voltages by up to 10%. Deviations in this range are acceptable for a period not longer than 10 consecutive minutes. In MV networks, shunt capacitors and OLTC's are mainly used for voltage regulation thereby assisting in the maintenance of the voltage standards.

- ***Can MV loads be modelled by a Beta distribution function as done in LV systems? What other approaches have been used to model MV loads?***

Load modelling can be classified into two groups, deterministic and statistical. Deterministic modelling involves the description of load by a constant value. The basis of most current practise in load modelling is the After Diversity Maximum Demand (ADMD) approach. The ADMD is the average maximum power demand per customer for a group of customers approaching infinity. This value is usually derived from annual demand data. The ADMD value varies with the number of customers in a selected group and the interval of demand as well. Correction factors such as the diversity factor (DF) and loss of diversity are used to tune the value to the context of application. The method has shortfalls characteristic of deterministic methods. Voltage analysis using ADMD values only gives information of voltage quality for only one case of demand and without an indication of the statistical risk of violation. Statistical methods are required in the assessment of the stochastic load models.

The dependency of load size and patterns on weather, network parameters and customer profiling makes load demand an uncertain variable. Statistical methods based on probability distribution functions are required to fully represent the variation. In MV design, the Gaussian fit has been prevalently used for load modelling. However, due to the skewness sometimes noted in load distributions, some researchers have used the Gaussian Mixture Model to account for non-Normal distributed loads. The method however increases computational burden significantly. Distribution functions like the log-normal, Weibull, Erlang and Beta have consequently been used in attempts to adequately model load data without restriction to symmetry as imposed by the Gaussian fit. Amongst these methods, the beta distribution stands out to have a lot of advantages, particularly its ability to model a wide range of skewness. Its flexibility in representing various data types makes it suitable for load modelling in MV networks.

- ***What methods have been used to calculate voltage drop in MV systems?***

A lot of voltage calculation methodologies have been used in MV systems. These can also be grouped into deterministic and probabilistic categories. Deterministic Load Flow (DLF) approaches such as the backward/forward sweep method and the Newton-Raphson are some of the most commonly used. These methods are based on fixed input parameters and hence conduct power system analysis only for one input condition, usually the average demand. This has been proven insufficient in modern power systems in which uncertainties associated with load demand and power generation are to be considered. Besides the inability to represent uncertainties, the backward/forward sweep method is usually time-consuming as inflicted by the iterative approach that is uses. On the other hand, the Newton-Raphson method suffers increased computational effort as matrix dimensions increase with network size. The shortfalls of DLF methods inspired the development of Probabilistic Load Flow (PLF) techniques.

The Monte-Carlo Simulation (MCS) is one of the most used numeric PLF methods in MV feeder design. It is merely a deterministic calculation iterated a number of times (usually above 10000 times) picking different input parameters each time. It is therefore very accurate, given that a high number of iterations is used. However, this requirement for a large number of iterations has restricted the use of the Monte-Carlo simulation to the validation of analytical methods which are in most cases faster.

Analytical methods based on convolution techniques, mathematical series and parameter estimation have been used on MV feeders. Methods based on the FFT and those that make use of the Cumulants and Charlier series are reported to have a well reduced computational burden. However, these methods have quite complex formulations. Methods based on parameter estimation are gaining popularity as they are both fast and not very complex.

Renowned work on MV feeders using parameter estimation was done by Celli *et al.* [23] using Normally distributed inputs. The use of this distribution however restricts the inputs to symmetrically distributed data. However, this is rarely the nature of loads or generation patterns from DG. Load and generation data collections reveal skewed distributions in data. This find makes the Gaussian orientated methodology a limited tool.

- ***What assumptions were made in the formulation of the Herman-Beta algorithm? Are these assumptions still valid in an MV network context?***

The HB algorithm was formulated for voltage computation specifically for passive and, later, active LV feeders. Assumptions made in the formulation of the HB method that are still valid within the MV system context are as follows:

I. *With regards to passive networks, maximum voltage drop occurs during the interval of maximum load demand. For active feeders, maximum voltage rise occurs during the interval of minimum load demand and maximum DG generation whereas the condition of* *maximum voltage drop occurs in the interval of minimum generation amidst maximum load demand.*

II. *The load and DG currents can be represented as statistics which are distributed by a Beta probability density function* – ability of beta distribution function in the modelling of differently skewed data makes it suitable for MV application. However, there is need for real load data collection and testing.

III. *The customer load currents are considered as independent statistical variables* – valid if the statistic is considered at a single interval.

IV. *Generators can be modelled as negative loads using the beta density function* – assumption is valid and was extended to the calculation of voltage drop on feeders with shunt capacitors.

The assumptions in the HB algorithm that were of conflict to MV systems are given below along with explanations.

I. *Loads can be represented as currents at unity power factor* – this assumption is invalid and becomes significant in the MV system context. Much of the connected loads on the MV network are of lagging power factor. The range of power factors associated with many MV substations is between 0.85 and 0.98. The variation of consumer voltage with load power factor verified the significance of this variable on voltage calculations. Thus loads cannot be assumed to be of unity power factor.

II. *The distributions feeders are assumed to be mostly resistive with negligible reactance* – MV feeders are characterised by relatively higher X/R ratios, typically unity. The reactance has approximately the same effect as the resistive element of the feeder. Hence, voltage drops across the reactance element are not negligible. Investigation on the effects of reactance on consumer voltage supports this claim.

- ***How can the input parameters in the HB algorithm be modified to make the HB algorithm suitable for voltage calculations in MV networks? Does the new application agree with proven methods such as the Monte-Carlo Simulation for voltage calculation?***

  Since some of the assumptions made in the HB method for LV networks are unsuitable for MV, motivation to modify the use of the algorithm arises.

  - With regards to feeder impedance, the reactance element has to be factored in the calculation. Since the addition of reactance increases the voltage drop on the feeder, using the absolute value of impedance in place of the resistance can mimic the effect. Upon comparison with the Monte-Carlo method, this approach was found to work satisfactorily.

However, this approximation of impedance used causes a linear error dependent on the length of the feeder and the size of customer currents. This makes the method undependable.

- Lagging power factor loads have been found to increase voltage drops on feeders by increasing the flow of current in the network. To simulate this effect, the load current was inflated by the power factor, thereby increasing the current. This obtained the desired effect of increase in voltage drop as caused by the drawing of reactive power by the loads. When compared to the Monte-Carlo simulation, the suggested method also worked satisfactorily well. The approximation method however suffers from errors proportional to the size of load current. Nonetheless, some combinations of load power factor and feeder X/R ratios were observed to achieve minimal errors. This is because the error signs in the two approximations are opposite which can result in error compensation.

- ***How can the new approach to voltage calculations on MV feeders be extended to accommodate an active network with DG interconnections?***

  DG connections to MV feeders can be regarded as negative loads in the same way done in LV active networks. On such a network, voltage calculations for the load nodes are done in the same way as applied to passive networks i.e. with compensation of reactance and lagging power factor loads. However, for voltage calculations on the added DG nodes, it was found that the compensation of feeder reactance for DG operating at unity power factor resulted in over-estimations of voltage rise. Under this condition of unity power factor, disregarding feeder reactance in the calculations was seen to obtain better estimates of feeder voltages. This research only covered the connection of unity power factor DG without reactive power injections or consumption by generators. Reactive power compensation through capacitors was however covered.

- ***How can the HB algorithm for MV be extended to allow for voltage calculations on shunt capacitor compensated feeders?***

  Shunt capacitors have an effect of voltage regulation on distribution feeders. Due to their leading currents, shunt capacitor connections result in the increase of nodal voltages. This 'generator-like' effect that they cause makes the modelling of shunt capacitors as negative loads a reasonable approach. This means that the algorithm for active feeders can be applied to shunt capacitor connections. However, the HB algorithm does not accept current input parameters of imaginary type. To correct this, a similar compensation approach to the effects of an imaginary current as that applied to lagging power factor can be used. The effect of the imaginary current is approximated through scaling the capacitor current with the feeder power factor. The resulting current is then regarded as a negative as if it flowed into the feeder in the same way the generator currents flow. This approach was found not to add any significant errors to the calculation of voltage on the compensated feeder.

10.2. Validity of research hypothesis

The hypothesis stated in the beginning of this dissertation was, ***"The Herman-Beta algorithm can be adopted for voltage calculation in Medium Voltage (MV) feeders through inclusion of line reactance and power factor variations in the formulation of the input parameters. Following validation of this new approach with a Monte-Carlo simulation, it is possible to further extend the application for voltage calculation on feeders with shunt capacitor compensation."***

Subsequent studies performed to test this hypothesis have shown it to be valid.

The extension of the HB algorithm to MV feeders has been shown to be feasible through the approximate modelling of the missing variables in the method for LV feeders. The developed method is a better tool than the HB algorithm without adjustments. However, its accuracy in comparison to the Monte-Carlo simulation cannot be easily quantified as errors are not constant. Nevertheless, the general improvements in accuracy compared to the HB algorithm without adjustments encourage the full, more precise, development of the algorithm for voltage calculations on both passive and active MV feeders. This finding is quite valuable as the accurate inclusion of power factor and feeder X/R ratio in the HB algorithm would allow the same algorithm to be used for both MV and LV feeders by setting the input parameters accordingly. This would mean that the slight errors associated with the HB algorithm for LV due to the assumption of unity power factor loads and purely resistive feeders could be eliminated.

10.3. Future work and proposals

Based on the findings made, the following are implications of the research:

1. **Correction of the South African National Standard for Electricity Distribution**

   In the beginning of this research, a follow-up derivation of the HB algorithm was done. This work helped in the discovery and correction of some errors in the NRS034 (1) -2007 publication which stipulates the guidelines for the provision of electricity distribution networks in residential areas. The errors pertained to the representation of the design algorithm for LV feeders, the Herman-Beta method. A compilation of the correct algorithms has been successfully accomplished and prepared for publication (see Appendix C).

2. Further studies

- *Further improvement on voltage drop algorithm*

  The work covered in this research has indicated there is scope for using the Herman-Beta algorithm for voltage drop calculations on MV feeders. However, the methods discussed in this work are based on approximate models. There would be value in reducing the error further and identifying the limits of error.

- *Development of excel spreadsheet for MV voltage drop calculations*

  The HB algorithm for LV feeders was programmed onto an Excel spreadsheet, which is currently a ready to use product available under Creative Commons Licence. This was found to be a very effective way of using the algorithm as the Excel environment allows good interaction with users. The extension of this idea to the MV algorithm will be useful for network planners.

- *Assessment of DG penetration limits on MV feeders*

  The investigation of DG penetration limits is essential in the utility company's planning for increased DG connections. With the development of the recommended voltage analysis tool in preceding points, it is possible to perform analysis of active networks to determine the maximum permissible DG interconnections that the grid can handle.

10.4. Concluding Remarks and Final Thoughts

The modification of the application of the HB algorithm has been successfully accomplished and results show appreciable improvement to the accuracy of voltage calculations for MV feeders compared with using the algorithm in the 'normal' way. The obtained results encourage the further investigation of ways of improving the error and consistency of MV feeder calculations.

REFERENCES

[1] R. Herman and C. T. Gaunt, "A Practical Probabilistic Design Procedure for LV Residential Distribution Systems," *IEEE Trans. Power Deliv.*, vol. 23, pp. 2247–2254, 2008.

[2] Eskom, "NRS 034-1:2007 Electricity distribution — Guidelines for the provision of electricity distribution networks in residential areas Part 1 : Planning and design of distribution networks," 2007.

[3] R. L. Sellick and C. T. Gaunt, "Comparing methods of calculating voltage drop in low voltage feeders," *Trans SA Inst. Electr. Eng.*, vol. 86, no. 3, 1995.

[4] R. Herman and J. Kritzinger, "The statistical description of grouped domestic electrical load currents," *Electr. Power Syst. Res.*, vol. Volume 27, no. 1, pp. 43–48, 1993.

[5] P. Dondi, D. Bayoumi, C. Haederli, D. Julian, and M. Suter, "Network integration of distributed power generation (ABB)," *J. Power Sources*, vol. 106, pp. 1–9, 2002.

[6] M. Delfanti, M. Merlo, G. Monfredini, V. Olivieri, M. Pozzi, and A. Silvestri, "Hosting dispersed generation on Italian MV networks: towards smart grids," in *Harmonics and Quality of Power (ICHQP) 14th International Conference on. IEEE*, 2010, pp. 1–6.

[7] E. Zio, M. Delfanti, L. Giorgi, V. Olivieri, and G. Sansavini, "Electrical Power and Energy Systems Monte Carlo simulation-based probabilistic assessment of DG penetration in medium voltage distribution networks," *Int. J. Electr. Power Energy Syst.*, vol. 64, pp. 852–860, 2015.

[8] G. Celli and F. Pilo, "MV network planning under uncertainties on distributed generation penetration," in *2001 Power Engineering Society Summer Meeting*, 2001, vol. 1, pp. 485–490.

[9] S. Repo, H. Laaksonen, and P. Jarventausta, "Statistical Models of Distributed Generation for Distribution Network Planning," in *CIRED 18th International Conference on Electricity Distribution*, 2005, pp. 1–5.

[10] C. T. Gaunt, R. Herman, G. Celli, and S. Mocci, "MV and LV distribution feeder design using probabilistic approaches to load and DG Introduction," in *Tutorial at CIRED 21st International Conference on electricity Distribution, Frankfurt Germany*, 2011, p. Not Published.

[11] M. Meldorf, T. Täht, and J. Kilter, "Stochasticity of the electrical network load," *Oil Shale*, vol. 24, no. 2 SUPPL., pp. 225–236, 2007.

[12] A. Augusto, A. de Souza, N. Kagan, K. de Geus, and M. E. M. Udaeta, "Impact of Distributed Generation on the Operational Planning of Medium Voltage Distribution Networks Using Genetic Algorithms," in *Innovative Smart Grid Technologies Conference Europe (ISGT-Europe), 2014 IEEE PES. IEEE*, 2014, vol. 5, pp. 1–5.

[13] Eskom, "NRS 048-2: Electricity Supply - Quality of Supply Part 2 : Voltage characteristics , compatibility levels , limits and assessment methods," 2003.

[14] J. Ward and H. Hale, "Digital Computer Solution of Power Flow Problems," *Trans. AIEEE*, vol. 2, no. 7, p. 961, 1956.

[15] L. C. Siebert, L. R. Ferreira, A. Aoki, A. Bonelli, A. R. R. Souza, and F. D. O. Toledo, "Deterministic versus Probabilistic approaches to self-healing in Smart Grid," in *22nd International Conference and Exhibition on Electricity Distribution (CIRED)*, 2013, no. 1413, pp. 10–13.

[16] F. Adinolfi, F. Baccino, M. Marinelli, S. Massucco, and F. Silvestro, "Model of a real medium voltage distribution network for analysis of distributed generation penetration in a SmartGrid scenario," *2012 3rd IEEE PES Innov. Smart Grid Technol. Eur. (ISGT Eur.*, pp. 1–7, 2012.

[17] R. Herman and C. T. Gaunt, "Electrification : Uncertainties , Models and Design Procedures townhouses," *CIGRE*, vol. 6, no. Coll, pp. 6–7, 2005.

[18] D. D. Le, A. Berizzi, C. Bovo, E. Ciapessoni, D. Cirio, A. Pitto, and G. Gross, "A probabilistic approach to power system security assessment under uncertainty," in *2013 IREP Symposium Bulk Power System Dynamics and Control - IX Optimization, Security and Control of the Emerging Power Grid*, 2013, pp. 1–7.

[19] B. Borkowska, "Probabilistic load flow," *IEEE Trans. Power Appar. Syst.*, vol. 93, no. 3, pp. 752–759, 1974.

[20] V. Neimane, "Distribution network planning based on statistical load modelingapplying genetic algorithms and Monte-Carlo simulations," *2001 IEEE Porto Power Tech Proc. (Cat. No.01EX502)*, vol. 3, 2001.

[21] M. Skok, S. Krajcar, and D. Skrlec, "Dynamic Planning of Medium Voltage Open- Loop Distribution Networks under Uncertainty," in *Intelligent Systems Application to Power Systems*, 2005, pp. 551–556.

[22] A. Dimitrovski and K. Tomsovic, "Uncertainty in Load Flow Modeling : Application of the Boundary Load Flow," in *Automation of Electric Power Systems 16th edition*, 2006, pp. 1–10.

[23] G. Celli, S. Mocci, F. Pilo, and R. Cicoria, "Probabilistic optimization of MV distribution network in presence of distributed generation," in *Proc. PSCC Conf*, 2002, pp. 24–28.

[24] C. T. Gaunt, R. Herman, M. Dekenah, R. L. Sellick, and S. W. Heunis, "Data collection, load modelling and probabilistic analysis for LV domestic electrification," in *International Conference on Electricity Distribution (CIRED)*, 1999.

[25] C. T. Gaunt and R. L. Sellick, "Comparing methods of calculating voltage drop in low voltage feeders," in *Trans SA Institute of Electrical Engineers*, 1995, vol. 86, no. 3.

[26] S. Repo, H. Laaksonen, and P. Jarventausta, "Statistical Models of Distributed Generation for Distribution Network Planning," in *18th International Conference on Electricity Distribution*, 2005.

[27] R. Herman and C.T. Gaunt, "A Practical Probabilistic Design Procedure for LV Residential Distribution Systems," *IEEE Trans. Power Deliv.*, vol. 23, pp. 2247–2254, 2008.

[28] A. S. Safigianni, V. C. Poulious, and G. N. Koutroumpezis, "Penetration of Mixed Distributed Generators in a Medium Voltage Network," in *Universities Power Engineering Conference (UPEC), 2012 47th International*, 2012, pp. 1–6.

[29] M. Delfanti, M. Merlo, G. Monfredini, V. Olivieri, M. Pozzi, and A. Silvestri, "Hosting dispersed generation on Italian MV networks: towards smart grids," in *Harmonics and Quality of Power (ICHQP) 14th International Conference on. IEEE*, 2010, pp. 1–6.

[30] G. Celli, S. Mocci, and F. Pilo, "PROBABILISTIC OPTIMIZATION OF MV DISTRIBUTION NETWORK IN PRESENCE OF DISTRIBUTED GENERATION," in *Proc. PSCC Conf*, 2010, pp. 24–28.

[31] C. L. Masters, "Voltage rise the big issue when connecting emmbedded generation to long 11kV overhead lines," *Power Eng. J.*, vol. 16, no. 1, pp. 5–12, 2002.

[32] G. Celli, S. Mocci, and F. Pilo, "PROBABILISTIC OPTIMIZATION OF MV DISTRIBUTION NETWORK IN PRESENCE OF DISTRIBUTED GENERATION," in *Proc. PSCC Conf*, 2002, pp. 24–28.

[33] M. Hasheminamin, V. G. Agelidis, and A. Heidari, "Impact study of high PV penetration in low and medium-voltage networks when considering residential and industrial load profile," in *Renewable Energy Research and Applications (ICRERA), 2013 International Conference*, 2013, no. 1, pp. 347–352.

[34] S. Conti and S. Raiti, "Probabilistic load flow using Monte Carlo techniques for distribution networks with photovoltaic generators," *Sol. Energy*, vol. 81, no. 12, pp. 1473–1481, 2007.

[35] S. Repo, H. Laaksonen, and P. Jarventausta, "Statistical Models of Distributed Generation for Distribution Network," in *CIRED 18th International Conference and Exibition on Electricity Distribution (CIRED)*, 2005, pp. 6–9.

[36] N. Hosseinzadeh and S. Mastakov, "Load modelling for medium voltage SWER distribution networks," *2008 Australas. Univ. Power Eng. Conf.*, pp. 1–5, 2008.

[37] A. K. Ghosh, D. L. Lubkeman, M. J. Downey, and R. H. Jones, "Distribution circuit state estimation using a probabilistic approach," *IEEE Trans. Power Syst.*, vol. 12, no. 1, pp. 45–51, 1997.

[38] C. Bary, "Coincidence-Factor Relationships of Electric-Service-Load Characteristics," *Trans. Am. Inst. Electr. Eng.*, vol. 9, no. 64, pp. 623–628, 1945.

[39] R. Hamilton, "The summation of load curves," *AIEEE*, vol. 63, no. 1, p. 729, 1944.

[40] S. Rusck, "The simultaneous demand in distribution network supplying domestic consumers," *ASEA*, vol. 10, no. 1, p. 59, 1956.

[41] I. A. Ferguson and C. T. Gaunt, "LV network sizing in electrification projects - Replacing a deterministic method with a statistical method," in *17th International Conference on Electricity Distribution (CIRED)*, 2003, no. 68, pp. 1–6.

[42] R. Singh, B. C. Pal, and R. Jabr, "Statistical representation of distribution system loads using Gaussian Mixture Model," *IEEE Trans. Power Syst.*, vol. 25, no. 1, pp. 29–37, 2010.

[43] C. Carmona-Delgado, E. Romero-Ramos, and J. Riquelme-Santos, "Probabilistic load flow with versatile non-Gaussian power injections," *Electr. Power Syst. Res.*, vol. 119, pp. 266–277, 2015.

[44] A. Herrera-Orozco, S. Perez-Londobo, and J. Mora-Florez, "Load modeling for fault location in distribution systems with distributed generation," *2012 Sixth IEEE/PES Transm. Distrib. Lat. Am. Conf. Expo.*, pp. 1–8, 2012.

[45] R. E. Brown and L. A. A. Freeman, "Analyzing the reliability impact of distributed generation," *Power Eng. Soc. Summer Meet. Conf. Proc. (Cat. No.01CH37262)*, vol. 2, no. 1, pp. 1013–1018, 2001.

[46] E. J. Kim and J. S. Hwang, "Distributed, Islanding Detection of System, Units Connected to Power Distribution Systems," in *International Conference on Power System Technology*, 2000, pp. 643–647.

[47] J. Schwippe, O. Krause, and C. Rehtanz, "Probabilistic Load Flow Calculation based on an enhanced convolution technique," *2009 IEEE Bucharest PowerTech*, pp. 1–6, 2009.

[48] C. Wan, Z. Xu, Z. Y. Dong, and K. P. Wong, "Probabilistic load flow computation using first-order

second-moment method," *IEEE Power Energy Soc. Gen. Meet.*, pp. 1–6, 2012.

[49] W. El-Khattam, Y. G. Hegazy, S. Member, and M. M. a Salama, "Investigating Distributed Generation Systems Performance Using Monte Carlo Simulation," *IEEE Trans. Power Syst.*, vol. 21, no. 2, pp. 524–532, 2006.

[50] G. Carpinelli, P. Caramia, and P. Varilone, "Multi-linear Monte Carlo simulation method for probabilistic load fl ow of distribution systems with wind and photovoltaic generation systems," *Renew. Energy*, vol. 76, pp. 283–295, 2015.

[51] Q. Xiao, "Comparing three methods for solving probabilistic optimal power flow," *Electr. Power Syst. Res.*, vol. 124, pp. 92–99, 2015.

[52] R. N. Allan and M. R. G. Al-Shakarchi, "Probabilistic a.c. load flow," *Proc. Inst. Electr. Eng.*, vol. 123, no. 6, p. 531, 1976.

[53] P. Zhang and S. Lee, "Probabilistic Load Flow using the method of combined cumulants and Gram-Charlier expansion," *IEEE Trans. Power Syst.*, vol. 19, no. 1, pp. 676–682, 2004.

[54] D. P. Stojanović, L. M. Korunović, and J. V. Milanović, "Dynamic load modelling based on measurements in medium voltage distribution network," *Electr. Power Syst. Res.*, vol. 78, no. 2, pp. 228–238, 2008.

[55] A. Dimitrovski and R. Ackovski, "Probabilistic load flow in radial distribution networks," in *Proceedings of 1996 Transmission and Distribution Conference IEEE*, 1996, pp. 15–20.

[56] C. T. Gaunt, R. Herman, G. Celli, and S. Mocci, "MV and LV distribution feeder design using probabilistic approaches to load and DG Introduction," *CIRED Tutor.*, no. June, 2011.

[57] J. D. Glover, M. S. Sarma, and T. J. Overbye, *Power System Analysis and Design*, 5th ed. United States of America, 2010.

APPENDIX A

Appendix A HERMAN-BETA ALGORITHM FOR LV FEEDERS

The formulations listed below are for the Herman-Beta method for voltage calculations on LV feeders. The equations cover both passive and active feeders.

List of symbols

The symbols used in the formulations were chosen to avoid Greek or other non-alphabetic symbols and, where possible, to avoid subscripts and superscripts. For example, ai is used rather than a_i

Vs	is the nominal supply voltage, in volts
ai	is the Beta probability density function parameter, alpha at node i
bi	is the Beta probability density function parameter, beta at node i
ci	is the scaling factor in amperes (usually the circuit-breaker size) at node i
mai	is the number of consumers connected to the a-phase at node I
mbi	is the number of consumers connected to the b-phase at node i
mci	is the number of consumers connected to the c-phase at node i
N	is the total number of nodes in the radial feeder section
Rp	is the temperature-corrected resistance of the phase conductor per span
Rn	is the temperature-corrected resistance of the neutral conductor per span
p	is the percentage risk in the probabilistic calculation
G	is the first statistical moment
H	is the second statistical moment
ki	is a resistance ratio
Ri	is a phase resistance index
Vmax	is the maximum consumer voltage
Vmin	is the minimum consumer voltage
Vd	is a voltage drop
L, K	are node counters
Vc	is the consumer voltage
vc	is the normalized consumer voltage
av	is the alpha parameter of scaled consumer voltage
bv	is the beta parameter of scaled consumer voltage
betainv	is the Beta inverse function
DVrmaxi	is the real component of maximum volt drop at node i
DVjmaxi	is the imaginary component of maximum volt drop at node i

DVrmini	is the real component of minimum volt drop at node i
DVjmini	is the imaginary component of minimum volt drop at node i
E()	is the expected value of ()

C1i, C2i, C3i, C4i, C5i, C6i, pi, qi and F1i, F2i, F3i are constants.

Procedure for voltage calculations on passive and active 3-phase feeders

In the equations listed below, it should be noted that all formulae apply to all nodes (load and generator nodes) except symbols denoted with *'symbol'*$_{LOAD}$ for load nodes and *'symbol'*$_{DG}$ for generator nodes.

For passive feeders:

DG node calculations are ignored since no DG customers are connected. By doing this, all variables involving subscript 'DG' are equated to zero thereby having no effect on the calculation of voltages.

For active feeders with DG

DG nodes are taken into consideration through specification of the number of connected generators (as directed in the procedure below) at the relevant nodes. Equations with subscript 'DG' are consequently considered in the calculation.

Step-wise procedure for calculating three-phase system voltage drops

Step 1 – Select the network parameters

1. Supply voltage, ***Vs***.
2. Load description in Beta pdf form: ***ai, bi, ci***. Where ***ci*** is the scaling factor – usually the circuit-breaker size.
3. Specify the number of consumer connections at each load node, i: ***mai, mbi*** and ***mci*** (loads in load nodes and embedded generators in generator nodes).
   A positive number represents a load and a negative number is an embedded generator.
4. Specify total number of nodes in the radial section, ***N***.
5. Specify the phase and neutral conductor resistances for each section: ***Rp*** and ***Rn***, allowing for temperature rise.
6. Specify a design risk value: ***p***, in percent.

Step 2 – Calculate constants Gi and Hi

$$Gi = \frac{ai}{(ai+bi)} \qquad Hi = \frac{ai(ai+1)}{(ai+bi)(ai+bi+1)}$$

Step 3 – Calculate Ri, Rp and ki

$$Ri = \sum_{j=1}^{i} Rn(j) \qquad Rp = \sum_{j=1}^{i} Rp(j) \qquad ki = \frac{Ri}{Rp}$$

Where

Rn (j) is the neutral conductor resistance for section *(i–1)* to *(i)*;

Rp (j) is the phase conductor resistance for section *(i–1)* to *(i)*.

Step 4 – Calculate maximum and minimum voltages, Vmax and Vmin

Real parts are indexed with *r* and imaginary parts with *j*. The symbol D is used to indicate voltage drop and *i* index indicates the *i*-th node.

$$DVrmaxi_{LOAD} = -0.5ki \times Ri \times ci(mbi + mci)$$

$$DVjmaxi_{LOAD} = \frac{\sqrt{3}}{2} ki \times Ri \times ci(mbi - mci)$$

$$DVrmini_{LOAD} = (1 + ki) \times Ri \times ci \times mai$$

$$DVjmini_{LOAD} = 0$$

$$DVrmaxi_{DG} = (1 + ki) \times Ri \times ci \times mai$$

$$DVrmini_{DG} = -0.5ki \times Ri \times ci(mbi + mci)$$

$$DVrmini_{DG} = -0.5ki \times Ri \times ci(mbi + mci)$$

$$DVjmini_{DG} = \frac{\sqrt{3}}{2} ki \times Ri \times ci(mbi - mci)$$

$$Vmax = \sqrt{\left(Vs - \sum_{i=1}^{N} DVrmaxi\right)^2 + \left(\sum_{i=1}^{N} DVjmaxi\right)^2}$$

If $\sum_{i=1}^{N} DVrmini < Vs$:

$$Vmin = +\sqrt{\left(Vs - \sum_{i=1}^{N} DVrmini\right)^2 + \left(\sum_{i=1}^{N} DVjmini\right)^2}$$

If $\sum_{i=1}^{N} DVrmini > Vs$:

$$Vmin = -\sqrt{\left(Vs - \sum_{i=1}^{N} DVrmini\right)^2 + \left(\sum_{i=1}^{N} DVjmini\right)^2}$$

Step 5 – Calculate the constants: C1i, C2i, C3i, C4i, C5i and C6i and F1i, F2i and F3i

$$F1i = |mai|(|mai| - 1) - |mai|(|mbi| + |mci|) + 0.25(|mbi| + |mci| - 1)(|mbi| + |mci|)$$

$$F2i = |mai|(2|mai| - |mbi| - |mci| - 2)$$

$$F3i = |mai|(|mai| - 1)$$

$$C1i = (1+ki)mai - 0.5ki(mbi + mci)$$

$$C2i = ki^2[(|mai| + 0.25|mbi| + 0.25|mci|)] + |mai|(2ki + 1)$$

$$C3i = F1i \times ki^2 + F2i \times ki + F3i$$

$$C4i = \frac{3ki^2}{4}(|mbi| + |mci|)$$

$$C5i = \frac{3ki^2}{4}[(|mbi| - |mci|)^2 - (|mbi| + |mci|)]$$

$$C6i = \frac{\sqrt{3}}{2}ki(mbi - mci)$$

Step 6 – Calculate the expected values: E (Dvri), E (DVr), E (DV²ri) and E (DV²r)

$$E(DVri) = C1i \times Ri \times ci \times Gi$$

$$E(DVr) = \sum_{i=1}^{N} E(DVri)$$

$$E\left(DV^2ri\right) = Ri^2 \times ci^2[C2i \times Hi + C3i \times Gi^2]$$

$$E\left(DV^2r\right) = \sum_{i=1}^{N} E(DV^2ri) + \sum_{K=1}^{N}\sum_{\substack{L=1 \\ L\neq K}}^{N} E(DVr_K) \times E(DVr_L)$$

Step 7 – Calculate expected values: E (DVji), E (DVj), E (DV²ji) and E (DV²j)

$$E(DVji) = C6i \times Ri \times ci \times Gi$$

$$E(DVj) = \sum_{i=1}^{N} E(DVji)$$

$$E\left(DV^2ji\right) = Ri^2 \times ci^2[C4i \times Hi + C5i \times Gi^2]$$

$$E\left(DV^2j\right) = \sum_{i=1}^{N} E(DV^2ji) + \sum_{K=1}^{N}\sum_{\substack{L=1 \\ L\neq K}}^{N} E(DVj_K) \times E(DVj_L)$$

Step 8 – Calculate E (Vc) and E (V²c)

$$E(Vc) = Vs[1 - \frac{E(DVr)}{Vs} + 0.5\frac{E(DV^2j)}{Vs^2}]$$

$$E\left(Vc^2\right) = Vs^2 - 2Vs \times E(DVr) + E\left(DV^2r\right) + E\left(DV^2j\right)$$

Step 9 – Calculate the scaled values of E (vc) and E (vc²)

$$E(vc) = \frac{E(Vc) - Vmin}{Vmax - Vmin}$$

$$E(vc^2) = \frac{E\left(Vc^2\right) - 2Vmin \times E(Vc) + Vmin^2}{(Vmax - Vmin)^2}$$

Step 10 – Calculate the Beta parameters of vc: av and bv

$$av = \frac{E(vc^2)\text{-}E(vc)}{E(vc)\text{-}\frac{E(vc^2)}{E(vc)}} \qquad bv = \frac{av}{E(vc)} - av$$

Step 11 – Select a risk percentage p and calculate percentile value v%

Use the Beta inverse function:

$$v\% = \text{betainv}[\left(\frac{p}{100}\right), |av|, |bv|]$$

A percentile value of 90% (or 95%) is used for calculating voltage rise in active feeders with embedded generation whereas a value of 10%(or 5%) is used for calculations on passive feeders.

Step 12 – Rescale the consumer voltage, Vc% according to whether the net current is into or out of the feeder

$$Vc\% = v\%(Vmax - Vmin) + Vmin$$

A.2. THE HERMAN-BETA ALGORITHM WITH MODIFIED INPUTS FOR MV FEEDERS

The modifications done to the input parameters of the HB algorithm to accommodate feeder reactance and non-unity power factor are as given in Table A1 below. The algorithm as detailed in the preceding section remains the same.

Table A-1: Modified terms in HB algorithm for voltage calculations on MV feeders

Term in HB_{LV}	Inflated term
Rpi	$Rpi = sqrt(Rpi^2+Xpi^2)$
Ci	Ci = Ci/pfi

Where,

pfi is the average power factor of the loads connected at node i

Xpi is temperature-corrected reactance of the phase conductor per span

APPENDIX B

Appendix BUSING THE MONTE-CARLO SIMULATION FOR VOLTAGE CALCULATIONS ON MV FEEDERS

In this work, the Monte-Carlo Simulation (MCS) is used as a validation tool. The accuracy of the Herman-Beta (HB) algorithms is decided on the basis of comparison with MCS results. This section serves to give a description of how the MCS was used in the calculation of voltages on MV feeders and more importantly, how the output results were used.

B.1. Voltage Drop Equations

A MCS utilises deterministic voltage equations in an iterated process carried out using different input quantities. With iteration, input variables are picked from given distributions using random number generators. These picked numbers are then used to compute voltages on the feeder using the equations derived below.

For a load consuming power denoted by $P_i + jQ_i$ from the grid at node i, the current that it draws can be calculated using the apparent power formula as follows,

$$S_i = I_i^* V_i$$

$$I_i^* = \frac{P_i + jQ_i}{V_i}$$

$$I_i = I_{Ri}\text{-}jI_{Ii} \ldots\ldots\ldots\ldots\ldots\ldots\ldots\ldots (1)$$

Where, $I_{Ri} = \frac{P_i}{Vi}, I_{Ii} = \frac{Q_i}{Vi}$

V_i is assumed to be the nominal voltage

The equation labelled (1) above can then be used to model the load. The calculation of voltage drop on a feeder with impedance given by $Z_{pi} = R_{pi} + jX_{pi}$ is performed as follows:

$$\Delta V_{ai} = I_{ai}Z_{pi} + I_{ni}Z_{ni} \quad \text{(for Red phase)}$$

After long and tedious calculations, the voltage drop equations obtained given separately in real and imaginary components are shown below. In these equations, the subscripts 'R' and 'I' are used to denote the real and imaginary components of the load current.

$$\Delta V_{Ri} = R_{pi}\left[I_{ai\text{-}R}(1+k)\text{-}0.5k(I_{bi\text{-}R}+I_{ci\text{-}R})+\frac{\sqrt{3}}{2}k(I_{bi\text{-}I}\text{-}I_{ci\text{-}I})\right]$$

$$+X_{pi}\left[I_{ai\text{-}I}(1+k)\text{-}0.5k(I_{bi\text{-}I}+I_{ci\text{-}I})\text{-}\frac{\sqrt{3}}{2}k(I_{bi\text{-}R}\text{-}I_{ci\text{-}R})\right]$$

$$\Delta V_{Ii} = X_{pi}\left[I_{ai\text{-}R}(1+k)\text{-}0.5k(I_{bi\text{-}R}+I_{ci\text{-}R})\right.$$

$$\left.+\frac{\sqrt{3}}{2}k(I_{bi\text{-}I}\text{-}I_{ci\text{-}I})\right]\text{-}R_{pi}\left[I_{ai\text{-}I}(1+k)\text{-}0.5k(I_{bi\text{-}I}+I_{ci\text{-}I})\text{-}\frac{\sqrt{3}}{2}k(I_{bi\text{-}R}\text{-}I_{ci\text{-}R})\right]$$

In this research, real power data and power factor values associated with it at a given substations are used in the computation of voltage drops on MV feeders. Using this information, the imaginary component of the load current is projected using the power angle $\emptyset$ as in the equation below.

$$I_{ai\text{-}I} = I_{ai\text{-}R}\tan\emptyset$$

However, if reactive power load data is available, the two distributions (for real and imaginary) are used in the drawing of load currents thereby eliminating the need of projection using power angle.

B.1.1. Voltage equations for the inclusion of shunt capacitors

In order to include shunt capacitors in the calculation of feeder voltages, the reactive power supplied by the capacitor is used to determine the capacitor current in a similar way done in the preceding section.

$$S_i = I_i^* V_i$$

$$I_i^* = \frac{-jQ_i}{V_i}$$

$$I_i = jI_{Ii} \dots\dots\dots\dots\dots\dots\dots\dots (2)$$

Where, $$I_{Ii} = \frac{Q_i}{V_i}$$

V_i is assumed to be the nominal voltage

The current given in equation 2 is used in the calculation of voltage drop in the same way done in the previous section.

B.1.2. Voltage equations for the inclusion of DG

In active feeders, connected generators inject currents into the utility grid. This current can be modelled by a beta pdf and used in the same way as in the calculations for loads. The only difference is that the generator currents are negative since they flow in the opposite direction to those of loads.

B.2. MATLAB Implementation

The general procedures taken in performing a MCS in MATLAB are illustrated in the flow chart given in Fig. B1. The main tasks in this procedure are:-

- Random number generation (for selection of customer currents)
- Iteration implementation
- Graphical representation of output voltage profiles

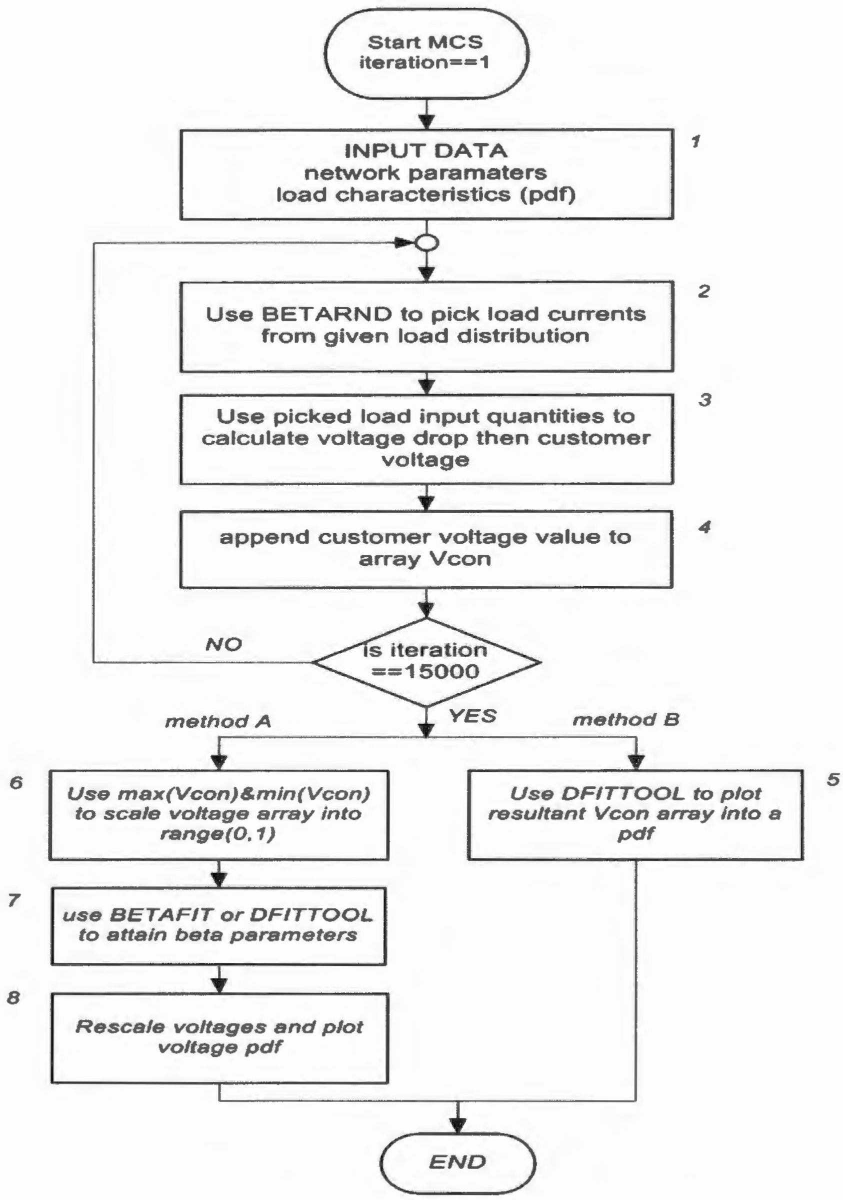

Figure B.1:Process Flow for voltage computations using the MCS

A ***Betarnd*** function is used to draw customer load values from a given load distribution function. The betarnd function is specially tailored for random number sampling from beta functions. Besides being a specific tool, the function allows sampling with equal chance which eliminates errors in the selection process. This process is marked by a process identifier '2' on the flowchart.

Once customer currents at a specific node are picked, the voltage equations given in the preceding section are used to calculate voltage drops due to that node and the resulting nodal voltage at that point.

The result of this calculation is stored in the voltage array, Vcon, at a location indexed by the iteration cycle (processes 3 and 4). This process is repeated up until the value of iterations specified by the user (15000 in our case) is reached. When this happens, the array Vcon has voltage values equal to the iterations performed. This array can be used to plot the distribution of voltages using the function ***dfittool*** (process 5, method B).

However, since the voltage values in Vcon are more or less around the nominal voltage 11kV, the Beta pdf cannot be used to fit the distribution of voltages since it requires inputs restricted to the open interval (0, 1). A normal distribution can however be used to fit this data such that comparisons with the outcomes of the HB method can be done. For such a comparison to be made, the mean and variance of the voltage pdf from the HB method are required to plot a similar pdf to that of the MCS.

For beta pdf plotting, the voltage array Vcon is required to be scaled to values in the interval (0, 1). To do this, the maximum and minimum voltages on the feeder are calculated using the equations given in section B1 above (process 6 on flow chart). The scaled array is then used to determine the beta parameters of the voltage pdf. The array is rescaled and used to plot the voltage pdf (processes 7 & 8). The achievement of this allows meaningful comparison of plots and beta parameters as well.

SUPPLEMENTARY WORK

Appendix CREVIEW OF THE HB ALGORITHM'S PRESENTATION IN THE NRS034-1/2007

This document serves as errata to the presentation of the HB algorithm in the NRS-34/2007. The corrections presented here are as a result of a rigorous follow up derivation of the algorithm. The Table below summarises the corrections made.

Table C-1: Correction of the HB algorithm in the NRS034-1 Document

SUBJECT VARIABLE OF CORRECTED EQUATION	NRS034 QUOTED EXPRESSION	CORRECTED EXPRESSION
Expected nodal voltage drop value, $E(V_d{}^2)$	$\sum_{k=1}^{N}\sum_{\substack{k=1\\k\neq l}}^{N} E(V_{d_k})E(V_{d_l})$	$\sum_{i=1}^{N} E(V_i{}^2)+\sum_{k=1}^{N}\sum_{\substack{l=1\\k\neq l}}^{N} E(V_{d_k})E(V_{d_l})$
Nodal maximum voltages, DVr_{maxi}	$\frac{1}{2}k_iR_iC_i(m_b+m_c)$	$-\frac{1}{2}k_iR_iC_i(m_b+m_c)$
Summated, end of feeder maximum voltages, V_{max}	$\sqrt{\left(V_s+\sum_{i=1}^{N} DVr_{maxi})\right)^2+\left(\sum_{i=1}^{N} DVj_{maxi})\right)^2}$	$\sqrt{\left(V_s-\sum_{i=1}^{N} DVr_{maxi})\right)^2+\left(\sum_{i=1}^{N} DVj_{maxi})\right)^2}$
Constant C_{2i}	$k_i{}^2\left[\left(V_s+\frac{1}{4}m_{bi}+\frac{1}{4}m_{ci}\right)+(2k_i+1)m_{ai}\right]$	$k_i{}^2\left[\left(V_s+\frac{1}{4}m_{bi}+\frac{1}{4}m_{ci}\right)\right]+(2k_i+1)m_{ai}$
Normalized expected voltage, $E(v_c{}^2)$	$\frac{E(V_c{}^2)-2V_{min}+V_{min}{}^2}{(V_{max}-V_{min})^2}$	$\frac{E(V_c{}^2)-2V_{min}E(V_c)+V_{min}{}^2}{(V_{max}-V_{min})^2}$